



AVERTISSEMENT

Ce document est le fruit d'un long travail approuvé par le jury de soutenance et mis à disposition de l'ensemble de la communauté universitaire élargie.

Il est soumis à la propriété intellectuelle de l'auteur. Ceci implique une obligation de citation et de référencement lors de l'utilisation de ce document.

D'autre part, toute contrefaçon, plagiat, reproduction illicite encourt une poursuite pénale.

➤ Contact SCD Nancy 1 : theses.sciences@scd.uhp-nancy.fr

LIENS

Code de la Propriété Intellectuelle. articles L 122. 4

Code de la Propriété Intellectuelle. articles L 335.2- L 335.10

http://www.cfcopies.com/V2/leg/leg_droi.php

<http://www.culture.gouv.fr/culture/infos-pratiques/droits/protection.htm>



FACULTE DES SCIENCES & TECHNIQUES

U.F.R. Sciences & Techniques Biologiques, Ecole Doctorale Sciences et Ingénierie Ressources Procédés Produits Environnement
Département de Formation Doctorale Sciences Agronomiques et Forestières, Biologie et Ecologie, Biotechnologies

UNIVERSITY of Sydney, School of Biological Science

Thèse

présentée pour l'obtention du titre de

Docteur en Biologie Végétale et Forestière

de l'Université Henri Poincaré, Nancy I

par **Cyril DOUTHE**

Relations entre échanges gazeux foliaires et discrimination isotopique du Carbone-13 pendant la photosynthèse: Estimations et variations rapides de la conductance mésophyllienne au CO₂

Soutenue publiquement le 7 novembre 2011

Rapporteurs:

Jaume FLEXAS - Pr, Universitat de les Illes Balears

Arthur GESSLER - Pr, University of Freiburg

Examineurs

Erwin DREYER - DR, INRA Nancy

Daniel EPRON - Pr, Université Nancy I

Charles R. WARREN - Pr, The University of Sydney

Margaret BARBOUR - Dr., The University of Sydney

Liste du Jury

Rapporteurs :

Jaume Flexas Sans (Dr.)

Departament de Biologia, Universitat de les Illes Balears
Carretera de Valldemossa Km 7.5
E-07122 Palma de Mallorca, Espagne
Tel : 0034 971 17 23 65
email : jaume.flexas@uib.es

Arthur Gessler (Pr.)

Humboldt-University at Berlin
Faculty of Agriculture and Horticulture
Lentze-Allee 75
14195 Berlin, Allemagne
Tel : 0049 33432-82 326
email : gessler@zalf.de

Examineurs :

Erwin Dreyer (D.R.)

Centre INRA de Nancy
UMR INRA UHP 1137 "Ecologie et Ecophysiologie Forestières"
54280 Champenoux, France
Tel : 0033 3 83 39 40 78
email dreyer@nancy.inra.fr

Daniel Epron (Pr.)

UMR INRA UHP 1137 "Ecologie et Ecophysiologie Forestières"
Nancy-Université - Université Henri Poincaré, Faculté des Sciences
BP 70239 - 54506 Vandoeuvre les Nancy, France
Tel : tel 0033 3 83 39 73 42
email : daniel.epron@scbiol.uhp-nancy.fr

Charles Warren (Assoc. Prof.)

The University of Sydney
School of Biological Sciences
Heydon-Laurence Building A08
NSW 2006, Australia
Tel : 0061 2 9351 2678
email : charles.warren@sydney.edu.au

Margaret Barbour (Dr.)

The University of Sydney
Faculty of Agriculture, Food and Natural Resource
107 Cobbitty Road, Cobbitty
NSW 2570, Australia
Tel : 0061 2 9351 8821
email : margaret.barbour@sydney.edu.au

Remerciements

Avant de rentrer dans des propos scientifiques certains (ou certains propos scientifiques..), rendons à César ce qui est à César. Étant donné que cette thèse a été effectuée en cotutelle mi-francophone, mi-australienne, les remerciements seront aussi dans les deux langues.

Tout d'abord, les chefs. Je tiens à remercier Erwin qui, lors de l'entretien "d'embauche" m'a entendu dire "la physio, j'y connaît rien" mais m'a quand même donné ma chance. Il m'a soutenu tout du long, et je pense avec le recul ça ne devait pas toujours être facile. Au final, la principale leçon qu'il m'aura apprise c'est... de bien poser la question. Et oui après quatre ans de thèse en recherche, ça paraît bizarre d'avoir juste appris à poser une question, mais en fait c'est très important. Un grand merci aussi à Oliver, pour nos conversations passionnantes et réellement stimulantes, qui très souvent partaient à la dérive, et qui faisait que le sujet à la fin de la conversation n'était jamais le même que celui du départ. Mais c'est aussi comme ça qu'on fait de la recherche! Merci aussi à Daniel, pour son encadrement plus lointain, mais tout aussi efficace. And finally I would like thanks Charlie, for his strong support during my journey at the University of Sydney, even if my English at the beginning was horrible.. Charlie let me organize my work independently, but was everytime present when I needed help. A special thanks as well for his incredible capacity to provide corrections of the manuscripts very fastly! At Usyd, I would to thanks as well Adrienne. We share the same room for several mouths, and I especially appreciated our passionate conversations.

À l'INRA de Nancy, beaucoup de personnes sont aussi à remercier. On commence par qui? Disons Pascal et Rémy, les deux compères de la thèse. Je ne dirait pas tout ici (ma conscience me l'impose), mais merci pour toutes les soirées (et les lendemains difficiles), les bons moments au labo, le Grand Détournement et les vodkas polonaises. Merci à Marion et Magali pour toutes les rigolades et les randos dans le Vosges. Merci à Silvere pour nos conversations enflammées sur le modèle de Farquhar (il est pas encore au point ce truc..), et aussi sur la "sécurité" des réseaux... Merci à Jacqueline, pour continuer à prendre soins des petits thésard apeurés au début de la thèse (et aussi pour m'expliquer comment marche un labo de bioch..), à Claude et Christian le duo isotopique de choc (accompagnés maintenant de Nicolas), merci à la Irène pour ces commentaires toujours pertinents (j'ai pas dit méchant !), ainsi que Marie-Béa et David. Un grand Merci aussi à Rosine. Rosine a toujours été présente, et m'a sauvé la vie plusieurs fois lorsque je me perdais dans les méandres de l'administration. Merci à Pierre pour son aide en stats, et nos conversations botanico-ornithologiques. Merci à Patrick pour m'avoir initié aux échanges gazeux, et aussi un grand merci à Caroline qui a pris beaucoup de temps pour m'expliquer le fonctionnement de la TDL et pour toutes ces heures passées à ...trouver les fuites de CO₂.. Merci à l'équipe de la Fac qui m'a accueilli pendant quelques temps, ainsi que Yves et Ata pour les extractions enzymatiques.

Je tiens aussi à remercier ma famille pour leur soutien, et sans qui ce manuscrit ne serait pas là. Mes parents, pour m'avoir donné la chance de faire des études et me laisser choisir ma voie, mes grand parents pour toujours être là quand on en a besoin, ainsi que Matthieu, mon frère. Un merci aux cousins de Chalosse pour leur amitié sans faille, en attendant les retrouvailles...ardues. A special thanks to my friends in Australia, Jhony and Federica for all the good moments, and also Damien (Carton Gaston!). Enfin, un merci tout particulier à la Tribu Teixiera pour leur amitié, leur soutien, les soirées, les bouffes, les discussions, tout quoi!

Pour finir un grand merci à Blandine, pour m'avoir soutenu jusqu'au bout et à continuer à la faire, pour supporter mon mauvais caractère, pour tout ce temps passé et à venir.

Bonne Lecture

Enjoy

Relations entre discrimination isotopique du carbone-13 et échanges gazeux foliaires pendant la photosynthèse: Estimations et variations rapides de la conductance mésophyllienne au CO₂

Résumé: Les travaux de cette thèse se sont situés autour de la relation entre discrimination isotopique du carbone 13 et échanges gazeux foliaires. Le modèle établi par Farquhar et al. (1982) permet de prédire la discrimination contre le ¹³C pendant la photosynthèse ($\Delta^{13}\text{C}$) en tenant compte des processus de diffusion, de carboxylation et décarboxylation engagés pendant la photosynthèse. Cette relation permet d'utiliser $\Delta^{13}\text{C}$ comme indicateur de l'efficacité d'utilisation de l'eau (WUE, quantité de carbone fixé en fonction de l'eau consommée), un paramètre particulièrement important dans un contexte de changement climatique, d'agriculture et de sylviculture. Le modèle de $\Delta^{13}\text{C}$ a également été utilisé pour estimer la conductance mésophyllienne au CO₂ (g_m), un paramètre qui limite fortement la photosynthèse *via* la disponibilité en carbone dans le chloroplaste. Au cours de nos travaux, nous avons analysé le modèle $\Delta^{13}\text{C}$ pour identifier les paramètres les plus influents dans le modèle, et mis en évidence que l'utilisation du "modèle simple" de $\Delta^{13}\text{C}$ (ignorant g_m et les processus de décarboxylation) peut induire un biais important dans l'estimation de WUE. Dans un second temps nous nous sommes concentrés sur les possibles variations à court-terme de g_m , un domaine encore sujet à débat. Nous avons confirmé que g_m était sensible aux variations de CO₂ et d'irradiance sur toutes les espèces d'arbres mesurées dans cette étude. Nous avons aussi montré que ces variations rapides ne peuvent pas être dues à des variations des autres paramètres du modèle, à l'exception possible du paramètre b (discrimination pendant la carboxylation). Nous suggérons que les prochaines études dans ce domaine portent sur (i) la possible variabilité environnementale et génétique du paramètre b et (ii) les mécanismes à l'origine des variations rapides de g_m (aquaporines et anhydrases carboniques).

Mots-clefs: discrimination isotopique du carbone, photosynthèse, conductance mésophyllienne, variabilité environnementale.

Relationship between carbon isotopic discrimination and leaf gas exchange during photosynthesis: Estimations of mesophyll conductance to CO₂

Abstract: This work was focused on the relationship between isotopic discrimination of ¹³C during photosynthesis ($\Delta^{13}\text{C}$) and leaf gas exchange. The model of Farquhar and colleagues (Farquhar *et al.* 1982) predicts $\Delta^{13}\text{C}$ by accounting for diffusion, carboxylation and decarboxylation processes during the photosynthesis. This relationship is widely used and $\Delta^{13}\text{C}$ is frequently considered as a proxy water use efficiency (WUE, the amount of water required to fix a amount of carbon), an interesting parameter in the context of climate change, crop production and sylviculture. The $\Delta^{13}\text{C}$ model is also used to assess mesophyll conductance to CO₂ (g_m), that strongly limits photosynthesis *via* the availability of carbon in the chloroplast. Along this work we analyzed the $\Delta^{13}\text{C}$ model and identified the most important parameters, and highlighted that using the "simple form" of the model (which ignores g_m and the decarboxylations) could lead to misestimating WUE. We also focused on the possible rapid variations of g_m , a subject still under debate. We confirmed that g_m was sensitive to rapid variations of CO₂ and irradiance in all species tested in this study. We also showed that apparent rapid variations of g_m could not be induced by variations of other parameters in the model, with the exception of parameter b (discrimination during carboxylation). We propose that future studies should focus on (i) the possible environmental and genetic variability of parameter b , and (ii) the physiological processes able to change g_m at short time scales (aquaporins and carbonic anhydrase).

Keywords: isotopic carbon discrimination, photosynthesis, mesophyll conductance, environmental variability

List of Publications

Cyril DOUTHE, Erwin DREYER, Daniel EPRON, Charles R. WARREN
Mesophyll conductance to CO₂, assessed from on-line TDL-AS records of ¹³CO₂ discrimination, displays small but significant short term responses to CO₂ and irradiance in Eucalypt seedlings.

Published in Journal of Experimental Botany, on 6 April 2011

Cyril DOUTHE, Erwin DREYER, Oliver BRENDEL, Charles R. WARREN
Is mesophyll conductance to CO₂ in leaves of three *Eucalyptus* species sensitive to short term changes of irradiance under ambient as well as low O₂?

Submitted to Functional Plant Biology, on 25 August 2011

Cyril DOUTHE, Oliver BRENDEL, Daniel EPRON, Charles R. WARREN, Erwin DREYER
Relationship between ¹³C discrimination and leaf gas exchange: analysis of the model, parameters and implications for estimating mesophyll conductance to CO₂.

In preparation

Cyril DOUTHE, Daniel EPRON, Oliver BRENDEL, Charles R. WARREN, Erwin DREYER
Mesophyll conductance of poplar leaves varies rapidly with changes in CO₂ and irradiance: an assessment from on line ¹³CO₂ discrimination records with TDL-AS.

In preparation

Table of Contents

INTRODUCTION.....	1
A brief history	2
A model linking between ^{13}C discrimination and plant gas exchange.....	3
CHAPTER I.....	7
Relationship between ^{13}C discrimination and leaf gas exchange: Analysis of the model, influence of the parameters and implications for estimating mesophyll conductance to CO_2.....	7
INTRODUCTION.....	8
Diversity of the W_i - $\Delta^{13}\text{C}$ relationships found in the literature	10
Using the complete form of the discrimination model.....	14
On the importance of the b parameter	26
Importance of non-photorespiratory decarboxylation: e and R_d	34
Importance of photorespiration: f and Γ^*	35
Concluding remarks	36
CHAPTER II	38
Mesophyll conductance to CO_2, assessed from on-line TDL-AS records of $^{13}\text{CO}_2$ discrimination, displays small but significant short term responses to CO_2 and irradiance in Eucalypt seedlings.	38
ABSTRACT	40
INTRODUCTION.....	41
MATERIAL & METHODS.....	44
RESULTS	52
DISCUSSION	57
Importance of the respiratory and photorespiratory terms in the estimation of mesophyll conductance	57
Response of g_m to CO_2 mole fraction.	59
Response of g_m to irradiance.....	60
CONCLUSION	61
CHAPTER III.....	63
Is mesophyll conductance to CO_2 in leaves of three <i>Eucalyptus</i> species sensitive to short-term changes of irradiance under ambient as well as low O_2?	63
ABSTRACT	65
INTRODUCTION.....	66
MATERIAL AND METHODS	69
RESULTS	75
DISCUSSION	86
Rapid response of mesophyll conductance to irradiance under 21 and 1% O_2	86
Sensitivity of g_m estimates to changes of model parameter values.....	87
Are the observed variations of g_m with O_2 realistic?	89
CONCLUSION	91
CHAPTER IV	94
Mesophyll conductance of poplar leaves varies rapidly with changes in CO_2 and irradiance: an assessment from on line $^{13}\text{CO}_2$ discrimination records with TDL-AS.....	94
ABSTRACT	96
INTRODUCTION.....	97
MATERIAL & METHODS.....	99
RESULTS	105

DISCUSSION	111
Rapid variations of g_m with PPFD and CO_2	111
Impact of a stable g_m on net CO_2 assimilation rate under PPFD variations	112
CONCLUSION	113
CONCLUSIONS.....	114
and PERSPECTIVES	114
ANNEX I	121
REFERENCES	134

List of abbreviations

Symbol	Unity	Description
ABA		Abscissic acid
A	$\mu\text{mol m}^{-2} \text{s}^{-1}$	Net CO ₂ assimilation rate
a	‰	Discrimination during CO ₂ diffusion in boundary layer
ab	‰	Discrimination during CO ₂ diffusion in air
ai	‰	Discrimination during CO ₂ diffusion in liquid phase
A _j	$\mu\text{mol m}^{-2} \text{s}^{-1}$	CO ₂ assimilation rate limited by electrons transport rate
A _c	$\mu\text{mol m}^{-2} \text{s}^{-1}$	CO ₂ assimilation rate limited by RubisCO
b	‰	Discrimination during carboxylation
b ₃	‰	Discrimination during carboxylation of CO ₂ by RubisCO
b ₄	‰	Discrimination during carboxylation by of HCO ₃ ⁻ PEPc (including CO ₂ hydration fractionation)
b ₄ *	‰	Pure discrimination during carboxylation by of HCO ₃ ⁻ PEPc
β		Relative amount of carbon fixed by PEPc
C _a	$\mu\text{mol mol}^{-1}$	CO ₂ mole fraction in the atmosphere (arround the leaf)
C _c	$\mu\text{mol mol}^{-1}$	CO ₂ mole fraction in chloroplast
C _e	$\mu\text{mol mol}^{-1}$	CO ₂ mole fraction entering the photosynthesis chamber
C _i	$\mu\text{mol mol}^{-1}$	CO ₂ mole fraction in intercular air-space (sub-stomatal cavity)
C _o	$\mu\text{mol mol}^{-1}$	CO ₂ mole fraction leaving the photosynthesis chamber
δ ¹³ C	‰	Carbon isotopic composition
Δ ¹³ C	‰	Discrimination against ¹³ C during photosynthesis
e	‰	Discrimination during Rd
e'	‰	Discrimination during Rd corrected by Wingates et al. (2007)
eb	‰	Discrimination during dissolution of CO ₂ in water
es	‰	Discrimination during hydration of CO ₂ in HCO ₃ ⁻
f	‰	Discrimination during photorespiration
Γ*	$\mu\text{mol mol}^{-1}$	CO ₂ compensation point in absence of Rd
g _m	$\mu\text{mol m}^{-2} \text{s}^{-1}$	Mesophyll conductance to CO ₂
g _{sw}	$\mu\text{mol m}^{-2} \text{s}^{-1}$	Stomatal conductance to water vapour
g _s	$\mu\text{mol m}^{-2} \text{s}^{-1}$	Stomatal conductance to CO ₂
g _t	$\mu\text{mol m}^{-2} \text{s}^{-1}$	Total conductance to CO ₂
J	$\mu\text{mol m}^{-2} \text{s}^{-1}$	Electrons transport rate
J _{max}	$\mu\text{mol m}^{-2} \text{s}^{-1}$	Maximum electrons transport rate
k		Carboxylation efficiency
K _c		Michaelis-Menten constant for carboxylase
K _o		Michaelis-Menten constant for carboxylase and oxygenase
O	kPa	O ₂ partial pressure in the chloroplast
PEPc		phospho <i>enol</i> pyruvate carboxylase
PPFD	$\mu\text{mol m}^{-2} \text{s}^{-1}$	photosynthetic photon flux density
R _d	$\mu\text{mol m}^{-2} \text{s}^{-1}$	Non-photorespiratory respiration
RubisCO		ribulose-1,5-diphosphate carboxylase/ oxygenase
V _{cmax}	$\mu\text{mol m}^{-2} \text{s}^{-1}$	Maximal carboxylation rate

INTRODUCTION

A brief history

Carbon is present in the biosphere in the form of two stable isotopes, ^{12}C , the most abundant ($\approx 98.9\%$) and ^{13}C , less abundant (1.1%), as well as in the form of a radioactive isotope ^{14}C . The first data about the carbon isotope ratio ($^{13}\text{C}/^{12}\text{C}$) were reported at the end of the 30's by Nier and Gulbransen (1939). They observed that components like plants, atmospheric CO_2 or lime-stone have different isotope ratios. The development of isotope-ratio mass spectrometer, as they are known now, was initiated by Nier (1947), based on the observation that particles of ionized gas are deflected by a magnetic field with a curvature depending on their mass. Such devices rapidly allowed the study of isotopic abundance at a largest scale, and the first “screening” studies were published. Wickman (1952) and Craig (1953, 1954) measured carbon isotope ratios in several plants. They observed that the relative abundance of ^{13}C differed among plant species and habitats. The first important information was that plants are depleted in ^{13}C compared to the atmosphere, meaning that some discrimination occurs between the source of carbon (the atmosphere) and the product (plant material). In his paper of 1953, Craig identified a grass species with a clearly higher carbon isotope ratio (^{13}C enriched) compared to others species. He had actually found a C_4 species but was not aware of this carbon fixation pathway, and it would be another 10 years before the C_4 pathway was described (Kortschak *et al.*, 1965). After these first “screening studies”, Park and Epstein gave rise to another step in the knowledge of carbon fractionation in plants. Their work on tomato (Park and Epstein, 1960) first proposed an explanation for the ^{13}C depletion in plant tissues. They observed that overall discrimination against ^{13}C was the result of a first fractionation against ^{13}C during CO_2 transfer from the atmosphere to the cytoplasm, and a second fractionation occurring during fixation of dissolved CO_2 . One year later, they pioneered work of the fractionation during respiration, pointing out that respired CO_2 has a different isotopic ratio than plant tissues, and that such differences could be dependent on the respiratory substrate used by the plants (Park and Epstein, 1961). Thus by 1961 the main bases for carbon isotope fractionation in plants were identified, allowing latter the establishment of a general model. However, it was not until 1982 that Farquhar and colleagues established a mechanistic model of ^{13}C discrimination for C_3 plants (Farquhar *et al.*, 1982), based on the relationship between the ratio intercellular vs atmospheric CO_2 concentration (C_i/C_a) and the isotopic discrimination during photosynthesis. They demonstrated that the overall ^{13}C discrimination reflects the balance between carbon diffusion to the site of carboxylation and the process of carboxylation. The relative contribution of each

component (diffusion vs carboxylation) explains a large fraction of the variability of carbon isotope ratio in plants.

A model linking between ^{13}C discrimination and plant gas exchange

The model of discrimination of Farquhar *et al.* (1982) established a link between leaf gas exchange and discrimination against ^{13}C during the photosynthesis. Because of its easy use and high predictive power, this model was widely used to approximate plant water use efficiency (WUE) from the $\Delta^{13}\text{C}$ signal (Farquhar and Richards, 1984). WUE represents the amount of water consumed to fix a given amount of carbon, and is especially interesting for genetic selection of crop species or to assess changes in plant ecophysiology under natural conditions. WUE can be computed as the net assimilation rate of CO_2 divided by the transpiration rate ($\text{WUE}=A/E$). This ratio can be computed at the ecosystem scale, the entire plant, or at the leaf scale as well on several time scales (plant life span until instantaneous). Since E is partially controlled by environmental factors (VPD, water vapour pressure deficit), plant physiologists use preferentially stomatal conductance to focus on the genetic component of WUE and compare data from different environments. In this study we thus focused on intrinsic WUE ($W_i = A/g_s$) and its positive linear relationship with $\Delta^{13}\text{C}$ predicted by the discrimination model.

The model (in its simple form, see below for details) is based on the fact that both W_i and $\Delta^{13}\text{C}$ are related to C_i , the CO_2 mole fraction in the intercellular air-space. The $\Delta^{13}\text{C}$ - WUE relationship was observed in several trees at the intra-specific scale, like in *Quercus robur* (Ponton *et al.*, 2002; Roussel *et al.*, 2009), *Pinus pinaster* (Guehl *et al.*, 1995), and in others conifers (Cregg *et al.*, 2000; Grossnickle *et al.*, 2005; Zhang and Cregg, 1996) or deciduous (Lauteri *et al.*, 1997; Roupsard *et al.*, 1998;). The original formulation of the model predicts the relationship between W_i and $\Delta^{13}\text{C}$ discrimination at the instantaneous scale, but for convenience most studies used ^{13}C abundance in leaf tissues or even in tree rings. This integrates the $\Delta^{13}\text{C}$ signal more or less over the leaf life-span, and includes a number of compounds with different turn over rates in the leaves. This leads to a discrepancy in time scale integration between the isotopic signal and gas exchange records. $\Delta^{13}\text{C}$ can also be measured in soluble sugars extracted from leaves, integrating the signal over a few (1-2) days (Brugnoli *et al.* 1988), or on starch, integrating over tens of days (Roussel *et al.*, 2009; Scartazza *et al.*, 1998). These differences in time scale integration can loosen the W_i - $\Delta^{13}\text{C}$ relationship. Moreover, measuring $\Delta^{13}\text{C}$ from bulk leaf tissue introduces another source of variation. The different components of a leaf display different isotopic signatures, with

sugars, starch, protein and organic acids being less depleted compared to bulk leaf tissue, while lignin and lipids are more depleted (Bowling *et al.*, 2008). Thus, differences in the proportion of these components in tissues can create a variability of $\Delta^{13}\text{C}$ not related to the variability of gas exchange (W_i).

To avoid such sources of variability, some studies tested $\Delta^{13}\text{C}$ variations during gas exchange measurements at an instantaneous scale. Such direct estimates of $\Delta^{13}\text{C}$ during photosynthesis are recorded by comparing isotopic composition ($\delta^{13}\text{C}$) of a gas before and after passing over a photosynthesising leaf. This approach was developed by Evans *et al.* (1986) who observed that variations of leaf gas exchange (basically net CO_2 assimilation and stomatal conductance) were well correlated to variations of $\Delta^{13}\text{C}$ at instantaneous scale. Nevertheless, they observed that the recorded discrimination was different from that predicted by the $\Delta^{13}\text{C}$ model. This was interpreted as due to the fact that the discrimination model assumed that the CO_2 concentration in the intercellular air spaces (C_i) was the same that the one in the chloroplast stroma (C_c), i.e., that mesophyll conductance (g_m), which influence the CO_2 flow between C_i and C_c , was infinite. They consequently highlighted the importance of mesophyll conductance and decarboxylation processes occurring during photosynthesis, processes not accounted for in the simple (and most used) form of the $\Delta^{13}\text{C}$ model. Mesophyll conductance induces a drop of CO_2 mole fraction between the intercellular air-space (the sub-stomatal cavity) and the site of carboxylation and thus influences the discrimination by the leaf. Decarboxylation processes (“day respiration” and photorespiration) produce CO_2 with a different $\delta^{13}\text{C}$ from that in the atmosphere, also affecting the measured discrimination. All these components have to be considered to interpret $\Delta^{13}\text{C}$ measurements and their relationship with gas exchange. Conversely, the deviation of observed $\Delta^{13}\text{C}$ from that predicted by the simple model was used as a way to estimate g_m .

Since a few years, a new topic emerged in the estimation of mesophyll conductance and the interpretation of $\Delta^{13}\text{C}$ variations at the instantaneous scale: the assessment of rapid variations of g_m . Initially, g_m was considered to depend only on leaf structure, thus remaining constant in the short-term. Nevertheless, some studies suggested that g_m could vary rapidly under varying conditions (Lloyd *et al.*, 1992; Centritto *et al.*, 2003). Practically at the same time, other studies suggested g_m was influenced by protein activity, especially aquaporins – a group of proteins that facilitate trans-membrane water transport (Terashima and Ono, 2002). A number of subsequent studies have examined rapid variations of g_m with CO_2 or irradiance (see for a review Flexas *et al.* (2008)). Nevertheless, the rapid variations of g_m is nowadays

still under debate, regarding studies where g_m was found to be stable with CO_2 and irradiance (Tazoe *et al.*, 2009). Since g_m can be estimated from $\Delta^{13}\text{C}$ *via* the model of discrimination, that the parameterization of the model is still problematic and that the impact of the parameterization of this model was not examined thoroughly yet, it is therefore timely to perform global sensitivity analysis of the $\Delta^{13}\text{C}$ model and check whether variations of the different parameters could induce apparent artifactual rapid responses of g_m .

This work was focused on the measurement of leaf gas exchange coupled with online discrimination during photosynthesis to improve our understanding of the relationship between $\Delta^{13}\text{C}$ and leaf gas exchange. Initial experiments demonstrated that mesophyll conductance had the largest effect on the $\delta^{13}\text{C}$ -WUE relationship, and thus we concentrated on the estimation of g_m and its ability to change with environmental conditions at the short-term scale. We estimated the influence of “day respiration” and that of photorespiration during photosynthesis on g_m estimation. We used variations of irradiance and CO_2 mole fraction to assess rapid variations of mesophyll conductance and variations of O_2 mole fraction in the air to change the influence of photorespiration. This work was carried out on four tree species (three Eucalypts and one Poplar) to extend the range of species tested. We addressed several questions:

- How sensitive is $\Delta^{13}\text{C}$ to the different parameters of the discrimination model? As a more specific question we will also address this for the estimation of g_m with the isotopic method.
- Does g_m respond to short term changes of CO_2 concentration and of irradiance in different species?
- Does accounting for the respiratory term change our estimates of g_m and their responses to CO_2 and irradiance variations, and does the presence or absence of photorespiration alter the response to irradiance?

*This manuscript is organized in four chapters: in **Chapter I** we will provide a full description of the $\Delta^{13}\text{C}$ model, a sensitivity analysis to highlight the respective influence of each parameter, and we will discuss the likely occurrence of rapid variations of each parameter under varying irradiance and CO_2 , in **Chapter II** we provide estimates of g_m under varying CO_2 and irradiance for three eucalypts species and check the importance of the respiratory term, in **Chapter III** we estimate variations of g_m with irradiance under high and low O_2 to*

vary the influence of photorespiration, and finally in **Chapter IV**, we perform estimations of g_m in three poplar clones under varying CO_2 and irradiance, and discuss the effects of a stable or a varying g_m on net CO_2 assimilation rates. In **Annex I**, we present the gas exchange systems used to provide data.

CHAPTER I

**Relationship between ^{13}C discrimination and leaf gas exchange:
Analysis of the model, influence of the parameters and
implications for estimating mesophyll conductance to CO_2 .**

INTRODUCTION

In the early 80's, a robust model based on a semi-mechanistic approach established for C_3 plants the relationship between discrimination against ^{13}C during photosynthesis ($\Delta^{13}\text{C}$) and leaf gas exchange (basically net CO_2 assimilation rate, A , and stomatal conductance to water vapour, g_{sw}) (Farquhar *et al.* 1982). This model in its complete form is based on the fact that the overall observed discrimination is the result of fractionation steps due to diffusion, carboxylation and decarboxylation processes, while under a simple form it ignores the decarboxylation processes and the influence of mesophyll conductance (g_m). $\Delta^{13}\text{C}$ predicted by the simple model (Δ_i) is computed as:

$$\Delta_i = a + (b - a) \frac{C_i}{C_a} \quad \text{Eq. 1}$$

with C_a the CO_2 mole fraction in the atmosphere, a is the fractionation during CO_2 diffusion in air and b the fractionation during carboxylation by RubisCO and phosphoenolcarboxylase (PEPc) (see detailed equations below). This mechanistic model predicts that higher CO_2 availability inside the leaf (i.e. higher C_i/C_a) leads to a larger discrimination against ^{13}C . Beyond the simple need to understand the variability of ^{13}C abundance in plants, some authors established a relationship between $\Delta^{13}\text{C}$ and water use efficiency (WUE), which is the ratio of the amount of carbon fixed to the amount of water consumed (Farquhar and Richards, 1984). WUE can be assessed at different spatial (ecosystem, whole plant or leaf) and temporal (leaf life-span or instantaneous) scales, but we will focus here at the leaf level and the instantaneous scale. Intrinsic water use efficiency ($W_i = A/g_s$) is a computation of WUE independent from VPD (vapour pressure deficit), allows to compare studies between themselves. W_i is related to $\Delta^{13}\text{C}$ by:

$$W_i = \frac{A}{g_{sw}} = \frac{C_a}{1.6} \frac{b - \Delta_i}{b - a} \quad \text{Eq. 2}$$

and reciprocally:

$$\Delta_i = b - \frac{W_i(1.6(b - a))}{C_a} \quad \text{Eq. 3}$$

where A is the net CO_2 assimilation rate and g_{sw} the stomatal conductance for water vapour; the term 1.6 accounts for the lower diffusivity of CO_2 compared to water vapour.

Assessing the temporal, phenotypic and possibly genetic variability of intrinsic water use efficiency (W_i) was the first main use of monitoring carbon isotope discrimination. Screening studies for genetic variability were used for selecting efficient crops in terms of

water consumption in regards of carbon gain (Farquhar and Richards, 1984). The large majority of studies used $\Delta^{13}\text{C}$ based on leaf bulk biomass to assess W_i integrated over the leaf life span. The relationship was tested among genotypes in many species including conifers, deciduous and evergreen broad-leaved trees and annuals, or under varying water, nutrient or light availability. Nevertheless, the use of leaf bulk tissue complicates our ability to relate $\delta^{13}\text{C}$ to leaf gas exchange. $\delta^{13}\text{C}$ of bulk tissues is an average of the $\delta^{13}\text{C}$ of the different components of the leaf. Since lignin and lipids are ^{13}C depleted, and sugars, starch and cellulose are enriched relative to bulk (Bowling *et al.*, 2008), the proportion of these components induces a variability of $\Delta^{13}\text{C}$ not related to gas exchange. Secondly, it is sometimes difficult to relate a $\Delta^{13}\text{C}$ signal integrated over several weeks, months or years (for conifers) with instantaneous gas exchange measurements. The difference in time scale integration could induce another bias in the $\Delta^{13}\text{C}$ - W_i relationship. Finally, the simple and most common form of the discrimination model (described above), is based on correlation of W_i and $\Delta^{13}\text{C}$ with CO_2 mole fraction in intercellular air-spaces (or sub-stomatal cavity, C_i). It is now accepted that mesophyll conductance (g_m) decreases CO_2 mole fraction in the chloroplast (C_c) compared to C_i . Since the fully developed model of $\Delta^{13}\text{C}$ is then related to C_c , not accounting for the difference between C_i and C_c possibly induces another bias in the $\Delta^{13}\text{C}$ - W_i relationship (Warren and Adams, 2006).

In this study, we firstly report W_i - $\Delta^{13}\text{C}$ relationships described in the literature to evidence the variability of this relationship, and then attempt to identify the sources of this variability (i.e. the parameters that influence the model). We then describe the “complete form” of the discrimination model and the different values found in the literature for each parameter of the model. We perform a sensitivity analysis of the $\Delta^{13}\text{C}$ model to quantify the potential effect of the variability of each parameter for the estimates of $\Delta^{13}\text{C}$. We then centre the next part of this study on the estimation of mesophyll conductance with online discrimination (instantaneous measurements), with a sensitivity analysis of the g_m estimation. Then, for each parameter we test the effect of using several values comprised in the range found in the literature on the g_m estimation, changing one parameter at a time, or two parameters to explore the “cumulative effect”. We analyse data of the response of g_m to irradiance in *Eucalyptus sieberi* (Douthe *et al.*, *in press*), and test whether rapid variations of other parameters could induce variations of $\Delta^{13}\text{C}$ independently of g_m . We explore the effect of other sources of variations and their potential effect on other parameters in the model, like

variations of O_2 , known to change the rate of photorespiration, and O_3 , suspected to change the relative amounts of RubisCO vs PEPc carboxylation.

Diversity of the W_i - $\Delta^{13}C$ relationships found in the literature

We provide here a comparison of 23 W_i - $\Delta^{13}C$ relationships from 16 studies (Table 1 and Figure 1, upper panel). The selection of data was restricted to tree species.

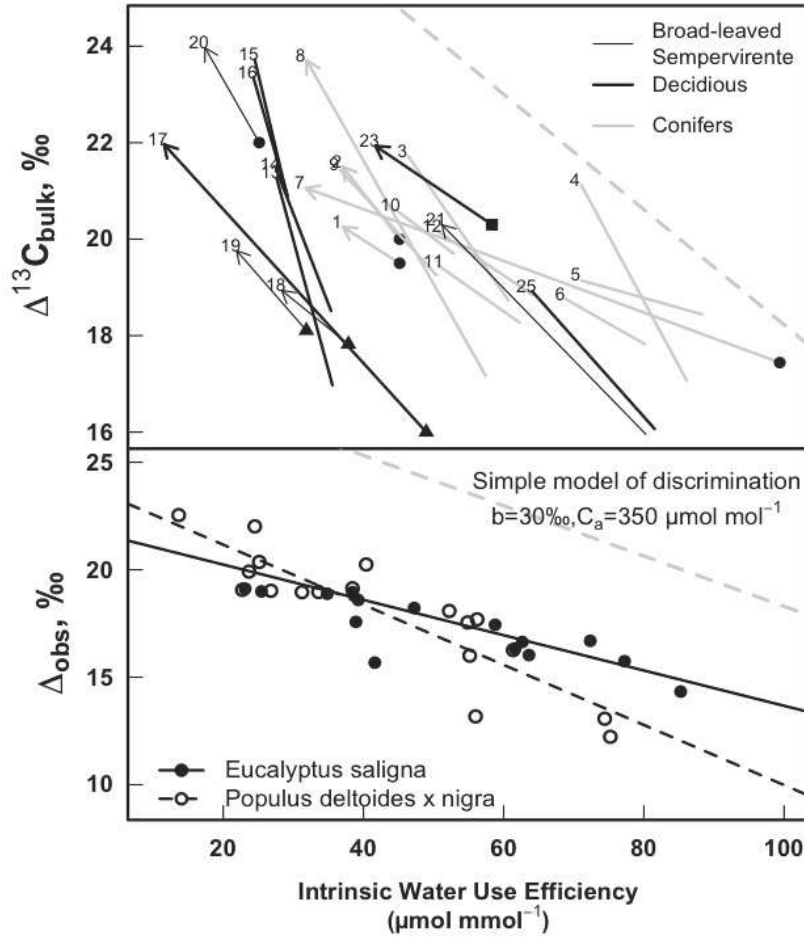


Figure 1: Upper panel: relationships between intrinsic water use efficiency (W_i) calculated with A/g_{sw} in $\mu\text{mol CO}_2 \text{ mol}^{-1} \text{ H}_2\text{O}$ and $\Delta^{13}C$ (in ‰) measured on leaf bulk biomass. Each line is a relationship of mean values induced by genetic (clones, populations or seed source) variations, except n°8 and 21 with genetic and drought confounded. Each arrow is a relationship induced by environmental variations, with the symbol at the beginning of the arrow determining the type of environmental variation (square for drought, circle for fertility and triangle for light). The direction of the arrow indicates from high to low drought or fertility or shade. Each number corresponds to the “ID” column in Table 1. Thick black line/arrow is for broad-leaved deciduous, thin black line/arrow is for broad-leaved sempervirent trees and grey line/arrow for conifers. The dashed grey line is the relationship predicted by the simple Farquhar model of discrimination (Eq. 3), with $b=30\text{‰}$ and $C_a=400 \mu\text{mol mol}^{-1}$.

Lower panel: W_i - $\Delta^{13}\text{C}$ measured with online discrimination on *Eucalyptus saligna* plants (filled circle, each is an average of $\Delta^{13}\text{C}$ and W_i recorded during 15 min) and *Populus deltoides x nigra* cuttings (empty circle, each is an average of $\Delta^{13}\text{C}$ and W_i recorded during 30-45 min). Irradiance was used to induce variations in $\Delta^{13}\text{C}$ and W_i , under 21% O_2 . $\Delta^{13}\text{C}$ was recorded with a calibrated tunable diode laser absorption spectrometer (TDL-AS) coupled to a gas exchange system. The dashed grey line is the relationship predicted by the simple model of discrimination (Eq. 3), with $b=30\text{‰}$ and $C_a=350 \mu\text{mol mol}^{-1}$ (i.e. the averaged C_a during the experiments).

The range of variation was from 10 to 110 $\mu\text{mol CO}_2 \text{ mol}^{-1} \text{ H}_2\text{O}$ for W_i , and from 16 to 24‰ for $\Delta^{13}\text{C}$. We collected data from studies presenting data of W_i (or A and g_{sw}) and isotopic discrimination performed from leaf bulk tissue. The very large majority of studies assumed $\delta^{13}\text{C}_{\text{air}}$ to be -8‰; when not indicated otherwise we assumed this value to recalculate $\Delta^{13}\text{C}$ from leaf bulk $\delta^{13}\text{C}$. In all studies there was a negative relationship between $\Delta^{13}\text{C}$ and W_i , as predicted by the model, but there was a very large diversity in slopes (from -0.03 to -0.52) and intercepts (from 21.2 to 39.9‰) of the W_i - $\Delta^{13}\text{C}$ relationship (see Table 1). The majority of broad-leaved trees presented values of W_i between 20 and 60 $\mu\text{mol CO}_2 \text{ mol}^{-1} \text{ H}_2\text{O}$ while conifers presented higher values, between 50 and 100 $\mu\text{mol CO}_2 \text{ mol}^{-1} \text{ H}_2\text{O}$. On the other hand, the whole range of $\Delta^{13}\text{C}$ was covered by both tree types. In all studies, the observed $\Delta^{13}\text{C}$ for a given W_i was systematically lower than predicted by the model.

The shift between predicted and measured $\Delta^{13}\text{C}$ was as large as 8‰ in some studies (Ponton *et al.* 2002). The large range of $\Delta^{13}\text{C}$ found for a given W_i and the systematic shift with the predicted $\Delta^{13}\text{C}$ can be explained by several hypotheses: (i) some fractionations steps and model parameters are not accounted for in the simple form of the model, (ii) differences in the time scale integration between W_i and $\Delta^{13}\text{C}$, or (iii) variability in $\Delta^{13}\text{C}$ due to varying leaf composition (e.g. lignin, lipids *etc.*).

- (i) since the simple form of the $\Delta^{13}\text{C}$ model ignores the influence of g_m ($C_i > C_c$), this model should in theory overestimate $\Delta^{13}\text{C}$ compared to the complete form. This rationale fits with the observed data (observed $\Delta^{13}\text{C} < \Delta_i$).
- (ii) the difference in time scale integration could also create a bias in the $\Delta^{13}\text{C}$ - W_i relationship, since instantaneous measurements of W_i do not reflect all variations over leaf –life-span integrated by the observed $\Delta^{13}\text{C}$ signal. We can note that this factor could either under or over-estimate $\Delta^{13}\text{C}$ for a given W_i .
- (iii) the $\delta^{13}\text{C}$ of the different leaf components tends to decrease the observed $\Delta^{13}\text{C}$ compared to that only influenced by W_i . Indeed, if we consider that $\delta^{13}\text{C}$ of

soluble sugars is closely related to short-term integrated gas exchange (Brugnoli *et al.* 1988), the proportion of others components in the leaf (lignin, lipids, proteins, cellulose etc..) and their respective $\delta^{13}\text{C}$ will decrease the observed $\Delta^{13}\text{C}$ by $\approx 1\text{‰}$ compared to that of soluble sugars (from data provided in Bowling *et al.* 2008), and thus the instantaneous $\Delta^{13}\text{C}$. This difference could partially explain the shift observed in our data (Figure 1).

When W_i and $\Delta^{13}\text{C}$ were recorded instantaneously and in parallel (Figure 1, lower panel) we still found an equivalent shift between measured and predicted $\Delta^{13}\text{C}$. This shows that the artefacts described above about integration time and leaf composition were probably not the main cause of the discrepancy. To take into account this shift, we have to account for more discriminating steps and for the fact that due to finite g_m , C_i differs from C_c , and thus use the complete version of the discrimination model.

Table 1: Slopes and intercepts of the W_i - $\Delta^{13}C$ relationship described in sixteen studies. The column “ID” identifies curves of Figure 1, the column “Source” describes the source of variation used to establish the W_i - $\Delta^{13}C$ relationship. In the column “Functionnal group”, deciduous and sempervirente refers to broad-leaved trees. The column “Case” precises different conditions used in the same study: for Boucher *et. al*, 1998 the measurement were performed at two different dates, for Cregg *et. al*, 2000 the comparative plantation was repeated in two different sites, and for Dawson *et. al*, 2004 the W_i - $\Delta^{13}C$ relationship was established for Male and Female trees, under two water regimes.

ID	study	source	species	functional group	Case	Slope	Intercept
1	Boucher <i>et. al</i> , 1998	silviculture	<i>Pinus strobus</i>	conifer	June	-0.15	27.46
2	Boucher <i>et. al</i> , 1998	silviculture	<i>Pinus strobus</i>	conifer	October	-0.17	29.14
3	Cregg <i>et. al</i> , 2000	provenance	<i>Pinus ponderosa</i>	conifer	Plattmouth	-0.17	31.12
4	Cregg <i>et. al</i> , 2000	provenance	<i>Pinus ponderosa</i>	conifer	Norman	-0.23	39.88
5	Grossnickel <i>et. al</i> , 1998	clones	<i>Picea glauca x engelmannii</i>	conifer		-0.03	21.98
6	Grossnickel <i>et. al</i> , 2005	provenance	<i>Thuja plicata</i>	conifer		-0.07	24.35
7	Guehl <i>et. al</i> , 1995	fertilization	<i>Pinus pinaster</i>	conifer		-0.04	22.28
8	Olivas-Garcia <i>et. al</i> , 2000	water+seed source	<i>Pinus ponderosa</i>	conifer		-0.21	31.5
9	Zhang <i>et. al</i> , 1994	families	<i>Larix occidentalis</i>	conifer		-0.13	27.03
10	Sun <i>et. al</i> , 1996	genetic	<i>Picea glauca</i>	conifer		-0.09	25.38
11	Zhang <i>et. al</i> , 1995	genetic	<i>Pinus ponderosa</i>	conifer		-0.08	24.48
12	Zhang <i>et. al</i> , 1995	genetic	<i>Psedotuga menziesii</i>	conifer		-0.08	24.94
13	Dawson <i>et. al</i> , 2004	genotype	<i>Acer negundo</i>	deciduous	Male watered	-0.46	35.38
14	Dawson <i>et. al</i> , 2004	genotype	<i>Acer negundo</i>	deciduous	Male droughted	-0.32	31.22
15	Dawson <i>et. al</i> , 2004	genotype	<i>Acer negundo</i>	deciduous	Female watered	-0.52	37.90
16	Dawson <i>et. al</i> , 2004	genotype	<i>Acer negundo</i>	deciduous	Female droughted	-0.43	34.88
17	Ponton <i>et. al</i> , 2002	shading	<i>Quercus robur</i> , <i>Q. petraea</i>	deciduous		-0.13	23.57
23	Sullivan <i>et. al</i> , 2007	site drought	<i>Salix arctica</i>	deciduous		-0.08	25.88
25	Roussel <i>et. al</i> , 2009	genetic	<i>Quercus robur</i>	deciduous		-0.14	29.15
18	Carelli <i>et. al</i> , 1999	shading	<i>Coffea arabica</i>	sempervirente		-0.10	22.09
19	Carelli <i>et. al</i> , 1999	shading	<i>Coffea cenaphora</i>	sempervirente		-0.14	23.16
20	Cernusak <i>et. al</i> , 2007	fertility	<i>Ficus insipida</i>	sempervirente		-0.21	28.02
21	Meinzer <i>et. al</i> , 1990	water+genotypes	<i>Coffea arabica</i>	sempervirente		-0.128	27.73

Using the complete form of the discrimination model

To take into account fractionation steps and processes neglected in the simple model, a more detailed model was developed by Farquhar *et al.* (1982). This model for $\Delta^{13}\text{C}$ accounts for mesophyll conductance (g_m) and the influence of decarboxylation processes due to photorespiration as well as respiration. The complete model for $\Delta^{13}\text{C}$ is computed following Evans *et al.* (1986) and Farquhar *et al.* (1982):

$$\Delta = a_b \frac{C_a - C_s}{C_a} + a \frac{C_s - C_i}{C_a} + (e_s + a_i) \frac{C_i - C_c}{C_a} + b \frac{C_c}{C_a} - \frac{\frac{eR_d}{k} + f\Gamma^*}{C_a} \quad \text{Eq.4}$$

where a_b is the discrimination due to diffusion in the boundary layer, e_s and a_i the discrimination due to dissolution and diffusion in the liquid phase, respectively, e and f the discrimination during “dark respiration” (R_d) and photorespiration, respectively and k the carboxylation efficiency ($k=(A+R_d)/(C_i-\Gamma^*)$) following (Farquhar *et al.*, 1982). This model predicts a smaller discrimination than the simple formulation due to: (i) the CO_2 draw-down between the intercellular air-space and the site of carboxylation (i.e., the influence of g_m) and (ii) the decarboxylation processes. Because some fractionation occurs during R_d and the photorespiration, the respired CO_2 has a different isotopic signature than the respiratory substrate. This shift has to be accounted for to fully explain the observed $\Delta^{13}\text{C}$. A global representation of the different carbon flows and associated fractionation factors described here is shown in Figure 2. The main problem of using this model is the parameterization, i.e., choosing the real value for each parameter. For most of the parameters, especially b , e and f , we do not know with certainty their absolute value or if they vary among genotypes or with environmental conditions. We provide here the range of values found in the literature. These values were used afterwards to set the sensitivity analysis (see Table 2).

Figure 2: Schematic representation of the different carbon fluxes and discrimination against ^{13}C in a leaf during photosynthesis. In blue are represented the carbon molar fractions (in $\mu\text{mol mol}^{-1}$) the atmosphere (C_a), the boundary layer (C_s), the intercellular air-space (C_i) and the chloroplast (C_c). In red are represented the different $^{13}\text{C}/^{12}\text{C}$ fractionation factors (in ‰) associated to CO_2 gaseous diffusion in the boundary layer (ab), in air through the stomata (a), CO_2 hydration in HCO_3^- (e_s), CO_2 diffusion in liquid phase (a_i), carboxylation by RubisCO (b_3) and by PEPc (b_4^*), during decarboxylation of glycine in serine (f) and to non-photorespiration decarboxylation (e)

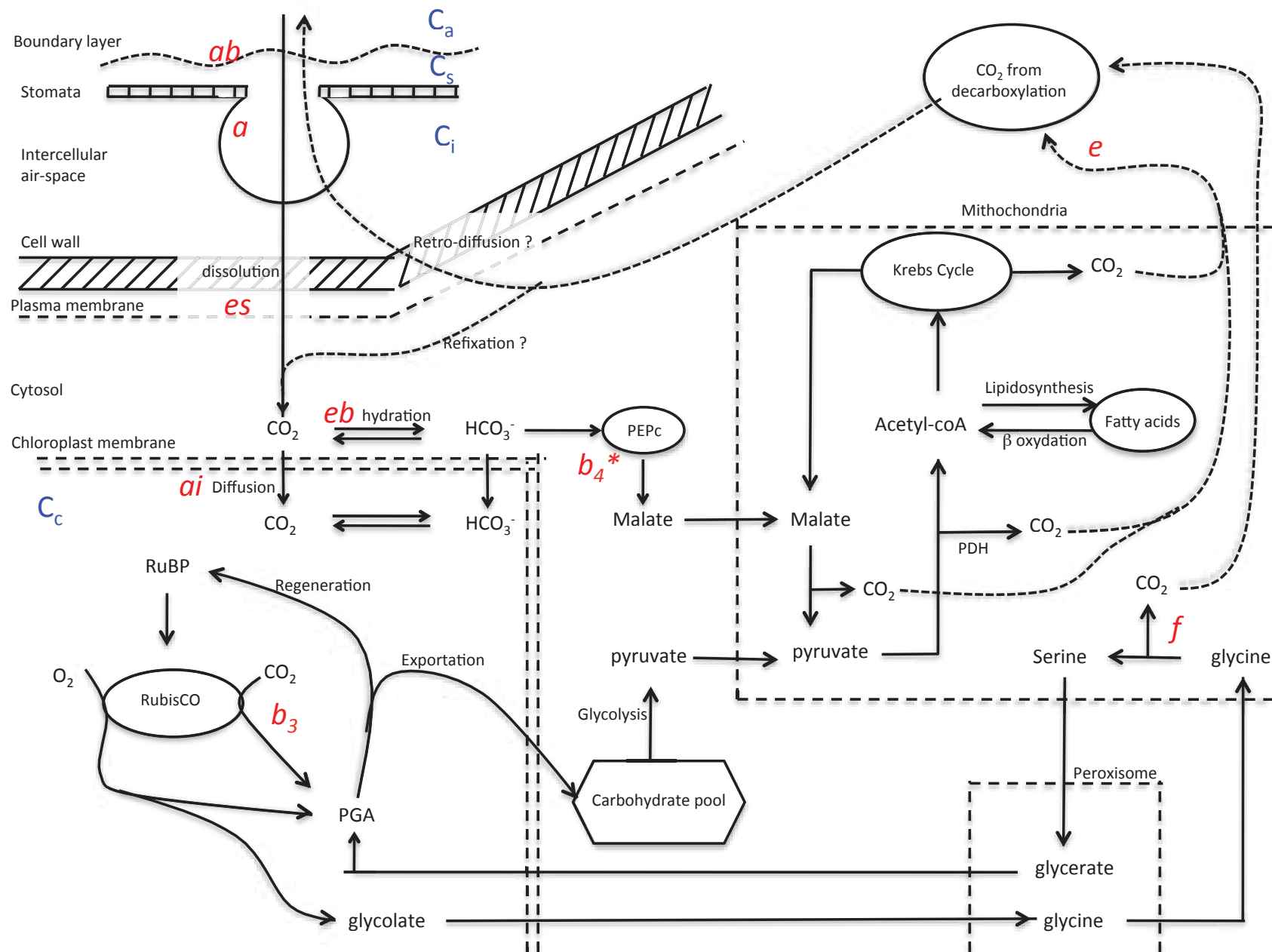


Table 2: Non-exhaustive list for parameters values of the Farquhar model of discrimination found in the literature

Parameter	Description	Value or range	Species	Conditions	Study	Remark
a (in ‰)	Gaseous diffusion of CO ₂	4.4			(Craig, 1954)	cited by (O'Leary, 1981)
a_b (in ‰)	Gaseous diffusion of CO ₂ in boundary layer	2.9			(Vogel, 1980)	cited by (Farquhar <i>et al.</i> , 1989)
a_i (in ‰)	Diffusion of CO ₂ in the liquid phase	0.7			(O'Leary, 1984)	cited by (Farquhar <i>et al.</i> , 1989)
b_3 (in ‰)	Fractionation during carboxylation by RubisCO	29.7 ± 0.8	<i>Spinacea oleracea</i>	25°C, pH=7	(Roeske and O'Leary, 1984)	cited by (McNevin <i>et al.</i> , 2006)
		29 ± 1	<i>Spinacea oleracea</i>	25°C, pH=8	(Roeske and O'Leary, 1984)	
		26.4 ± 0.6	<i>Spinacea oleracea</i>	25°C, pH=9	(Roeske and O'Leary, 1984)	
		29.0 ± 0.3	<i>Spinacea oleracea</i>	pH=7.6	(Guy <i>et al.</i> , 1993)	
		30.3 ± 0.8	<i>Spinacea oleracea</i>	pH=8.5	(Guy <i>et al.</i> , 1993)	
		26.2–29.8	<i>Spinacea oleracea</i>	24°C, pH=8.5	(Scott <i>et al.</i> , 2004)	
		28.9±1.5	<i>Spinacea oleracea</i>	25°C	(McNevin <i>et al.</i> , 2006)	
		27.4±0.9	<i>Nicotiana tabacum</i>	25°C, pH=8	(McNevin <i>et al.</i> , 2007)	
b_4 (in ‰)	Fractionation during carboxylation by PEPc	2.6 ± 0.2	<i>Zea mays</i>	25°C	(McNevin <i>et al.</i> , 2006)	cited by (McNevin <i>et al.</i> , 2006)
		2.7 ± 4.4	<i>Sorghum bicolor</i>	24°C, pH=8.5	(Whelan <i>et al.</i> , 1973)	
		2.03	<i>Zea mays</i>	25°C, pH=7.5	(Reibach and Benedict, 1977)	
		2.9 ± 0.5	<i>Zea mays</i>	25°C, pH=7.5	(O'Leary <i>et al.</i> , 1981)	
e_s (in ‰)	Fractionation during dissolution of CO ₂ in water	1.1			(Vogel, 1980)	cited by (Evans <i>et al.</i> , 1986)
		1.06		25°C	(Mook <i>et al.</i> , 1974)	
eb (in ‰)	Fractionation during hydration of aqueous CO ₂	-8.97		25°C	(Mook <i>et al.</i> , 1974)	from -12‰ at 0°C to -8.42‰ at 30°C
e (in ‰)	Fractionation during respiration (R _d , measured in the dark)	-8.1 to +10.3	15 species	Several assumed respiratory substrates	from a review by Ghashghaie <i>et al.</i> (2003)	cited by (Ghashghaie <i>et al.</i> , 2003)
		-2.5	<i>Helianthus annuus</i>	Leaf sucrose	(Ghashghaie <i>et al.</i> , 2001)	
		-3.0	<i>Nicotiana sylvestris</i>	Leaf sucrose		
		14 to -4	<i>Helianthus annuus</i>	Leaf organic matter, temperature	(Ghashghaie <i>et al.</i> , 2003)	
			<i>Nicotiana sylvestris</i>			
			<i>Helianthus annuus</i>	from 10°C to 30°C.		
		-5.8	<i>Phaseolus vulgaris</i>	Leaf sucrose	(Duranceau <i>et al.</i> , 1999)	
		-4.5	<i>Phaseolus vulgaris</i>	Leaf sucrose	(Barbour <i>et al.</i> , 2007)	
	Fractionation during respiration (R _d , estimated)	-0.2 to -0.8	<i>Helianthus annuus</i>	mesocosm level	(Tcherkez <i>et al.</i> , 2010)	

in the light)					
R_d (in $\mu\text{mol m}^{-2} \text{s}^{-1}$)	Non-photorespiratory respiration (measured in the dark)	0.5 to 2	<i>Helianthus annuus</i> <i>Nicotiana sylvestris</i> <i>Helianthus annuus</i>	10°C to 30°C	(Ghashghaie <i>et al.</i> , 2003)
		0.4 to 1.6	<i>Phaseolus vulgaris</i>	10°C to 30°C	(Tcherkez <i>et al.</i> , 2003)
		0.6	<i>Eucalyptus pauciflora</i>	25°C, PPFD from 200 to 2000 $\mu\text{mol m}^{-2} \text{s}^{-1}$	(Atkin <i>et al.</i> , 2000) Laisk method
	Non-photorespiratory respiration (estimated in the light)	0.6 ± 0.1	<i>Phaseolus vulgaris</i>	20°C, 450 $\mu\text{mol m}^{-2} \text{s}^{-1}$ PPFD	(Tcherkez <i>et al.</i> , 2005) ^{13}C labelling
		0.7 ± 0.2	<i>Eucalyptus regnans</i>	25°C	(Warren, 2008a) Laisk method
		0.73 ± 0.07	<i>Solanum lycopersicum</i>	25°C	(Warren, 2008b) Laisk method
		0.46 ± 0.06	<i>Phaseolus vulgaris</i>	25°C	(Warren, 2008b) Laisk method
		0.6 ± 0.1	<i>Eucalyptus regnans</i>	25°C	(Warren, 2008b) Laisk method
		0.41±0.09	<i>Eucalyptus globulus</i>	25°C	(Douthe <i>et al.</i> , 2011) Laisk method
		0.31±0.09	<i>Eucalyptus saligna</i>	25°C	(Douthe <i>et al.</i> , 2011) Laisk method
		0.68±0.07	<i>Eucalyptus sieberi</i>	25°C	(Douthe <i>et al.</i> , 2011) Laisk method
		8 to +16	Seven species	Several reactants	(Ivlev <i>et al.</i> , 1996) Large variability induced by the different reactants
	f (in ‰)	0.5	<i>Triticum aestivum</i>		(Gillon and Griffiths, 1997) cited by (Ghashghaie <i>et al.</i> , 2003)
		2	<i>Phaseolus vulgaris</i>		(Gillon and Griffiths, 1997)
		8	<i>Triticum aestivum</i> <i>Phaseolus vulgaris</i>		(Gillon, 1997)
		7	<i>Glycine max</i>		(Rooney, 1988)
		11.6	Three species		(Lanigan <i>et al.</i> , 2008) Determined from a statistical approach
		11			(Tcherkez, 2006) Determined from a theoretical approach
Γ^* (in $\mu\text{mol mol}^{-1}$)	CO_2 compensation point in absence of R_d	33 to 48.4	18 species	25°C	(Evans and Loreto, 2000) Several methods (values not corrected for g_m)
		37.43	<i>Nicotiana tabacum</i>	25°C	(Bernacchi <i>et al.</i> , 2002) O^{18} method
		48.8±2.1	<i>Juglans regia</i>	25°C, sun leaves	(Piel <i>et al.</i> , 2002) Laisk method
		49.4±2.7	<i>Juglans regia</i>	25°C, shade leaves	
		35 to 42.3	four species	25°C	(Pons and Westbeek, 2004) Laisk method
		38.6	<i>Spinacea oleracea</i>	25°C	(Von Caemmerer <i>et al.</i> , 1994) Isotopic method

Diffusion of CO₂ from the atmosphere to the chloroplast

The fractionation factor for diffusion in the air (a in ‰, see Table 2) is assessed from theoretical assumptions. Discrimination during CO₂ diffusion in air occurs because gas diffusion in air is modulated by the ratio of molar masses of ¹²CO₂ and ¹³CO₂ (see O'Leary, 1981 and Farquhar *et al.* 1982). Because ¹³CO₂ is heavier than ¹²CO₂ (molar masses of 45 and 44, respectively), the subsequent difference of diffusion leads to a discrimination (against ¹³CO₂) of 4.4‰ during diffusion in the air. This estimation was taken as discrimination factor for gas diffusion by Farquhar *et al.* (1982) in their model. Such a relationship is not likely to vary with temperature, pressure or CO₂ mole fraction (O'Leary, 1981). The parameter a in the model is therefore considered constant and independent of environmental conditions and genotypes.

Fractionation associated to dissolution of gaseous CO₂ in water (parameter es) was estimated to be 1.1‰ (Evans *et al.*, 1986), based on Vogel (1980). This corroborates an estimation by (Mook *et al.*, 1974) with $es=1.06$ ‰ at 25°C, where $\delta^{13}\text{C}$ was measured before and after dissolution. This fractionation factor is relatively insensitive to temperature and varies from 1.18‰ to 1.04‰ between 0°C and 30°C (Mook *et al.*, 1974).

Once dissolved, CO₂ has to diffuse in the liquid phase to the chloroplast stroma, with a fractionation factor ai . Reported estimations of ai are rare, but (Evans *et al.*, 1986) set $ai=0.7$ ‰ based on previous estimations from O'Leary (1984). However, the hydrated form (HCO₃⁻) diffuses faster in the liquid phase than the molecular form CO₂.

Hydration of aqueous CO₂ induces a fractionation of -9‰ at 25 °C (Mook *et al.*, 1974), leading to an overall hydration fractionation with respect to gaseous CO₂ of -7.9‰, the negative sign meaning ¹³C accumulation in HCO₃⁻. This parameter is not directly visible in Eq. 4, because it is associated with fractionation by phosphoenolpyruvate carboxylase (PEPc) fixation (see below).

Discrimination during carboxylation

Since the early 60's, it has been proposed that CO₂ fixation causes the largest discrimination in plants (Park and Epstein, 1960). Fractionation by carboxylation is noted b in the discrimination model. Two main enzymes are involved in the fixation of carbon in C₃ plants: RubisCO that fixes CO₂ in the chloroplast stroma and PEPc

that fixes HCO_3^- in the cytosol (see Figure 2), with fractionation factor b_3 for RubisCO and b_4 for PEPc. For b_3 , a review by O'Leary (1981) reported *in vitro* estimations around 30‰, but specified that there is a large uncertainty. A recent study reported very close values for purified RubisCO from tobacco, with $b_3=27.4\pm0.9\text{‰}$ (McNevin *et al.*, 2007). They compared their values with other published estimations and found a range from 27.5‰ to 29‰ (data for spinach and soybean), with respect to dissolved CO_2 . When expressed with respect to gas phase CO_2 , this leads to $b_3=28.5\text{‰}$ to 30‰, with upper and lower SDs covering a range from 26‰ to 30.5‰.

Fractionation by PEPc (noted b_{4*} in Farquhar *et al.*, 1989) is much smaller than by RubisCO, with b_{4*} between 2 and 2.5‰ (O'Leary, 1981), considering HCO_3^- as the main substrate. These estimations were recently confirmed, with $b_{4*}=2.6\pm0.2\text{‰}$ (McNevin *et al.* 2006), by monitoring CO_2 isotope concentrations *via* membrane inlet mass-spectrometer in a cuvette with carboxylating PEPc and the basic form of the Rayleigh equation. Usually, the term b_{4*} is expressed with respect to gas-phase CO_2 , taking into consideration the fractionation due to hydration of CO_2 (-7.9‰), thus $b_4=-5.7\text{‰}$ (Farquhar, 1983).

The relative amount of carbon fixed by PEPc is noted β , then b is:

$$b = \beta b_4 + (1 - \beta) b_3 \quad \text{Eq. 5}$$

It is well known that RubisCO fixes the largest amount of carbon in leaves, but the proportion fixed by PEPc and the exact value of β are uncertain. It is usually set between $\beta=0.05$ (i.e., 5% carbon fixed by PEPc) (Evans *et al.*, 1986), and $\beta=0.1$ (Farquhar and Richards, 1984). A few studies have estimated β , using indirect measurements. Most estimates originate from measurements of the ratio of enzyme activities as a proxy for the relative amount of carbon fixed. PEPc activity was found to be 2% to 4% relative to that of RubisCO in wheat (Von Caemmerer and Evans, 1991), 0.6% in *Betula pendula* (Saurer *et al.*, 1995), 10% in *Populus tremula* x. *Populus alba* (clone INRA 717-1B4) (Bagard *et al.*, 2008). Vu *et al.* (1985) obtained an upper value of 13% in *Citrus sinensis*. Holbrook *et al.* (1984) using ^{14}C labeling observed that less than 5% of the assimilated $^{14}\text{CO}_2$ was present in C_4 acids (malate and aspartate, metabolites related to the PEPc pathway). All these values lead to an average 5% of carbon fixed by PEPc, with possible interspecific variations.

To the best of our knowledge, no study tested the variability of β under changing irradiance or CO_2 , (the sources of variations we are interested by in this

study) and β is always considered stable during measurements. However, we can note that studies on ozone fumigation noted modification of both RubisCO and PEPC enzymatic activities, with a decrease of RubisCO and an increase of PEPC activity (Saurer *et al.*, 1995; Dizengremel, 2001; Bagard *et al.*, 2008).

Discrimination during “day respiration”

The term “dark” respiration, noted R_d in the discrimination model, represents the non-photorespiratory respiration by the leaf. When a carbohydrate enters the glycolytic pathway, it produces pyruvate which is decarboxylated into Acetyl-coA by the pyruvate dehydrogenase (PDH), resulting in a release of CO_2 (see Figure 2). Then Acetyl-coA can feed the lipid biosynthesis pathway, or enter the Krebs cycle (or tricarboxylic acid cycle, TCA) releasing again CO_2 . These metabolic pathways are fully functional during the night, but partially inhibited during the day (under light). Inhibition by light varies around 50% (53% in *Phaseolus vulgaris*, Tcherkez *et al.*, 2005, 66% in *Populus koreana x trichocarpa* cv Peace, Piel 2002 PhD thesis; $\approx 45\%$ at 25% in *Eucalyptus pauciflora*, Atkin *et al.*, 2000)). Tcherkez *et al.* (2005) evidenced that such a reduction in R_d was due to a 95% inhibition of the Krebs cycle activity, while the PDH was less affected (27% reduction) in light compared to dark. The inhibition under light of R_d can occur at pretty low levels of irradiance ($12 \mu\text{mol m}^{-2} \text{s}^{-1}$ PPFD), is maximum at $100 \mu\text{mol m}^{-2} \text{s}^{-1}$ PPFD and then stable with irradiance in *Eucalyptus pauciflora* (Atkin *et al.*, 2000).

Isotope fractionation during respiration (R_d) refers to a difference in isotopic composition between the respiratory substrate and the released CO_2 , noted e in the model. Park and Epstein (1961) first observed in tomato plants that respired CO_2 was enriched compared to the plant material. Later studies observed enriched or depleted respired CO_2 , with apparent fractionation varying between +10 and -8‰ (data reported by Ghashghaie *et al.*, 2003). It is important to note that the extreme values are based on the comparison between whole plant material (considered as respiratory substrate) and respired CO_2 in the dark. Selecting only data based on sucrose, the more likely respiratory substrate under non-stressed conditions, leads to respired CO_2 enriched by 2-5‰ (e thus negative) (Barbour *et al.*, 2007; Ghashghaie *et al.*, 2003; Ghashghaie *et al.*, 2001). There is a “positional effect” of ^{13}C in glucose molecules, with C-3 and C-4 being more ^{13}C enriched than the other ones. Because the PDH reaction will decarboxylate preferentially carbon C-3 and C-4, respired CO_2 from

PDH will be enriched and Acetyl-coA (the product of the PDH reaction) depleted. Thus, the CO₂ evolved from the Krebs cycle during degradation of Acetyl-coA will be depleted (Tcherkez *et al.*, 2003). This also explains that lipids, formed from Acetyl-coA are depleted. The depletion of CO₂ emitted from the Krebs cycle can be increased when plants use fatty acids as respiratory substrate, like under high temperature or long darkness. It has been concluded that the observed overall fractionation will be dependent on the relative influence of the PDH reaction (producing ¹³C-enriched CO₂) and the Krebs cycle (producing ¹³C-depleted CO₂, Tcherkez *et al.*, 2003). These processes reflect carbon metabolism in darkened leaves. Fractionation by respiration in the light is poorly known at present, regarding the difficulty to clearly separate discrimination by diffusion, carboxylation and photorespiration from that of R_d. However, CO₂ respired in the light has been estimated from experimental data to be depleted by less than 5‰ (Tcherkez *et al.*, 2011; Tcherkez *et al.*, 2010).

Discrimination during photorespiration

Photorespiration is a complex cycle that includes the fixation of a molecule of O₂ by RubisCO, the resulting production of glycolate which enters the peroxysome to produce glycine (Figure 2). Glycine then enters the mitochondria to be decarboxylated into serine which releases the photorespired CO₂. Serine comes back to the peroxisome, produces glycerate which re-enters the Calvin cycle as 3-phosphoglycerate. The ratio of oxygenation to carboxylation (ϕ) by RubisCO can be estimated from Γ^* , the CO₂ compensation point in absence of R_d. Γ^* is thus incorporated in the model of discrimination to account for photorespiration. Evans and Loreto (2000) provided a list of Γ^* estimated in 11 species, with extremes values varying between 33 and 47 $\mu\text{mol mol}^{-1}$, with average Γ^* lies around 40 $\mu\text{mol mol}^{-1}$.

It has been shown that photorespiratory decarboxylation fractionates against ¹³C glycine decarboxylation, (f in the discrimination model, see Ghashghaie *et al.*, 2003 for a review). *In vitro* estimations of f conducted on glycine decarboxylase extracted from eight plants species showed that the photorespired CO₂ could be ¹³C depleted (-8‰) or enriched (+16‰) with respect to the substrate (Ivlev *et al.*, 1996). The direction of fractionation was species-dependent, but also influenced by the pH and the enzyme co-factors used for the reaction. f was estimated from a theoretical approach which predicted that photorespired CO₂ should be ¹³C depleted by 11‰

compared to glycine (Tcherkez, 2006). A statistical approach provided close value with $f=11.6\text{‰}$ (Lanigan *et al.*, 2008). This approach consisted to set b , f and g_m as unknowns, and fix known values for Γ^* , e and R_d . The three unknowns were then estimated simultaneously to fit a modelled and a measured $\Delta^{13}\text{C}$ in three *Senecio* species. These latter values bring support for a positive f value, which implies emission of depleted CO_2 , and a fractionation around 11‰ . We can note that the enriched serine comes back to the Calvin cycle via glycerate and 3-phosphoglycerate. This can cause enrichment of the carbohydrate pool formed *via* the Calvin cycle. This influence is not accounted in the $\Delta^{13}\text{C}$ model, and was not estimated yet.

Sensitivity analysis of $\Delta^{13}\text{C}$ estimates

To our knowledge, there was no sensitivity analysis performed on the overall $\Delta^{13}\text{C}$ model yet. Indeed, quantifying at the same time the relative importance of all the parameters of a model can be difficult. We chose here two different methods. The first method consisted to generate a dataset with fixed values of $g_m=0.2, 0.5$ and $0.8 \mu\text{mol m}^{-2} \text{s}^{-1}$ (corresponding to a realistic range of V_{cmax} between 103 and $74 \mu\text{mol m}^{-2} \text{s}^{-1}$); $b=26, 28, 30\text{‰}$; $f=0, 5, 15\text{‰}$; $e=-15, 1, +15\text{‰}$; $R_d=0, 1, 2 \mu\text{mol m}^{-2} \text{s}^{-1}$; and $\Gamma^*=35, 42.5, 50 \mu\text{mol mol}^{-1}$, the range of each parameter being chosen following values found in the literature (Table 2). For each of the 3^5 possible combinations we calculated $\Delta^{13}\text{C}$ with a fixed value of $A=16.9 \mu\text{mol m}^{-2} \text{s}^{-1}$, $C_i=269.1 \mu\text{mol mol}^{-1}$ and $C_a=317.1 \mu\text{mol mol}^{-1}$, corresponding to measured data on *Eucalyptus sieberii* (Douthe *et al.*, *in press*). Then, a multiple linear regression was performed to explain the variations of the computed $\Delta^{13}\text{C}$ with g_m , b , e , f , R_d and Γ^* as covariates and partial R^2 for each parameter was compared to the total R^2 of the model. g_m appeared to be largely the most influent parameter in the discrimination model, with a relative R^2 of 70% (Figure 4, lower left panel). When g_m is fixed thus not accounted for in the analysis (Figure 4, lower right panel), b is the most important parameter (partial R^2 of 65%), followed by f (30%) and e (10%). R_d and Γ^* appeared to have a small effect on the model.

Another approach was tested to confirm these results. We used the Sobol's index, which compares the effect of a variation of the input parameters on the variance of the output variable (here $\Delta^{13}\text{C}$) (see R Development Core Team 2010, package "Sensitivity" version 1.4.0 and Saltelli 2002). Sobol's index is comprised between 0 and 1; higher values mean a higher relative influence on the given

parameter. We used the same range of variations for each parameter than for the first method. Again, g_m is largely the most influent parameter on $\Delta^{13}\text{C}$ (Figure 4, upper left panel), and b when g_m is fixed (Figure 4, upper right panel). e and f have approximately the same influence, and R_d and Γ^* are less influential parameters in the model.

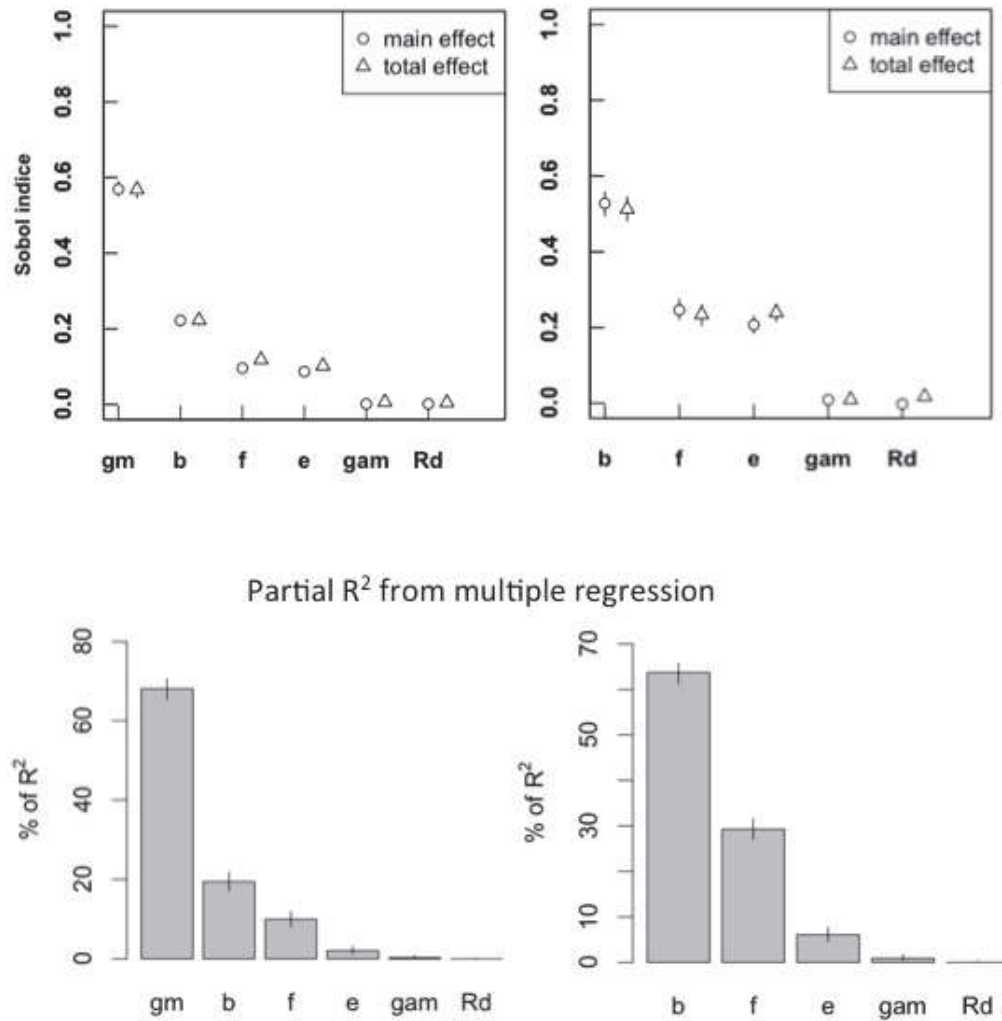


Figure 4: Two methods used to perform a sensitivity analysis of the model of $\Delta^{13}\text{C}$ (fully developed form). On the upper panels the Sobol's index (with and without g_m for the left and right, respectively), computed from a random dataset for each parameter and based on the decomposition of the variance of $\Delta^{13}\text{C}$ following the variations of the input parameters, where g_m , b , f , e and R_d are parameters described in Table 2 and “gam” refers to Γ^* . The higher the index ($[0,1]$), the higher the influence of the parameter. Main effect concerns only the effect of the given parameter while total effect concerns also the interaction with the other parameters in the model (an interaction exists when the effect of a given parameter on the output variable changes with the value of a second parameter). When main and total effects are close from each-other, no strong interaction exists. On the bottom panels, partial R^2 for each tested parameter from a multiple regression performed on $\Delta^{13}\text{C}$ (with and without g_m for the left and right, respectively), with three values fixed for each parameter (see text) within the range of variation

found in the literature. Fixed values were used for $A=16.9 \mu\text{mol m}^{-2} \text{s}^{-1}$, $C_i=269.1 \mu\text{mol mol}^{-1}$ and $C_a=317.1 \mu\text{mol mol}^{-1}$ and $g_m=0.5 \mu\text{mol m}^{-2} \text{s}^{-1}$ (when g_m is fixed) following measured data on *Eucalyptus sieberi* (unpublished data), under 21% O_2 . Each procedure was performed with g_m , b , e , f , R_d and Γ^* as parameters, then g_m was removed to highlight the effect of the other parameters.

Sensitivity of the $\Delta^{13}\text{C}$ - W_i relationship to parameters variations

To illustrate the impact of g_m and b , the two most influential parameters in the $\Delta^{13}\text{C}$ model, on the $\Delta^{13}\text{C}$ - W_i relationship, we simulated a leaf presenting a variation of A from 10 to 14 $\mu\text{mol m}^{-2} \text{s}^{-1}$ and g_s from 0.1 to 0.5 $\mu\text{mol m}^{-2} \text{s}^{-1}$. The corresponding $\Delta^{13}\text{C}$ was calculated for different values of g_m (Figure 3, left panel) and b (Figure 3, right panel).

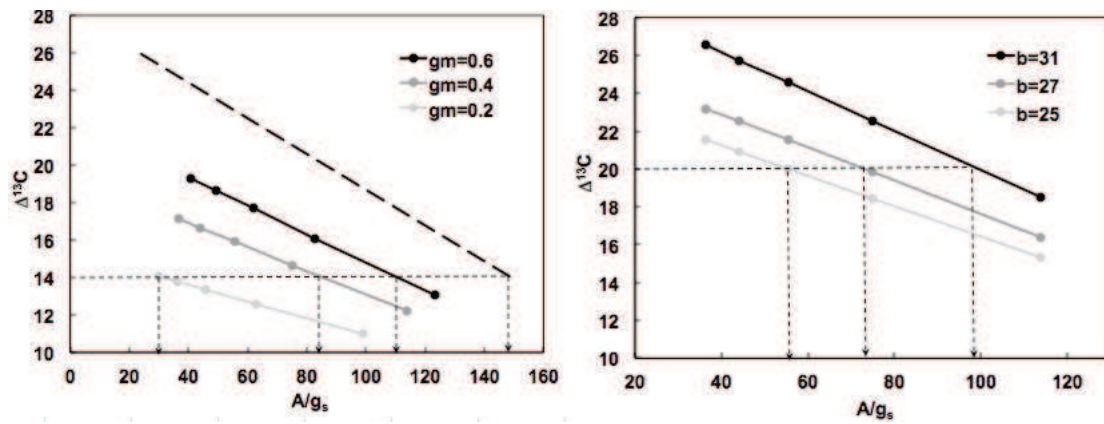


Figure 3: Left panel: simulation of the $\Delta^{13}\text{C}$ - W_i relationship (intrinsic water use efficiency, A/g_s), following the simple model of discrimination (broken line), the complete form of the model of discrimination (using the standard parameterization described in Table 3) but with different values for mesophyll conductance (g_m , in $\mu\text{mol m}^{-2} \text{s}^{-1}$). The horizontal dashed line represents the data for a single value of $\Delta^{13}\text{C}=14\text{‰}$, and each vertical dashed arrow the corresponding value of A/g_s .

Right panel: simulation of the $\Delta^{13}\text{C}$ - W_i relationship (intrinsic water use efficiency, A/g_s), following the simple model of discrimination (broken line) but with different values for discrimination during carboxylation (b , in ‰). The horizontal dashed line represents the data for a single value of $\Delta^{13}\text{C}=20\text{‰}$, and each vertical dashed arrow the corresponding value of A/g_s .

This highlights the large error potentially done when estimating A/g_s from $\Delta^{13}\text{C}$ signal if actual values of g_m are not accounted or if the b or value is mis-estimated.

The influence of g_m for a given value of $\Delta^{13}\text{C}$ ($=14\text{‰}$) is very large as the estimated A/g_s varies from 150 if using the simple form of the model (ignoring g_m), to 110 if using the complete form when $g_m=0.6 \mu\text{mol m}^{-2} \text{s}^{-1}$, and down to 30 if $g_m=0.2 \mu\text{mol m}^{-2} \text{s}^{-1}$ (Figure 3). Similarly, a value of $\Delta^{13}\text{C}=20\text{‰}$ using the simplified model leads to

estimated A/g_s from 100 to 55 for the different values of b (31 to 25‰). The influence of these two parameters is therefore quite large.

These results highlight the crucial importance to (i) set an adapted value for the parameter b and (ii) account for g_m to provide accurate estimates of W_i from $\Delta^{13}C$. We also tested the influence of the overall respiratory term and the influence of respiration and photorespiration separately, but they had little influence on the $\Delta^{13}C$ - W_i relationship.

Sensitivity analysis of the mesophyll conductance estimation

Since the “complete form” of the $\Delta^{13}C$ model was used to estimate mesophyll conductance to CO_2 (g_m), it is important to assess the impact of choosing different values for a given parameter on these estimates. We used the g_m equation as described in (Pons *et al.*, 2009), firstly established by (Lloyd *et al.*, 1992) and based on the fully developed model of discrimination (Evans *et al.*, 1986):

$$g_m = \frac{(b - es - ai)A/C_a}{(\Delta_i - \Delta_{obs}) - \frac{eR_d/k - f\Gamma^*}{C_a}} \quad \text{Eq. 6}$$

where Δ_i is the discrimination predicted by the “simple form” of the model of discrimination and Δ_{obs} the observed $\Delta^{13}C$. This approach is called the “single point method” because g_m can be estimated from one measurement of Δ_{obs} and gas exchange plus estimates of e and f . This contrasts with the “slope method” first developed by (Evans *et al.*, 1986), which requires a range of A and $\Delta_i - \Delta_{obs}$ to estimate g_m and assumes that g_m is not affected by the source of variation of A . To perform the sensitivity analysis we used the Sobol’s index and the same range of parameter values as above. To estimate g_m , the observed $\Delta^{13}C$ (Δ_{obs}) has to be known. We used $\Delta_{obs} = 19.21\text{‰}$ based on measurements from the same dataset as for A , C_i and C_a , as described above.

Figure 5 clearly shows that b is the most influential parameter in the estimation of g_m , explaining over 50 % of variation in g_m , followed by f and e with around 40%. R_d and Γ^* have a small influence on the estimation of g_m . We observed strong differences between the main and the total effect of b , f and e , which denotes interactions between parameters. In other words, following the values taken by b , for example, the effect of f on g_m estimate will change.

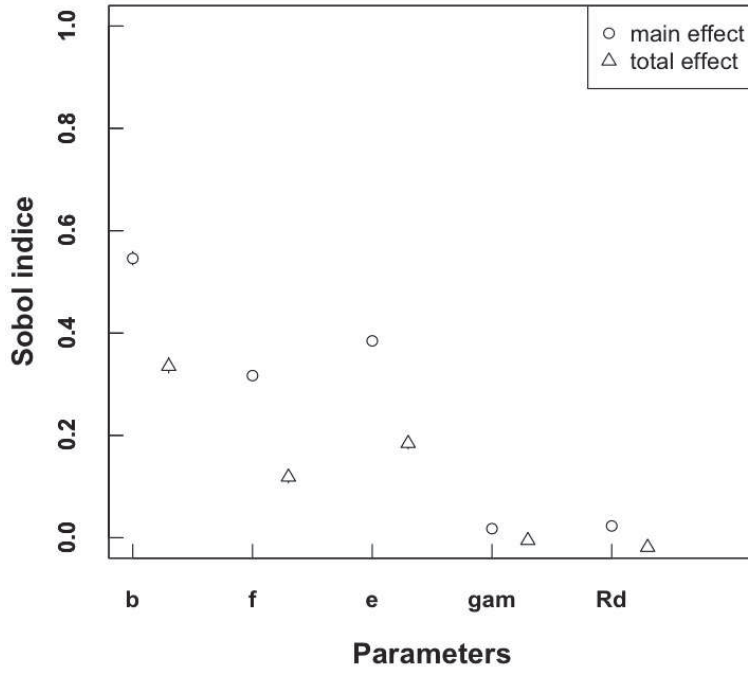


Figure 5: Sensitivity analysis of the mesophyll conductance to CO₂ estimate (g_m) using Sobol's index. Fixed values were used: $A=16.9 \mu\text{mol m}^{-2} \text{s}^{-1}$, $C_i=269.1 \mu\text{mol mol}^{-1}$ and $C_a=317.1 \mu\text{mol mol}^{-1}$ and observed $\Delta^{13}\text{C}=19.21\%$ following measured data on *Eucalyptus sieberi*, under 21% O₂. We filtered data to select only realistic g_m values between 0 and $1 \mu\text{mol m}^{-2} \text{s}^{-1}$.

In conclusion, it appears important to use the fully developed model of discrimination to better interpret observed variations of $\Delta^{13}\text{C}$. On the other hand, the parameterization of this model is still problematic, particularly for the estimation of mesophyll conductance. There is still poor knowledge about the “true” value of some parameters, like b or f , or about their genetic or environmental variability. Regarding the large range of variation reported in the literature, choosing a non-appropriate (but still realistic) value can lead to misleading values of g_m . In the following part of the study, we focused on the use of the $\Delta^{13}\text{C}$ model to estimate g_m , and addressed two main questions:

- What is the effect of choosing different values for a given parameter on the estimated g_m ?
- In the context of rapid variations of g_m with irradiance, could variations of model parameters explain $\Delta^{13}\text{C}$ variations attributed to g_m ?

On the importance of the b parameter

Results of our sensitivity analysis and literature reports indicate the b parameter (fractionation during the carboxylation) has a large influence on the estimation of g_m

(Pons *et al.*, 2009; Tazoe *et al.*, 2011). Following the standard parameterization (Table 3), and the data set used previously (see “*Sensitivity analysis of $\Delta^{13}C$ estimates*” section), $g_m=0.33 \mu\text{mol m}^{-2} \text{s}^{-1}$ and we considered this value as reference for the following analyses. When b is varied from the standard 28‰ to 26‰ g_m increases by 60%, while if b is varied from the standard 28‰ to 30‰ g_m decreases by 20% respectively (Figure 6). Choosing $b=26‰$ affected even more g_m when f takes a value of 15‰ (g_m changed by +150%), or $e=-15‰$ (+100%), highlighting the interaction found with sensitivity analysis (Sobol index, Figure 5). On the other hand, when $b=30‰$, g_m values are less affected by other parameters (Figure 6).

Table 3: Values of parameters used to perform the simulation in Figure 3 and the sensitivity analysis showed in Figure 6. The range for each parameter is set following literature value (Table 2).

Parameter	Range used for sensitivity analysis	Value for “Standard parameterization”
b (in ‰)	26 to 30	28
f (in ‰)	0 to 15	7.5
e (in ‰)	-15 to +15	1
R_d (in $\mu\text{mol m}^{-2} \text{s}^{-1}$)	0 to 2	1
Γ^* (in $\mu\text{mol mol}^{-1}$)	35 to 50	42.5

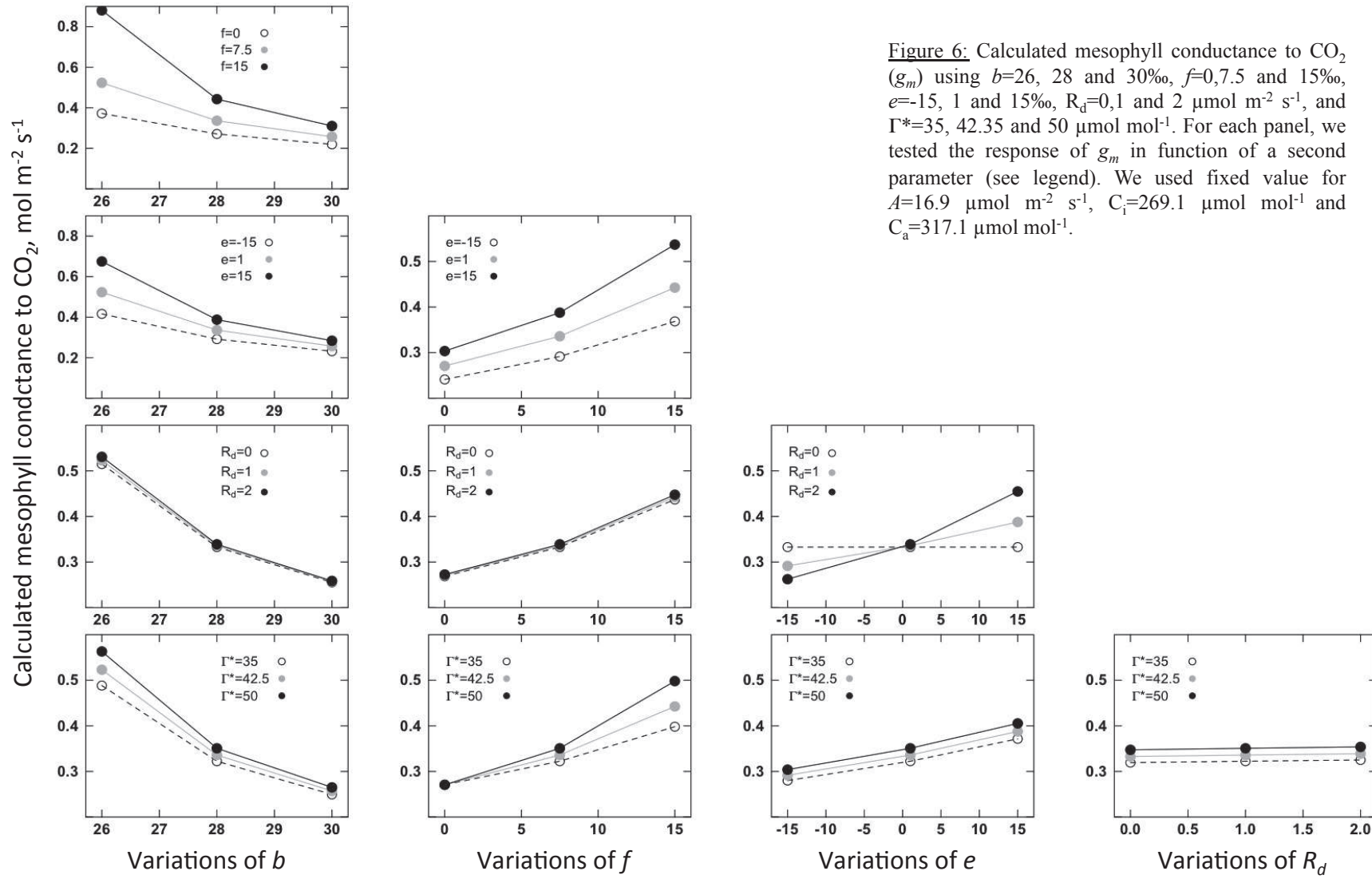


Figure 6: Calculated mesophyll conductance to CO_2 (g_m) using $b=26, 28$ and 30% , $f=0, 7.5$ and 15% , $e=-15, 1$ and 15% , $R_d=0, 1$ and $2 \mu\text{mol m}^{-2} \text{s}^{-1}$, and $\Gamma^*=35, 42.35$ and $50 \mu\text{mol mol}^{-1}$. For each panel, we tested the response of g_m in function of a second parameter (see legend). We used fixed value for $A=16.9 \mu\text{mol m}^{-2} \text{s}^{-1}$, $C_i=269.1 \mu\text{mol mol}^{-1}$ and $C_a=317.1 \mu\text{mol mol}^{-1}$.

Could variations of b with irradiance or O_2 cancel short-term response of g_m ?

There is an increasing number of studies testing and observing a rapid (within minutes) response of g_m to changes of environmental conditions (CO_2 and irradiance, in particular, see Flexas *et al.*, 2008 for review). In these studies it has been considered that other fractionation factors used in the g_m equation remain stable with time. This is a crucial hypothesis to validate the rapid response of g_m , but has not yet been tested. Here we focus on possible variations of b during changes of irradiance to test if b could vary enough to fully account for the observed changes of $\Delta^{13}C$. We based this analysis on irradiance response curves from 200 to 1000 $\mu mol\ m^{-2}\ s^{-1}$ PPFD performed on *Eucalyptus sieberii* with a calibrated TDLAS, under 21% and 1% O_2 to vary the influence of photorespiration, with all parameters constant with O_2 , except $\Gamma^*=38.7$ and $1.85\ \mu mol\ mol^{-1}$ respectively (Figure 7). Considering that g_m was stable with irradiance and equal to the maximum value measured at an irradiance of 1000 $\mu mol\ m^{-2}\ s^{-1}$ (Figure 7, $g_m=0.37\ \mu mol\ m^{-2}\ s^{-1}$ under 21% O_2), b should vary from 28‰ at high irradiance to 26‰ at low irradiance. The same pattern was observed under 1% O_2 , according to a constant $g_m=0.49\ \mu mol\ m^{-2}\ s^{-1}$, with b should be 27‰ at low irradiance. Under 21% O_2 , a decrease of b from 28 to 26‰ could be explained by an increase of β (relative amount of carbon fixed by PEPc) from 0.055 to 0.11 (i.e. 5.5% to 11% carbon fixed by PEPc), for $b_3=30‰$ and $b_4=-5.7‰$ and constants with irradiance. There are however several possible combinations of b and β to explain this variation (see Figure 8). These values of b and β are comprised in a realistic range of variation, according to the literature (Table 2), suggesting that b variations with irradiance are plausible. Such phenomena could occur since RubisCO carbon fixation is directly dependent of irradiance (via electron transport chain) but not that of PEPc. Thus, β could be higher at low compared to high irradiance. However, to the best of our knowledge, such hypothesis was not directly tested yet. This possibility was mentioned by Von Caemmerer and Evans (1991) and Lloyd *et al.* (1992), but the authors concluded in favour of a constant β . Von Caemmerer and Evans (1991) cited estimation of β at low light being of the same range as in high light and Lloyd *et al.* (1992) concluded that the variations of b needed was very unlikely because too large (from 20 to 35‰, for *Citrus*) to fully explain the variations of $\Delta^{13}C$ attributed to g_m . Nevertheless, there is a real need to estimate β with independent methods. At the moment, only estimations via RubisCO and PEPc activities are used to assess the relative part of carbon fixed by each enzyme, but we don't know if maximum activities can be systematically related to the effective amount of carbon fixed.

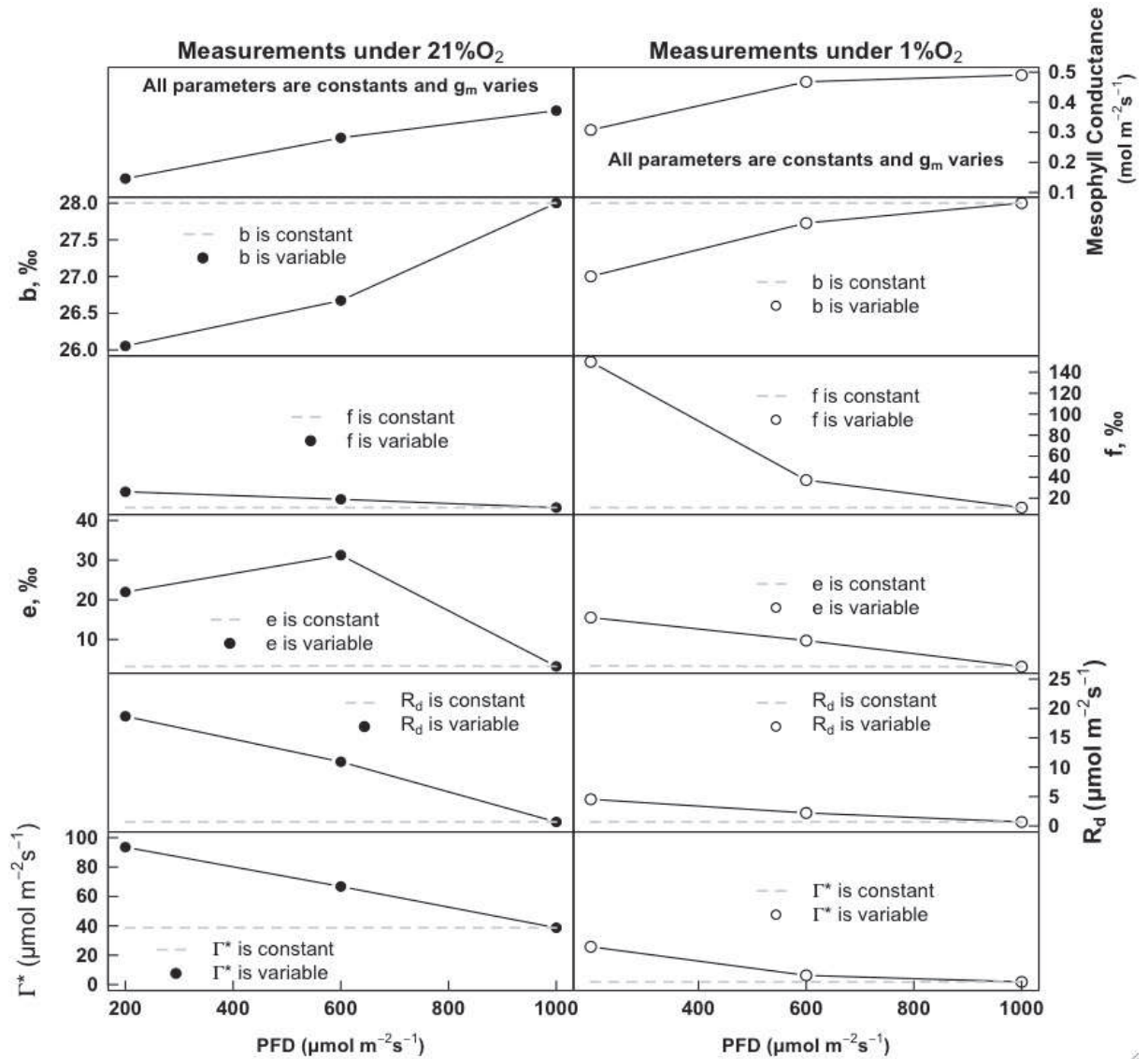


Figure 7: We tested the hypothesis of a stable g_m and calculated the variations of each parameter needed to obtain the same $\Delta^{13}\text{C}$ as observed with a constant g_m across irradiance variations, for each parameter (from the top to the bottom: b , f , e , R_d and Γ^*). Left panels (filled circles) indicate measurement under 21% O_2 and right panels (empty circles) indicate measurement under 1% O_2 . Data were recorded on *Eucalyptus sieberii* (unpublished). g_m was calculated with the isotopic method from measurements performed with a calibrated TDLAS, using the standard parameterization described in Table 3, except $\Gamma^*=38.7$ and $1.85 \mu\text{mol mol}^{-1}$ under 21% and 1% O_2 , respectively. Each point is an average of three measurements taken at 180s intervals.

Using the standard parameterization, we observed that g_m increased \sim two fold when O_2 was switched to 1% O_2 compared to 21% O_2 . There are only few data about g_m variations under changed O_2 . We can note that Flexas *et al.* (2007) and Von Caemmerer and Evans (1991) did not observe such variations while measuring g_m with online discrimination. We then tested the hypothesis that b could change with O_2 , inducing an artefactual variation of g_m .

In such a case, b should increase by on average 4‰ at 1% O_2 ($b=30.4$ ‰ or 32.7‰ at 1000 and 600 $\mu\text{mol m}^{-2} \text{s}^{-1}$ PFD, respectively) to compensate variations of g_m (see Figure 9). Such variations could happen if the rate of carboxylation by RubisCO is dependent of O_2 concentration (via the competing oxygenase activity) but not that of PEPc. In that case, we can expect an increase of b (via a decrease of β) with decreasing O_2 . A value of $b=30.5$ ‰ can be easily reached with realistic values of b_3 and β (Figure 8).

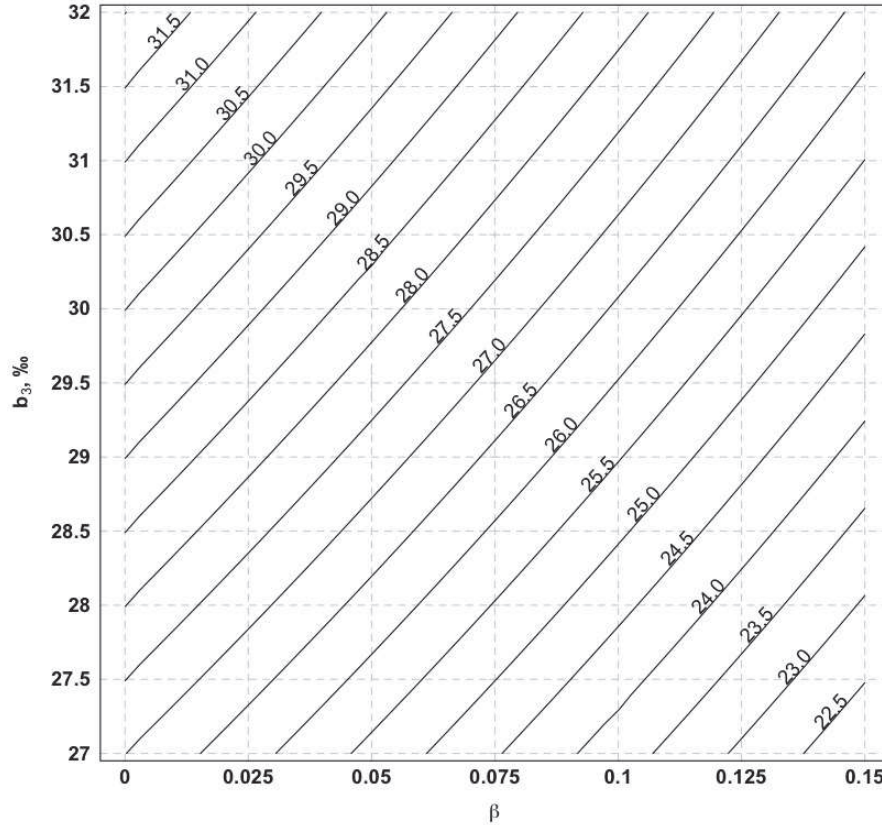


Figure 8: Values of b , fractionation during carboxylation according to b_3 (fractionation by RubisCO) varying from 27‰ to 32‰ and β (relative amount of carbon fixed by PEPc) from 0 to 0.15 (corresponding to 0% and 15%). Each value of b was computed from $b=b_3(1-\beta)+b_4\beta$ (Farquhar and Richards, 1984) and is shown on each continuous line, with $b_4=-5.7$. The range of b_3 values was set according to McNevin *et.al* (2007) based on estimations of purified RubisCO discrimination in wild-type tobacco and spinach. The range of b_3 corresponds to extremes SDs given by the authors, calculated with respect to gaseous CO_2 . The range of β corresponds to lowest (0%, no carbon fixed by PEPc) and highest values found in the literature (0.13 from Vu *et al.*, 1985 estimated from ratio of RubisCO and PEPc activities).

On the other hand, high b values like 31.5‰ and 32.7‰ are unlikely to happen, or would require both very high b_3 and low β (Figure 8). Moreover, this hypothesis also requires that b is influenced by irradiance, regarding the increase and then the decrease of recalculated

b with increasing PFD (Figure 9). Regarding these results, it appears unlikely that b could vary with O_2 with an intensity such as to fully explain variations of g_m .

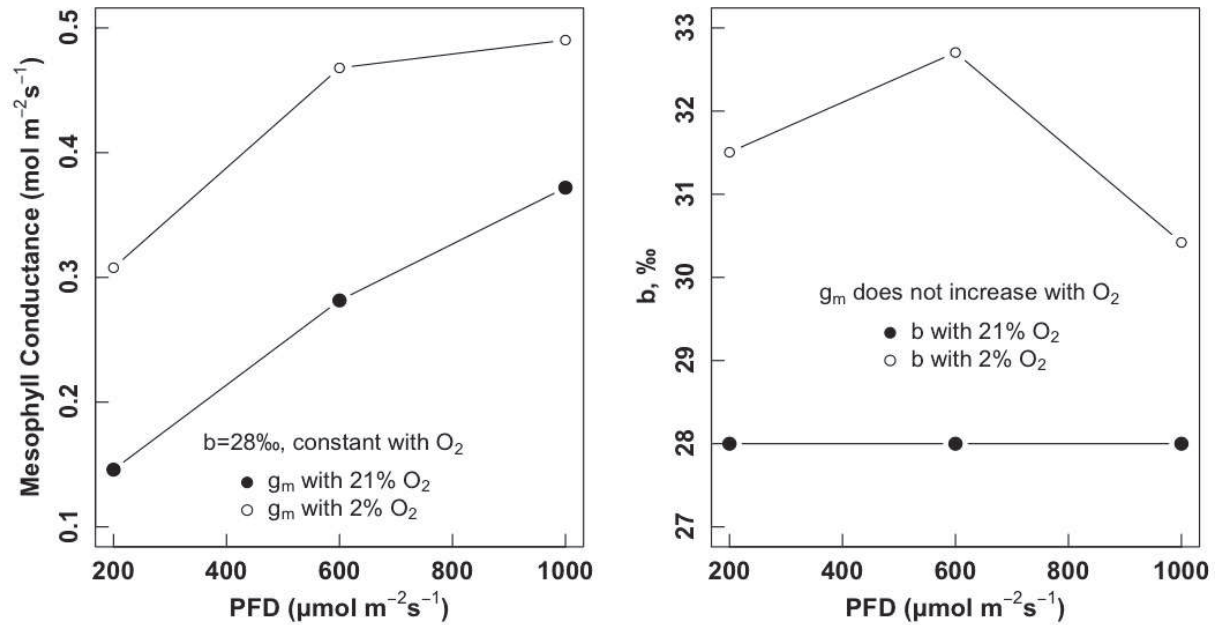


Figure 9: On the left panel, values of mesophyll conductance estimated from online discrimination with a calibrated TDLAS (unpublished data) under varying irradiance for a plant of *Eucalyptus sieberii*, under 21% O_2 (filled circles) and 1% O_2 (empty circles). We used the standard parameterization described in Table 3, except $\Gamma^*=38.7$ and $1.85 \mu\text{mol mol}^{-1}$ under 21% and 1% O_2 , respectively.

On the right panel, we calculated for each PFD the variation of b needed to have g_m does not increase with O_2 . Each point is an average of three measurements taken at 180s intervals.

Could b be changed by ozone fumigation?

It has been recognised that exposing plants to ozone (O_3) fumigation decreases photosynthesis and plant growth. Biochemical modifications occur a few days after starting the O_3 exposure, with generally a decrease of photosynthesis, photorespiration (assessed by gas exchange) and RubisCO activity, with a concomitant increase of PEPc activity (Dizengremel, 2001). These results were confirmed in poplar plants (*Populus tremula* Mich x. *Populus alba* L. clone INRA 717-1B4) exposed to 120 ppb O_3 for 13 hours / day. After 14 days of exposure, photosynthesis decreased by 20-40%, photorespiration by 50% compared to control plants, and the PEPc/RubisCO ratio of total activities increased from 0.1 to 0.3 (Bagard *et al.*, 2008). If the PEPc/RubisCO ratio of total activities can be related to the relative amount of carbon fixed by each enzyme, then it can be used as a proxy for the β parameter in the discrimination model. We can note that the value of 0.1 for control plants corresponds to the value of β set in (Farquhar and Richards, 1984). To test if ozone exposure could change β , we measured the online $\Delta^{13}C$ of control and ozone exposed plants of poplar,

using the protocol described by Bagard *et al.* (2008). After 14 days of ozone exposure to 120 ppb (control plants exposed to air <10ppb), the assimilation rate was decreased from 20 to 15 $\mu\text{mol m}^{-2} \text{s}^{-1}$ (25 % decrease). For the two plants presenting low C_i/C_a (~ 0.5) $\Delta^{13}\text{C}$ was unchanged between control and ozone exposed plants, but for $C_i/C_a > 0.7$ $\Delta^{13}\text{C}$ was 2‰ lower in ozone exposed compared to control plants (Figure 10).

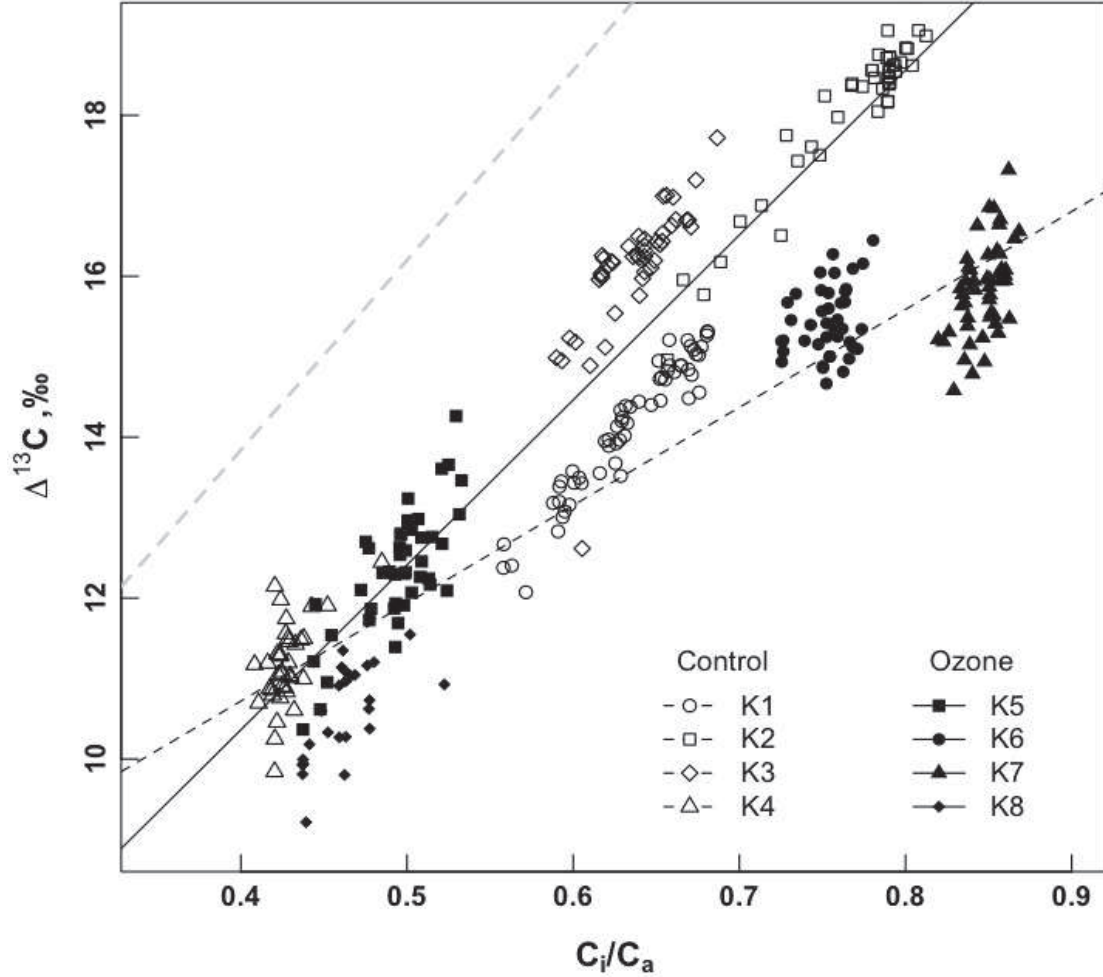


Figure 10: Online discrimination against $^{13}\text{CO}_2$ versus C_i / C_a ratio measured for four control plants (empty symbols) and four ozone exposed plants (filled symbols) of poplar (*Populus deltoides x nigra*), each symbol denotes a different plant. CO_2 entering the photosynthesis chamber was varied from 450 to 950 $\mu\text{mol mol}^{-1}$ to obtain C_i/C_a variations under an irradiance of 550-650 $\mu\text{mol photons m}^{-2} \text{s}^{-1}$. Ozone fumigation was set at 120ppb for 13 hours / day during 14 days before starting measurements while air for control plants was usually <10ppb.

A decrease of $\Delta^{13}\text{C}$ can be due to a decrease of g_m or b , or both since the influence of (photo)respiration (rate and associated fractionation factors) remains unchanged. Under the first hypothesis, with b set at 30‰ and not affected by ozone exposure, g_m was on average 50% lower than in control plants, decreasing from 0.2 to 0.1 $\text{mol m}^{-2} \text{s}^{-1}$. Under the second hypothesis, we considered g_m to remain unaffected by exposure to ozone, and used the g_m

response to C_i measured in control plants to calculate a g_m for plant exposed to ozone. Then, we adjusted b and results were $b=27.6$, 24.8 , 21.2 and 22.1‰ for K5, K6, K7 and K8, respectively (plants shown in Figure 10). A low b value like 21‰ , for $b_3=30\text{‰}$, means a value of β of ~ 0.25 . This is very close to the value estimated by Bagard *et al.* (2008) with total enzyme activities ($\beta=0.3$). These first results suggest that the parameter b could potentially vary due to ozone exposure. This could be useful to better understand its influence in the discrimination during photosynthesis, other than using simulation. Nevertheless, confirmatory studies must be carried out to strengthen this hypothesis. Because of the inextricable dependence of b and g_m estimation using the $\Delta^{13}\text{C}$ method, a second approach to estimate g_m could be a useful solution. Carrying out studies with simultaneously online discrimination and chlorophyll fluorescence methods appear to be a very promising approach for future studies.

Importance of non-photorespiratory decarboxylation: e and R_d

Fractionation during respiration other than from photorespiration (R_d), so-called “day respiration”, has only a small influence on the estimation of g_m , as highlighted by the sensitivity analysis. Using the standard parameterization (Table 3) and changing R_d from 0 to $2 \mu\text{mol m}^{-2} \text{s}^{-1}$ affected g_m by only 1% (see Figure 6). Even with extreme values of b , f or Γ^* , R_d has a small influence. An exception was when R_d and e varied together. With $e=-15\text{‰}$, increasing R_d decreased g_m by $0.1 \text{ mol m}^{-2} \text{s}^{-1}$ (20%) and when $e=+15\text{‰}$, enhanced R_d increased g_m by $0.15 \text{ mol m}^{-2} \text{s}^{-1}$ (35%). This close relationship is obviously induced by the $e \cdot R_d$ factor in the equation. The e parameter has a larger effect on g_m estimation than R_d . Variation between extreme values ($e=-15$ and $+15\text{‰}$) changed g_m by almost $0.1 \text{ mol m}^{-2} \text{s}^{-1}$ (i.e 30% variation). This effect is larger when $f=15\text{‰}$ or $b=26\text{‰}$ is used (60% or 100% increase compared to the standard parameterization, respectively).

It has been reported that $\delta^{13}\text{C}$ of respired CO_2 could change with leaf temperature and by maintaining the leaf under prolonged darkness (Tcherkez *et al.*, 2003). These variations are mainly caused by a change of respiratory substrate, with decarboxylation of sucrose resulting in enriched respired CO_2 and that of lipids or proteins resulting in depleted respired CO_2 . Such changes could impact $\Delta^{13}\text{C}$ recorded during photosynthesis, and should be included in the discrimination model via the e parameter. This is the same rationale as (Wingate *et al.*, 2007) who considered that if the $\delta^{13}\text{C}$ of source CO_2 during the experiment is different from that during growth, then the respired CO_2 would be affected because of a mix between freshly synthesised and older carbon pool. We tested the possibility that such changes in isotopic signature of respired CO_2 during an experiment could give rise to artefactual short-term

variations g_m . We estimated that e would have to change from ~3‰ to 25-30‰ under 21% O₂, and from ~3‰ to 15‰ under 1% O₂ with decreasing irradiance to negate the computed variation of g_m . Values of e for 21% O₂ are clearly out of the range found in the literature for darkened leaves. Under 1% O₂, the values of e are within the range found in the literature (for darkened leaves), except if we consider estimations based on sucrose as respiratory substrate (then $e=2-5‰$). If we now compare to recent estimations of e during the light period ($e<1‰$, Tcherkez *et al.*, 2011; Tcherkez *et al.*, 2010), these variations of e are even more unlikely. However, such rapid variations would need large change of the respiratory substrate during the experiment but this phenomenon remains very unlikely due to the constant temperature used in our experiment, and the fact that carbohydrate starvation probably did not occur. This clearly shows that potential changes of e cannot lead to the short-term response of g_m to irradiance. We then considered that using values of e close to 0 for estimating mesophyll conductance is probably adapted. It is the same story for R_d . To fully explain the change in g_m , R_d would have to increase up to 20 $\mu\text{mol m}^{-2} \text{s}^{-1}$ under 21% O₂ which is not possible. Under 1% O₂, R_d would have to increase to 2.2 and 4.5 $\mu\text{mol m}^{-2} \text{s}^{-1}$ at 600 and 200 $\mu\text{mol m}^{-2} \text{s}^{-1}$, respectively. These values are far higher than values reported in the literature. Moreover, there is no study observing increasing R_d in such proportions, with decreasing irradiance (between 1000 and 200 $\mu\text{mol m}^{-2} \text{s}^{-1}$). We conclude that R_d can't explain short-term variations of g_m under either 21% or 1% O₂.

Importance of photorespiration: f and Γ^*

The fractionation during photorespiration, noted f , is the second most influential parameter in the estimation of g_m , according to the sensitivity analysis (Figure 4). Enhanced f increases the value of g_m , with g_m lowered by 20% when $f=0‰$ and increased by 30% when $f=15‰$ (Figure 7). In terms of absolute values this represents a change of g_m by 0.3 $\text{mol m}^{-2} \text{s}^{-1}$ with f varying from 0 to 15‰ for $b=30‰$, but for $b=26‰$ g_m changed by $\approx 0.5 \text{ mol m}^{-2} \text{s}^{-1}$ (higher sensitivity of g_m to f with low b). Comparatively, Γ^* has only a small effect on the estimation of g_m , with variations remaining 0.05 $\text{mol m}^{-2} \text{s}^{-1}$ when Γ^* varies between 35 and 50 $\mu\text{mol mol}^{-1}$. There is a larger effect with $f=15‰$, with g_m varied by 0.1 $\mu\text{mol mol}^{-1}$.

Changes in f are unlikely to explain g_m variations with irradiance, with respect to the large range of values needed (Figure 6). f should switch from 11‰ under high irradiance up to 26‰ under low irradiance (21% O₂), which is double recent estimates (Lanigan *et al.*, 2008; Tcherkez, 2006). Moreover, it has been never suggested that f could vary with irradiance. We found a very large value, with $f=150‰$ at 1% O₂, clearly a computation

consequence, regarding of the low Γ^* ($1.85 \mu\text{mol mol}^{-1}$) associated with f . To account for variation in g_m at low irradiance, Γ^* would have to increase to $60 \mu\text{mol mol}^{-1}$ (compared to 38.7) at 21% O_2 and $25 \mu\text{mol mol}^{-1}$ (compared to 1.85) at 1% O_2 . This represents very large increases compared to the value under high irradiance, and since Γ^* reflects RubisCO affinity for CO_2/O_2 , it is not likely to vary with O_2 . This evidence that neither variations of Γ^* or f could explain g_m variations with irradiance.

Concluding remarks

In this analysis we first performed comparisons of the $\Delta^{13}\text{C}/W_i$ relationship among several species and functional groups using an integrated signal of $\Delta^{13}\text{C}$ recorded from bulk leaf material. We observed that $\Delta^{13}\text{C}$ can be used as an estimator of W_i , but that the relationship changes between species and with the source of variation (i.e. light, water availability or genetic). In other words, variations of $\Delta^{13}\text{C}$ are related to variations of W_i , but it is not possible to estimate the absolute values of W_i . This can be easily explained by the fact that (i) the $\Delta^{13}\text{C}$ signal from bulk is influenced by the $\delta^{13}\text{C}$ and the proportion of the different leaf components, and that $\delta^{13}\text{C}$ and the proportion of each component can vary between species and by the treatment used, and (ii) the use of the simple model of discrimination ignore important parameters like g_m . The second observation explored the systematic shift between observed $\Delta^{13}\text{C}$ and $\Delta^{13}\text{C}$ predicted by the simple form of the discrimination model (Eq. 1). This shift was also observed using online discrimination, which avoids differences of time integration between $\Delta^{13}\text{C}$ and W_i , and the problem with leaf composition. This highlights the importance to account mesophyll conductance and respiratory components described in the fully developed model of discrimination to correctly interpret $\Delta^{13}\text{C}$ information.

In the second part, we focused our attention on the fully developed $\Delta^{13}\text{C}$ model, and its use to derive mesophyll conductance. A sensitivity analysis highlighted the importance of the b parameter to obtain absolute values of g_m . Moreover, b appeared to be a critical parameter in the assessment of rapid variations of g_m (within minutes), there is thus a pressing need to determine if b can effectively vary with changes in environmental variations or not. We also showed that b variations could happen during O_2 variations or ozone fumigation. Nevertheless, the direct inter-relationship between g_m and b in the $\Delta^{13}\text{C}$ model prevents a clear understanding of their specific variations, since one must be fixed to estimate the other. Chlorophyll fluorescence method could be used as a second approach to estimated g_m , since only estimations of R_d and Γ^* are shared parameters with the two approaches (except A and

C_i , but these latter can be considered as known parameters, not estimated), and the assumptions inferred from the biochemical model of photosynthesis of Farquhar and colleagues. The estimations of g_m is also sensitive to values of f but less so than for b . Following the last estimations, f lies around 10-11‰. A slight under or over-estimation (by 1-2‰) of f will not have a large consequence for estimates of g_m and using $f \approx 11‰$ should not strongly mislead g_m estimations. For e , only using extreme coupled to high R_d would strongly affect g_m estimation. There an increasing body of evidence that respired CO_2 is only slightly depleted (e close to 1‰), and as for f , even if this value is biased by a few per mil, it will not affect g_m estimation. It appeared that estimates of g_m from $\Delta^{13}C$ are not very sensitive to R_d and Γ^* values, thus, the slight errors inferred by the use of the “Laik method” should not have a large impact on the g_m estimate. Finally, we estimated that short-term variations of g_m are unlikely to be artifactual because of rapid variations of any parameter of the respiratory component. An independent approach is now needed to confirm previous results. Measuring simultaneously both leaf discrimination and chlorophyll fluorescence seems to be an attractive solution, since in the second method is not based on fractionation approaches.

CHAPTER II

Mesophyll conductance to CO₂, assessed from on-line TDL-AS records of ¹³CO₂ discrimination, displays small but significant short term responses to CO₂ and irradiance in Eucalypt seedlings.

Mesophyll conductance to CO₂, assessed from on-line TDL-AS records of ¹³CO₂ discrimination, displays small but significant short term responses to CO₂ and irradiance in Eucalypt seedlings.

Cyril DOUTHE^{1,2,3}, Erwin DREYER^{1,2*}, Daniel Epron^{1,2}, Charles R. WARREN³

Addresses

1. INRA, Unité Mixte de Recherches 1147 "Ecologie et Ecophysiologie Forestières", F 54280 CHAMPENOUX, France

2. Nancy Université, Unité Mixte de Recherches 1147 "Ecologie et Ecophysiologie Forestières", Faculté des Sciences, F 54500 VANDOEUVRE, France

3. University of Sydney, School of Biological Sciences, Heydon-Laurence Building, A08, The University of Sydney, NSW 2006, Australia.

Emails: Cyril.Douthé@nancy.inra.fr; dreyer@nancy.inra.fr; daniel.epron@scbiol.uhp-nancy.fr; charles.warren@sydney.edu.au

*Correspondence and reprints

Short title: Mesophyll conductance varies with CO₂ and irradiance

Additional Keywords: Photosynthesis, stomatal conductance, *Eucalyptus globulus*, *Eucalyptus sieberii*, *Eucalyptus saligna*, tunable diode laser absorption spectrometry

Number of words: Figures: 6 Tables: 1

ABSTRACT

Mesophyll conductance (g_m) is now recognized as an important limiting process for photosynthesis, as it results in a significant decrease of CO₂ diffusion from sub-stomatal cavities where water evaporation occurs, to chloroplast stroma. Over the past decade, an increasing number of studies proposed that g_m can vary in the short-time (e.g. minutes), but these variations are still under controversy, especially those potentially induced by changing CO₂ and irradiance. In this study we present g_m data estimated with on-line ¹³C discrimination recorded with a tunable diode laser absorption spectrometer (TDL-AS) during leaf gas exchange measurements, and based on the single point method. The data were obtained with three *Eucalyptus* species. We observed a 50% decrease of g_m when CO₂ mole fraction was increased from 300 to 900 $\mu\text{mol mol}^{-1}$, and a 60% increase when irradiance was increased from 200 to 1100 $\mu\text{mol m}^{-2} \text{s}^{-1}\text{PPFD}$. We also estimated the relative contribution of respiration and photorespiration to overall ¹³C discrimination. Not taking this contribution into account may lead to a 50% underestimation of g_m but had little effect on the CO₂ and irradiance induced changes. As a conclusion, we state that (i) the observed responses of g_m to CO₂ and irradiance were not artefactual, (ii) the respiratory term is important to assess absolute values of g_m but has no impact on the responses to CO₂ and PPFD; and (iii) increasing irradiance and reducing CO₂ mole fraction results in rapid increases of mesophyll conductance in *Eucalypt* seedlings.

INTRODUCTION

During photosynthesis, CO₂ diffuses from the atmosphere (at a mole fraction C_a) to the sites of carboxylation (C_c) inside the chloroplasts (Farquhar *et al.*, 1980; Gaastra, 1959). CO₂ crosses the leaf boundary layer and traverses stomatal pores into the sub-stomatal cavity. CO₂ then diffuses through the gas phase between mesophyll cells before reaching cell walls, where it is solubilised. In the liquid phase, CO₂ crosses the plasma membrane, the cytosol and finally the chloroplast membranes to reach the sites of carboxylation in the chloroplast stroma. Most of the carboxylation is by Rubisco while a small fraction (estimated at 5%) is by phosphoenolpyruvate carboxylase (PEPc) in the cytosol. The mesophyll conductance to CO₂ (g_m) represents the conductance from the sub-stomatal cavities at a mole fraction C_i, to the sites of carboxylation, and includes gas and liquid phase transfer.

In early leaf photosynthesis models, g_m was considered to be infinite. This was an explicit assumption in the original formulation of Farquhar's model of C₃ photosynthesis. However, many subsequent studies showed that there was a difference between C_i and C_c suggesting that g_m might be finite (Evans *et al.*, 1986; Lloyd *et al.*, 1992) and that it affects estimation and interpretation of photosynthetic parameters like the maximal carboxylation activity of RubisCO (V_{cmax}) or the maximal light-driven electron flux (J_{max}) (Epron *et al.*, 1995; Niinemets *et al.*, 2009a). g_m can limit the rate of photosynthesis by 25-30% (Epron *et al.*, 1995) and this limitation may be as large as stomatal conductance (Flexas *et al.*, 2007c; Warren and Adams, 2006). The range of g_m variation among species is similar to that of stomatal conductance, from 0.005 up to 0.5 mol m⁻² s⁻¹ (see the reviews by Evans and Von Caemmerer, 1996 and Flexas *et al.*, 2008), with high g_m occurring in herbaceous annuals and lower values in evergreen gymnosperms. g_m is apparently influenced by leaf traits like thickness, tissue density (and therefore leaf dry mass per unit area, LMA ; see Flexas *et al.*, 2008 and Niinemets *et al.*, 2009b, for meta analyses), cell wall thickness or the proportion of gaseous versus liquid mesophyll phases (Evans *et al.*, 2009; Piel *et al.*, 2002; Terashima *et al.*, 2006). Such morphological leaf properties would confer stable g_m in the short term (e.g., a few days).

Since the early 90's, g_m was shown to be affected by environmental factors. At first, changes were thought to be rather long-term changes like for instance the decline induced by leaf ageing (Scartazza *et al.*, 1998), by a gradual drought stress (Cornic *et al.*, 1989; Rouspard *et al.*, 1996; Warren, 2008b), or by salinity (Bongi and Loreto, 1989). More recently, short

term changes were shown to occur in response to temperature (Bernacchi *et al.*, 2002; Pons and Welschen, 2003; Warren, 2008a; Warren and Dreyer, 2006). Similarly rapid responses of g_m (at the minutes scale) were reported to occur under varying CO₂ mole fraction. A review by Flexas *et al.* (2008) reported that g_m decreases with increasing CO₂ (data from Harley *et al.*, 1992, During, 2003 and Flexas *et al.*, 2007b). This pattern was also observed by Hassiotou *et al.* (2009) among seven *Banksia* species, by Vrabl *et al.* (2009) in *Helianthus annuus*, and by Bunce (2010) in *Glycine max* and *Phaseolus vulgaris*. Tazoe *et al.* (2011) recently observed the same decreasing pattern among three species with contrasting photosynthetic capacities. Only a few studies have tested the rapid response of g_m to irradiance. Flexas *et al.* (2008) reported an increase of g_m with increasing irradiance (data from Gorton *et al.*, 2003 and Flexas *et al.*, 2007b).

Nevertheless, there is still no consensus about the reality of such rapid responses of g_m to CO₂ and irradiance. Several studies reported g_m to be stable in response to changes in CO₂ (Loreto *et al.*, 1992; Tazoe *et al.*, 2009; Von Caemmerer and Evans, 1991) and irradiance (Tazoe *et al.*, 2009; Yamori *et al.*, 2010). Some of the discrepancy may be due to measurement accuracy and/or artefacts. This can be true with the two main methods used to estimate g_m : the fluorescence/gas exchange technique (Loreto *et al.*, 1992) and the isotopic discrimination method (Pons *et al.*, 2009). One of the complications with the isotopic method, which we used here, is that the contribution of ¹³C discrimination during respiration and photorespiration needs to be taken into account (see model description below). Some studies have ignored discrimination during respiration and photorespiration (Flexas *et al.*, 2007b, 2007c ; Vrabl *et al.*, 2009), or approximated respiration in the light by that in the dark (Tazoe *et al.*, 2009, 2011). The fractionation factors associated with respiration and photorespiration can be taken into consideration using recent estimates (Lanigan *et al.*, 2008). An alternate approach is to limit the impact of fractionation during photorespiration by using low O₂ in the measurement atmosphere (Tazoe *et al.*, 2009).

To date, there is no consensus regarding whether g_m responds rapidly to irradiance and CO₂ mole fraction, despite the importance of this for interpreting responses of photosynthesis to environmental variables. The aim of this research was to assess whether short-term variations of g_m occur in response to changes in irradiance and CO₂ mole fraction. Rapid response of g_m was assessed by recording online ¹³CO₂ discrimination during photosynthesis with a custom built photosynthesis chamber adapted to a LI-COR 6400, and coupled to a TDL-AS (or tunable diode laser absorption spectrometer). To examine the ubiquity of

responses we used three species of *Eucalyptus* with differing rates of photosynthesis, and took into consideration the respiratory term of on-line ^{13}C discrimination to reinforce our findings. Measurements were done on species with contrasting photosynthetic capacity to check whether g_m variability is species-dependent and how g_m is related to A and g_s within and among species.

MATERIAL & METHODS

Plant material

We used three species in the genus *Eucalyptus*: *E. globulus* Labill., *E. saligna* Sm. and *E. sieberi* L. A. S. Johnson. Plants were grown for 4 months in a naturally-illuminated greenhouse at an average daily temperature of 25 °C in 8L pots filled with compost-based substrate. They were watered with automatic drip irrigation. At the time of the experiment they were ~60 cm high.

Gas exchange measurements

We measured the response of net CO₂ assimilation rate (A , $\mu\text{mol m}^{-2} \text{s}^{-1}$) to variations in sub-stomatal CO₂ mole fraction (C_i) and photosynthetic photon flux density (PPFD, $\mu\text{mol m}^{-2} \text{s}^{-1}$) in each of four replicate plants of the three species, for each treatment (e.g. 2 treatments x 3 species x 4 replicates = 24 plants). All measurements were made on the youngest fully expanded leaves. Plants were transferred from the greenhouse to the laboratory at 25°C. To assess simultaneously photosynthesis and discrimination against ¹³CO₂ we used a LI-6400 portable gas exchange system (LI-COR, Lincoln, NE, USA) equipped with a custom built chamber of 18 cm² and coupled to a TDL-AS (TGA100A, Campbell Scientific, Logan, UT, USA).

Before measurements, leaves were exposed to 1000 $\mu\text{mol m}^{-2} \text{s}^{-1}$ PPFD and 400 $\mu\text{mol CO}_2 \text{mol}^{-1}$ for 30 minutes to induce photosynthesis and stomatal opening. CO₂-responses of photosynthesis were measured under a constant PPFD of 1000 $\mu\text{mol m}^{-2} \text{s}^{-1}$ while CO₂ mole fraction for the reference gas (C_e) was sequentially set at 300, 500, 700 and 900 $\mu\text{mol mol}^{-1}$. PPFD response at 200, 500, 800 and 1100 $\mu\text{mol m}^{-2} \text{s}^{-1}$ were measured under a constant CO₂ mole fraction of 400 $\mu\text{mol mol}^{-1}$. During each step of the CO₂ or PPFD responses, we waited at least 20 minutes for A and g_s to reach a steady-state, and recorded three individual points separated by 180 s. Each set of three individual data points was averaged to characterize the response at one step in the response curve. The standard error of the three individual points was used to assess the analytical variability.

Air flow into the chamber was set at 400 $\mu\text{mol s}^{-1}$, and leaf temperature at 25°C. Irradiance was provided by a LI-COR RGB light source (6400-18, LI-COR-0128), which covered the entire chamber surface. A sub-sample of air from the sample and reference gas lines of the LI-6400 was diverted to the TDL-AS. The TDL-AS measured sequentially gas

from two calibration tanks, the LI-6400 reference gas and finally the LI-6400 sample gas. Each intake was measured for 45 s, with the first 15 s ignored to minimise carryover and enable stabilisation between intakes. The total time for a sequence of measurements was therefore 180 s.

The TDL-AS gas was connected through a “T” tubing to the reference tube of the LI-6400 between the console and the IRGA. In the same way, the TDL-AS intake of sample gas was connected in-between the LI-6400 chamber exhaust. The TDL-AS was set to continuously withdraw 150 mL min⁻¹ (~102 µmol s⁻¹) from each of the sample and reference fluxes of the LI-6400. This withdrawal of air was much smaller than the flow through the LI-6400 chamber, which means that the TDL-AS could sample air from the LI-6400 while maintaining a positive pressure in the LI-6400 chamber. Existence of a positive pressure inside the LI-6400 chamber was checked through the curvature of the propafilm covering the top of the chamber. We matched TDL-AS with LI-6400 data by taking into account the time lag of 37 s that was recorded between the chamber and the TDL-AS. The TDL-AS data were only used to record the isotopic composition of the reference and sample gas while all photosynthesis parameters were estimated from the LI-6400 data.

Isotopic measurements and system testing

Discrimination by a leaf was assessed by measuring isotopic composition in reference (δ¹³C_e, ‰) and sample gas (δ¹³C_o, ‰). The isotopic composition (δ¹³C) was expressed as:

$$\delta^{13}C = \left(\frac{R_s}{R_{VPDB}} - 1 \right) \times 1000$$

where R_s is the isotopic ratio ($R = {}^{13}\text{CO}_2/{}^{12}\text{CO}_2$) of the sample and R_{VPDB} is the isotopic ratio of Vienna Pee Dee Belemnite (VPDB, 0.0112372).

The TDL-AS was calibrated with two tanks (T1 and T2) with CO₂ concentrations of respectively 419 ± 10 and 290 ± 7 µmol mol⁻¹ (mean ± CI) given by the provider and checked with a recently factory-calibrated LI-8100 IRGA (LI-COR, Lincoln, NE, USA). Isotopic composition of the each tank was measured by sampling air into 12-mL exetainers (Labco Limited, Buckinghamshire, UK) and analysed via the gas-bench inlet of an IRMS (Delta S, Finningan, Bremen) at INRA Nancy (n= 10 exetainers / tank). For T1 and T2, δ¹³C was -36.6 ± 0.08‰ and -36.9 ± 0.2‰ (mean ± S_d, n=10), respectively. Absolute values of ¹²CO₂ and ¹³CO₂ were respectively 414.51 and 4.487 µmol mol⁻¹ for T1 and 286.89 and 3.104 µmol mol⁻¹

¹ for T2, considering the CO₂ mole fraction indicated by the provider took into consideration both isotopologues. A linear interpolation was used between these two points for each isotopologue. For further calibration, we generated a range of CO₂ mole fractions of 200, 300, 500, 700, 1000, 1500 and 2000 $\mu\text{mol mol}^{-1}$ using the CO₂ injector of the LI-6400 fed with the same CO₂ cartridge during the whole test. CO₂ mole fractions above the calibration range led to a small deviation of +2.5‰. We fitted a second order polynom to describe the deviation of apparent $\delta^{13}\text{C}$ from reference values measured at $C_e=300 \mu\text{mol mol}^{-1}$ (because in the calibration range) along the extended CO₂ range ($\delta^{13}\text{C}=0.000007[\text{CO}_2]^2-0.0035[\text{CO}_2]-5.2922$; $R^2 = 0.92$, $n=140$). We corrected all TDL-AS values and obtained a stable $\delta^{13}\text{C}$ signal along the extended CO₂ mole fraction range.

The noise of the system was assessed by observing the standard deviation (S_d) of $\delta^{13}\text{C}$ values within each CO₂ step. We observed an average S_d of 0.16 ‰ for $\delta^{13}\text{C}$ ($n=21$). These values were used for the computation of the standard deviation of the observed discrimination by the leaf ($S_d\Delta_{\text{obs}}$, see below).

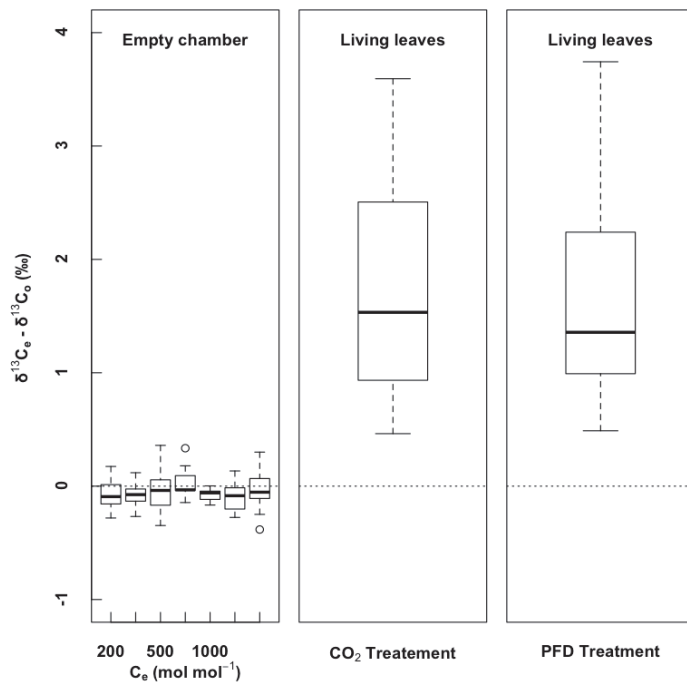


Figure 1: Boxplots of the difference in $\delta^{13}\text{C}$ between outlet and inlet of the 18 cm² chamber for (i) an empty chamber with inlet air CO₂ varying from 200 to 1000 $\mu\text{mol mole}^{-1}$ ($n=10$); (ii) the whole set of measurements under varying CO₂ concentrations (300 to 900 $\mu\text{mol mole}^{-1}$), $n=40$; (iii) the whole set of measurements under varying PPFD (from 200 up to 1100 $\mu\text{mol m}^{-2} \text{s}^{-1}$), $n=40$. The middle line represents the median, upper and lower box limit the 75% and 25% quartiles, respectively, and whiskers the extreme value.

Finally we used the empty photosynthesis chamber to test the absence of $\delta^{13}\text{C}$ difference between inlet and outlet that might be caused by leaks and/or CO₂ adsorption/desorption processes. We observed that the $\delta^{13}\text{C}_e - \delta^{13}\text{C}_o$ difference was stable along the CO₂ mole fraction range used during the test, and confirmed that the empty chamber did not affect isotopic composition of the air (i.e. leaks and CO₂ adsorption/desorption

processes were negligible). The observed $\delta^{13}\text{C}_e - \delta^{13}\text{C}_o$ difference was much smaller than the $\delta^{13}\text{C}$ difference recorded during actual measurements (Figure 1), although under specific conditions (low photosynthesis) the two could overlap. A data filtering procedure was therefore implemented (see below).

Model description

The observed discrimination (Δ_{obs}) is usually calculated following Evans *et al.* (1986):

$$\Delta_{\text{obs}} = \frac{\xi(\delta^{13}\text{C}_o - \delta^{13}\text{C}_e)}{1000 + \delta^{13}\text{C}_o - \xi(\delta^{13}\text{C}_o - \delta^{13}\text{C}_e)} \quad (\text{eq. 1})$$

where:

$$\xi = \frac{C_e}{C_e - C_o} \quad (\text{eq. 2})$$

ξ is the ratio of CO_2 entering the chamber over the CO_2 drawdown induced by the leaf.

Δ is the result of discrimination by diffusion processes during CO_2 movement from atmosphere to the chloroplast, and biochemical fractionation during carboxylation processes. Each fractionation step is characterized by a fractionation factor (due to diffusion or biochemistry) weighted by the gradient of concentration. In the complete form Δ is predicted by (Evans *et al.*, 1986):

$$\Delta = a_b \frac{C_a - C_s}{C_a} + a \frac{C_s - C_i}{C_a} + (e_s + a_i) \frac{C_i - C_c}{C_a} + b \frac{C_c}{C_a} - \frac{\frac{eR_d}{k} + \mathcal{F}^*}{C_a} \quad (\text{eq. 3})$$

where:

- a_b is the fractionation during CO_2 diffusion in the boundary layer (2.9‰, Farquhar, 1980);
- a is the fractionation during CO_2 diffusion in air through stomata into the leaf (4.4‰, O'Leary, 1981);
- e_s is the fractionation occurring when CO_2 is dissolved in the cell solution (1.1‰ at 25 °C, O'Leary, 1981);

- a_i is the fractionation during CO₂ diffusion in the liquid phase (0.7‰, O’Leary, 1981);
- b is the discrimination during carboxylation, and is depending on fractionation by both ribulose-1,5-bisphosphate carboxylase/oxygenase (RubisCO, $b_3 = 30$ ‰) and phosphoenolpyruvate carboxylase (PEPc, $b_4 = -5.7$ ‰),

$$b \text{ is computed as: } b = (1 - \beta) b_3 - \beta b_4 \quad (\text{eq. 4})$$

where β (between 0.05 and 0.1) is the relative amount of carbon fixed by PEPc (Farquhar and Richards, 1984). In our experiment we used a value of $b=28$ ‰, i.e., a β value of 0.055.

- f denotes overall discrimination during photorespiration. The value of f was set at 11‰, according to the theoretical approach of Tcherkez (2006), which was confirmed later by Lanigan *et al.* (2008);
- e denotes overall fractionation during day respiration relative to photosynthetic products (R_d), and can vary between -10 and +10 (Ghashghaie *et al.*, 2003). e was set at 1‰ before correction following Wingate *et al.* (2007);
- k is the carboxylation efficiency computed as (Farquhar *et al.*, 1982);

$$k = (A + R_d) / (C_i - \Gamma^*) \quad (\text{eq. 5})$$

- Γ^* is the CO₂ compensation point in the absence of day respiration (Brooks and Farquhar, 1985).

The estimation of g_m is based on the difference between the observed discrimination by the leaf (Δ_{obs}) and the discrimination predicted from the simplified form of the model (Δ_i) in which decarboxylation terms are ignored and g_m is considered to be infinite:

$$\Delta_i = a + (b - a) \frac{C_i}{C_a} \quad (\text{eq. 6})$$

With this ‘single point method’ first developed by Lloyd *et al.* (1992) and recently described by Pons *et al.* (2009), g_m can be estimated from a single value of Δ_{obs} :

$$g_m = \frac{(b - e_s - a_i) A / C_a}{(\Delta_i - \Delta_{obs}) - \frac{eR_d / k + f\Gamma^*}{C_a}} \quad (\text{eq. 7})$$

Model parameters

We estimated R_d and Γ^* with the “Laik method” (Viil *et al.*, 1977) for the three species, i.e., from the intersection of three A- C_i curves recorded at PPFDs of 100, 50 and 25 $\mu\text{mol photon m}^{-2} \text{s}^{-1}$ and C_e of 125, 100 and 50 $\mu\text{mol mol}^{-1}$. The “Laik method” provides C_i^* - or “apparent” CO_2 compensation point in the absence of day respiration (Von Caemmerer *et al.*, 1994), and was used as a proxy of Γ^* . Because these measurements are sensitive to errors due to CO_2 leak diffusion (low A and low C_a compared to the atmosphere), we estimated the potential CO_2 leaks due to diffusion through chamber gaskets (Flexas *et al.*, 2007a; Rodeghiero *et al.*, 2007). We computed a diffusion coefficient of the gaskets with the procedure provided in the user manual of LI-COR, and found a value of 0.938 $\mu\text{mol s}^{-1}$ (while it usually is 0.46 for smaller 6 cm^2 chambers). This correction was incorporated into all gas exchange computations used for Γ^* and R_d estimations. The computed values of Γ^* did not differ between species, so we used the mean ($\Gamma^*=38.7 \pm 0.51 \mu\text{mol mol}^{-1}$, $n=13$) as a common value for the three species. For *E. globulus*, *E. saligna* and *E. sieberi*, R_d was 0.41 ± 0.09 , 0.31 ± 0.09 and $0.68 \pm 0.07 \mu\text{mol m}^{-2} \text{s}^{-1}$, respectively.

As the isotopic signature of the reference gas provided by cartridges differed from that used by the leaves for earlier photosynthesis, e was replaced by $e' = e + \delta^{13}\text{C}_{\text{tank}} - \delta^{13}\text{C}_{\text{atmosphere}}$ (Wingate *et al.*, 2007). $\delta^{13}\text{C}$ in the cartridge was measured with the TDL-AS at the chamber inlet. In our case, the LI-6400 was fed with compressed CO_2 cartridges with $\delta^{13}\text{C}_{\text{tank}}$ varying between -1‰ and -4‰ except for two cartridges with $\delta^{13}\text{C}_{\text{tank}} = -19$ ‰. e' therefore varied between +4‰ and +6‰, except for two plants where it was -11‰.

C_c , the CO_2 concentration at the site of carboxylation was calculated from Fick’s Law as:

$$C_c = C_i - \frac{A}{g_m} \quad (\text{eq. 9})$$

Finally, we calculated the total leaf conductance to CO_2 following Ball (1988), assuming resistances in series as:

$$g_t = \frac{1}{\frac{1}{g_{sc}} + \frac{1}{g_m}} \quad (\text{eq. 10})$$

where the stomatal conductance to CO₂ is $g_{sc} = g_{sw}/1.6$.

Propagation of uncertainty from measurement to Δ calculation and data filtering

We estimated the uncertainty (standard deviation) of Δ_{obs} due to the finite precision of $\delta^{13}\text{C}$ measurements. This was achieved by propagating uncertainty (standard deviations) of $\delta^{13}\text{C}_e$ and $\delta^{13}\text{C}_o$ through the equations estimating Δ_{obs} (see Appendix I for details):

$$Sd_{\Delta_{\text{obs}}} = \left(\frac{\xi \sqrt{Sd_{\delta^{13}\text{C}_e}^2 + Sd_{\delta^{13}\text{C}_o}^2}}{\xi(\delta^{13}\text{C}_o - \delta^{13}\text{C}_e)} + \frac{1 + \sqrt{Sd_{\delta^{13}\text{C}_o}^2} - \xi \sqrt{Sd_{\delta^{13}\text{C}_e}^2 + Sd_{\delta^{13}\text{C}_o}^2}}{1 + \delta^{13}\text{C}_o - \xi(\delta^{13}\text{C}_o - \delta^{13}\text{C}_e)} \right) \Delta_{\text{obs}} \quad (\text{eq. 11})$$

The propagated uncertainty in Δ_{obs} (i.e., $\text{sd}\Delta_{\text{obs}}$) was used as the basis for a filter to remove unreliable estimates of Δ_{obs} . Computation of g_m is based on the difference between Δ_i and Δ_{obs} (i.e., $\Delta_i - \Delta_{\text{obs}}$), thus we reasoned that g_m estimates would be unreliable if the difference between $\Delta_i - \Delta_{\text{obs}}$ was smaller than $\text{Sd}_{\Delta_{\text{obs}}}$. Consequently we rejected all values where $\Delta_{\text{obs}} + \text{Sd}_{\Delta_{\text{obs}}} > \Delta_i$. We applied this filter to the individual points in the data set, rejecting 33 among 238 points.

Statistical analyses

All statistical analyses were performed with R (R Development Core Team 2010, <http://www.R-project.org>). Mixed-effect linear models were run to assess species and treatment effects on A , g_s , g_m , $\Delta_i - \Delta$, C_c and the $C_i - C_c$ drawdown, as shown in Table 1. For the CO₂ treatment, “species” (as a factor) and “C_i” (as a covariate) were incorporated into the model as fixed effects, and “individual within species” as a random effect. For variations of C_c and the $C_i - C_c$ drawdown, we used C_a as covariate. For PPFD treatment, species and PPFD were set as factors. Normality and heteroscedasticity were graphically checked with QQ-plots. In case of heteroscedastic data we weighted the mean as a function of the variance. In case of non-normal distribution, variables were log-transformed. The *species* \times *treatment* interaction was tested for each procedure, and was removed from the model when not significant. In the absence of interaction, we performed comparison of the intercepts to assess differences between species. In the case of interaction, slope comparisons were performed to

test if species response differed from each other. Significance was accepted at $P < 0.05$. We used mean least squares regression to assess the correlation between variables (R^2 and P -value).

RESULTS

Variation of g_m under changing C_e

CO₂ mole fraction was changed in the air entering the chamber in three steps from 300 to 900 $\mu\text{mol}\cdot\text{mol}^{-1}$, inducing a range of C_i from 185 to 745 $\mu\text{mol}\cdot\text{mol}^{-1}$. Net CO₂ assimilation rate (A) was positively related to C_i and varied between 3 and 18 $\mu\text{mol}\cdot\text{mol}^{-2}\cdot\text{s}^{-1}$, while stomatal conductance to water vapour (g_s) was negatively related to C_i and varied between 0.02 and 0.8 $\text{mol}\cdot\text{m}^{-2}\cdot\text{s}^{-1}$ (Figure 2). *E. sieberi* had significantly higher A and g_s than *E. globulus* and *E. saligna* (t-test $P < 0.05$, Figure 2).

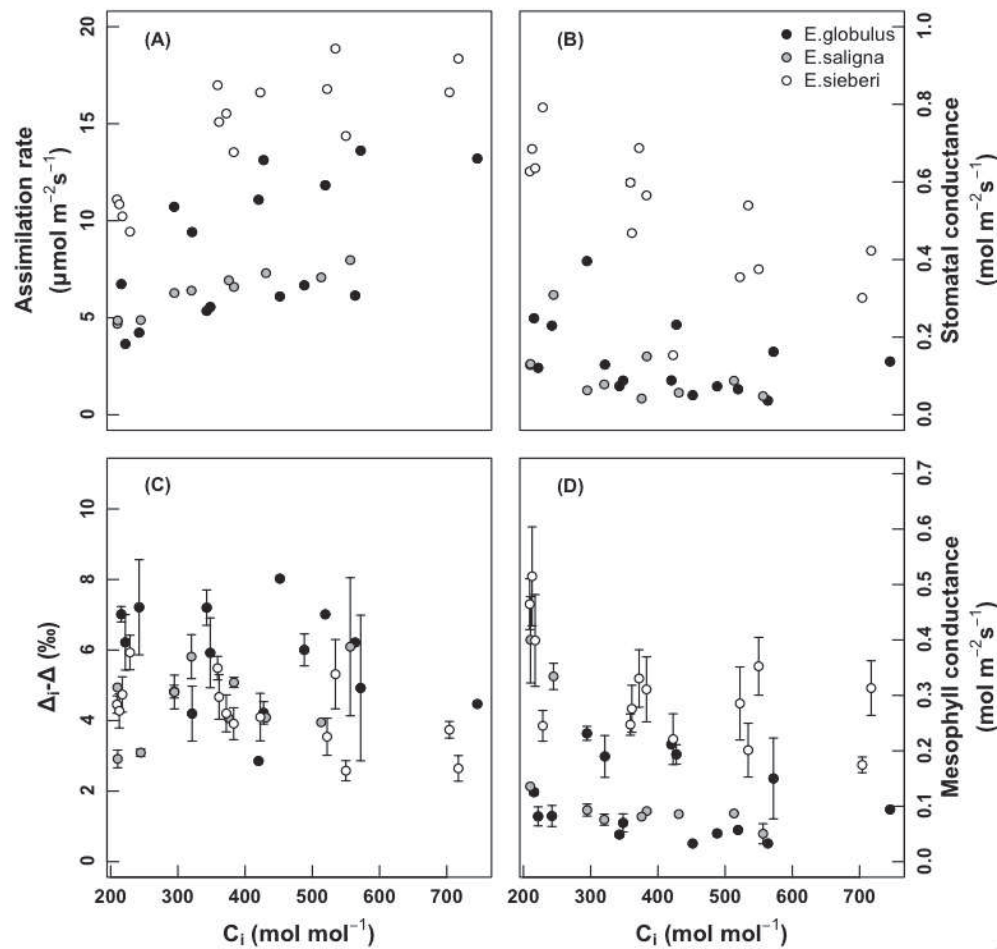


Figure 2: Relationships between CO₂ mole fraction in the substomatal cavities (C_i) and (A) net CO₂ assimilation rate (A), (B) stomatal conductance to water vapour (g_s), (C) difference between predicted and measured isotopic discrimination ($\Delta_i - \Delta$) and (D), mesophyll conductance (g_m). *E. globulus* in black, *E. saligna* in grey, and *E. sieberi* in white. SE is provided by the average of 3 measurements taken at 180 s intervals. Measurements were made at four levels of C_e on 4 plants per species, and were filtered against noisy values of $\delta^{13}\text{C}_e - \delta^{13}\text{C}_o$.

Table 1: Mixed effects model for A , g_s , g_m and $\Delta_i - \Delta$. *Species*, C_a and C_i or PPFD effects were incorporated into the model as fixed effects, and *individual plant* as a random effect. In case of heteroscedastic data the mean was weighted as a function of the variance. For C_i and C_a degree of freedom (df) was 1, for PPFD $df=3$, and for *species* $df=2$. Significant values ($p<0.05$) in bold.

		$\underline{C_i}$				$\underline{C_a}$		\underline{PPFD}					
		A	g_s	g_m	$\Delta_i - \Delta$	C_c	$C_i - C_c$	A	g_s	g_m	$\Delta_i - \Delta$	C_c	$C_i - C_c$
<u>Variable</u>	F	168.11	38.82	18.67	3.70	165.01	102.90	86.01	34.23	6.41	NS	NS	NS
	P	<0.001	<0.001	<0.001	(0.06)	<0.001	<0.001	0.001	<0.001	0.002	NS	NS	NS
<u>Species</u>	F	13.31	26.33	10.11	6.36	4.64	7.65	14.65	(2.91)	NS	NS	NS	NS
	P	0.002	<0.001	0.006	0.02	0.045	0.013	<0.01	(0.10)	NS	NS	NS	NS
<u>Interaction</u>	F	3.05	NS	3.44	NS	5.84	3.72	14.88	4.55	NS	NS	NS	NS
	P	(0.06)	NS	0.047	NS	0.008	0.038	<0.001	0.002	NS	NS	NS	NS

The difference between $\delta^{13}\text{C}_e$ and $\delta^{13}\text{C}_o$ decreased with increasing C_i (data not shown). Among all species, Δ_{obs} varied between 12‰ and 22‰ and was positively correlated to C_i/C_a ($R^2=0.79$, $P<0.001$, data not shown). The difference between Δ calculated with infinite g_m and no respiratory term (simple model) and observed Δ ($\Delta_i-\Delta_{\text{obs}}$) varied between 3 and 7‰ but showed no clear trend with C_i (Figure 2, Table 1).

Mesophyll conductance (g_m) computed by taking into account the respiratory component of discrimination varied from 0.025 to 0.55 $\text{mol m}^{-2} \text{s}^{-1}$ (Figure 2). g_m was larger in *E. sieberi* than in the other two species (t-test, $P<0.05$). g_m was affected by C_i (Table 1), and decreased when C_i increased. Post-hoc tests revealed that *E. globulus* and *E. saligna* displayed g_m - C_i slopes significantly different from zero. In *E. sieberi*, three individuals out of four showed a clear negative pattern when C_i increased, but not the fourth. The relationship between g_m and g_s was significant among all species ($R^2=0.54$, $P<0.001$), and within *E. globulus* and *E. saligna* when treated separately (data not shown).

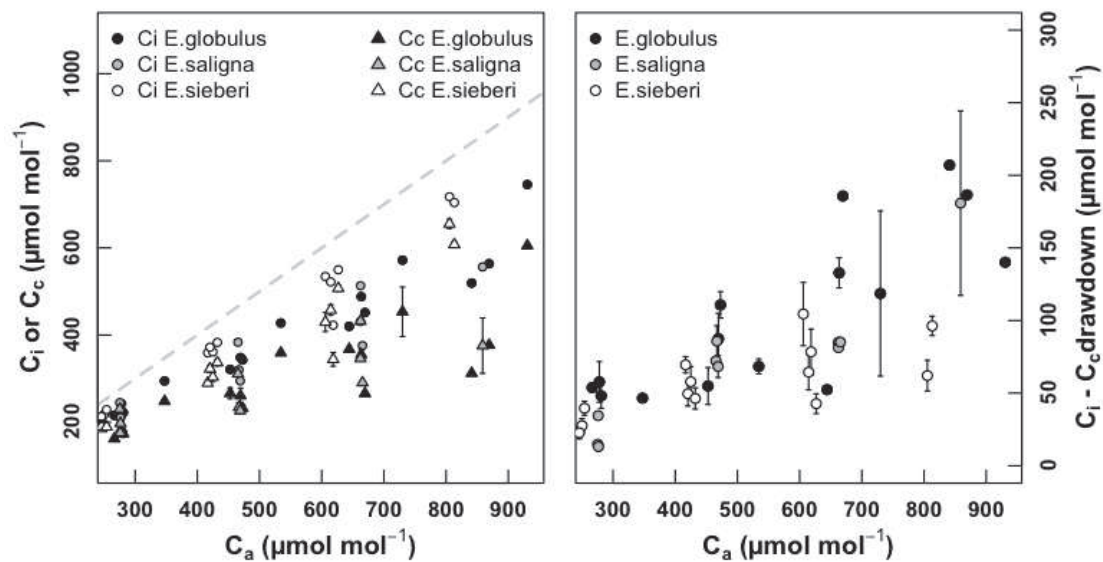


Figure 3: Left: CO₂ mole fraction in the substomatal cavities (C_i , disks) and at carboxylation sites (C_c , triangles) as a function of C_a . The dashed grey line is the 1:1 relationship. Right: C_i - C_c drawdown as a function of C_a . Each point represents the mean of 1-3 analytical measurement mean \pm SE, with *E. globulus* in black, *E. saligna* in grey, and *E. sieberi* in white.

C_c and the C_i - C_c drawdown were as expected severely affected by C_a (Table 1). The C_i - C_c drawdown was around $50 \mu\text{mol mol}^{-1}$ at $C_a=200 \mu\text{mol mol}^{-1}$ and increased up to 200 at $C_a=900$ (Figure 3). When tested individually, all slopes of the responses of C_c and C_i - C_c to C_i were different from zero.

Variation of g_m with changing irradiance

A and g_s increased significantly with irradiance (Table 1). A and g_s were larger in *E. sieberi* than in the two other species (see Figure 4, t-test $P<0.05$). In each species, g_s increased significantly from 200 to $500 \mu\text{mol m}^{-2} \text{s}^{-1}$ PPFD, and then stabilised (figure 4). A and g_s were positively correlated, all species treated together (Figure 5C, $R^2=0.76$, $P<0.001$). Across the range of irradiance, Δ_{obs} varied between 11‰ and 20‰ and was positively correlated with C_i/C_a ($R^2=0.74$, $P<0.001$, data not shown). Δ_i - Δ_{obs} varied between 3 and 9 ‰ but was not affected by irradiance nor by species (Table 1, Figure 4).

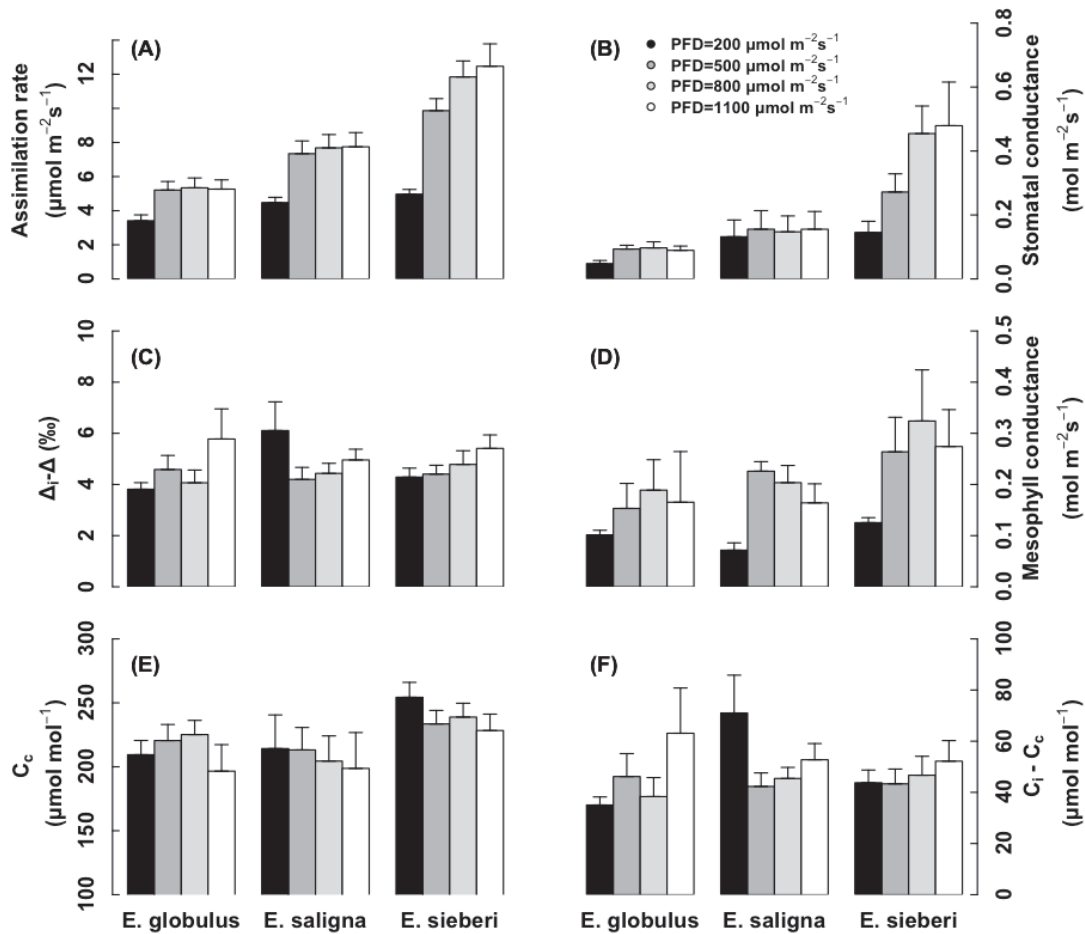


Figure 4. (A) Net CO₂ assimilation rate (A), (B) stomatal conductance to water vapour (g_s), (C) difference between predicted and measured isotopic discrimination (Δ_i - Δ_{obs}), (D) mesophyll conductance

(g_m), (E) CO_2 mole fraction at carboxylation sites (C_c) and (D) the C_i - C_c drawdown at 4 different levels of PPFD. Means \pm SE ($n=2-4$ replicate plants), with *E. globulus* in black, *E. saligna* in grey, and *E. sieberi* in white.

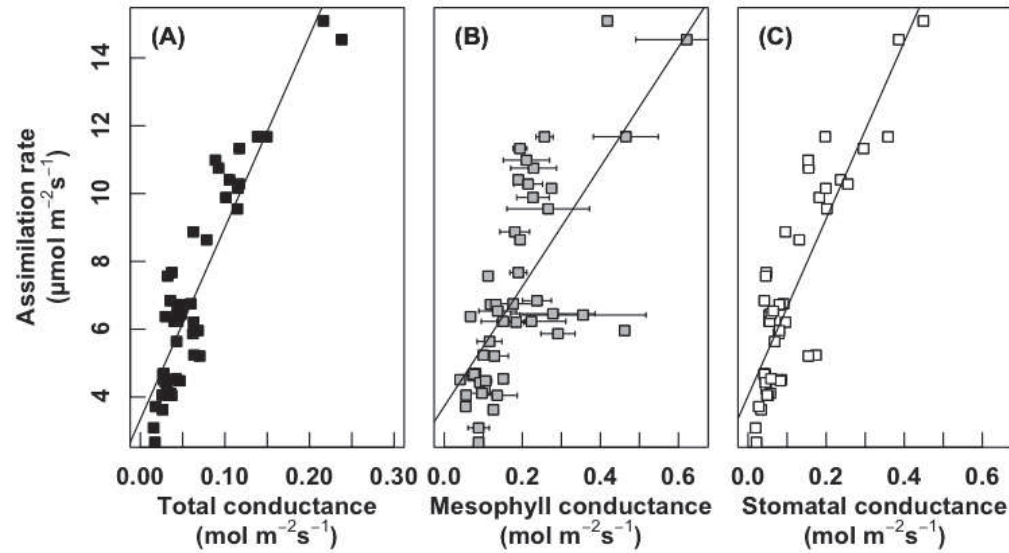


Figure 5: Relationships between net CO_2 assimilation rate (A) and (A) total leaf conductance to CO_2 (g_t , black squares), (B) internal conductance to CO_2 (g_m , grey squares) and (C) stomatal conductance to CO_2 (g_s , white squares) under varying PPFD.

g_m varied between 0.04 and 0.6 $\text{mol mol}^{-2}\text{s}^{-1}$, and was positively related to PPFD. As for g_s , the response consisted of a significant increase between 200 and 500 $\mu\text{mol m}^{-2}\text{s}^{-1}$ PPFD with a stabilisation above this threshold. g_m was positively correlated with g_s ($R^2=0.36$, $p<0.001$, data not shown) and A ($R^2=0.49$, $p<0.001$, Figure 5B), among all species. We also detected significant A - g_m and g_m - g_s relationships within each species (except for g_s - g_m in *E. saligna*).

Total leaf conductance to CO_2 (g_t) was strongly correlated to A ($R^2=0.83$, $P<0.001$) as shown in Figure 5A. Over the full set of irradiance values, C_c varied between 200 and 260 $\mu\text{mol mol}^{-1}$, and the C_i - C_c drawdown between 40 and 60 $\mu\text{mol mol}^{-1}$. None of these parameters displayed any variation with irradiance (Table 1), or with species.

DISCUSSION

This study provides support to recent evidence that mesophyll conductance (g_m) varies rapidly (within minutes) in response to environmental conditions. The rapid responses were observed under two different sources of variation: CO₂ mole fraction and irradiance. In seedlings of three *Eucalyptus* species we found a modest but significant decrease of g_m with increasing CO₂ mole fraction, and a significant increase with irradiance. The effect was visible in the three species irrespective of the photosynthetic capacity.

Importance of the respiratory and photorespiratory terms in the estimation of mesophyll conductance

The isotopic method estimates g_m from the ¹³CO₂ discrimination during photosynthesis by comparing observed values with those derived from a model based predicting discrimination under infinite mesophyll conductance. This approach requires a high precision in discrimination records, which is now achieved by combining precise leaf gas exchange measurements with online TDL-AS records of changes in ¹³CO₂/¹²CO₂ in the atmosphere around the leaf (see Pons et al, 2009; Tazoe et al, 2011 for a discussion of the technique). One of the important problems with this method is the fact that several discrimination steps during photosynthesis, respiration, and photorespiration need be taken into account. In particular, a number of earlier studies omitted the respiratory and photorespiratory terms (Flexas *et al.*, 2007b; Vrabl *et al.*, 2009). Moreover, the response of g_m was affected by the O₂ mole fraction in the air, i.e., by the occurrence photorespiration during measurements: it was visible only under low O₂ (Tazoe *et al.*, 2011).

In the present study, we incorporated these two terms into the g_m estimates displayed in our results. Absolute values of g_m were up to 50% larger when these terms were incorporated, and this enhancement was independent of the treatments applied (Figure 6). We tested whether this potentially large change had an impact on the observed effects of changing CO₂ mole fraction in the air or irradiance: the response of g_m to CO₂ mole fraction and irradiance remained significant even when the respiratory term was omitted (see table 2). We similarly tested the effects of substituting e (fractionation during day respiration) and f (fractionation during

photorespiration) with extreme values ($f=0\%$, $e=-10\%$, $e=+10\%$). Despite the fact that these changes resulted in significant differences of computed g_m , they did not result in any loss of significance of the observed effects of CO_2 or irradiance (data not shown). Vrabl *et al.* (2009) compared g_m estimated with the fluorescence method (which takes the respiratory terms implicitly into account) and with the isotopic method (without taking it into account) and found the same range of g_m values and the same negative response to C_i . Our computations suggest that the respiratory terms can be important in the estimation of the absolute values of g_m , but have only little influence on the observed CO_2 or irradiance responses of g_m . The respiratory terms of isotopic discrimination are unlikely responsible for the discrepancies among studies. We omitted in this discussion to address the question of changing e and f during the CO_2 and irradiance treatments: up to now, there is no reason to assume that these values are not stable across the whole range of environmental conditions.

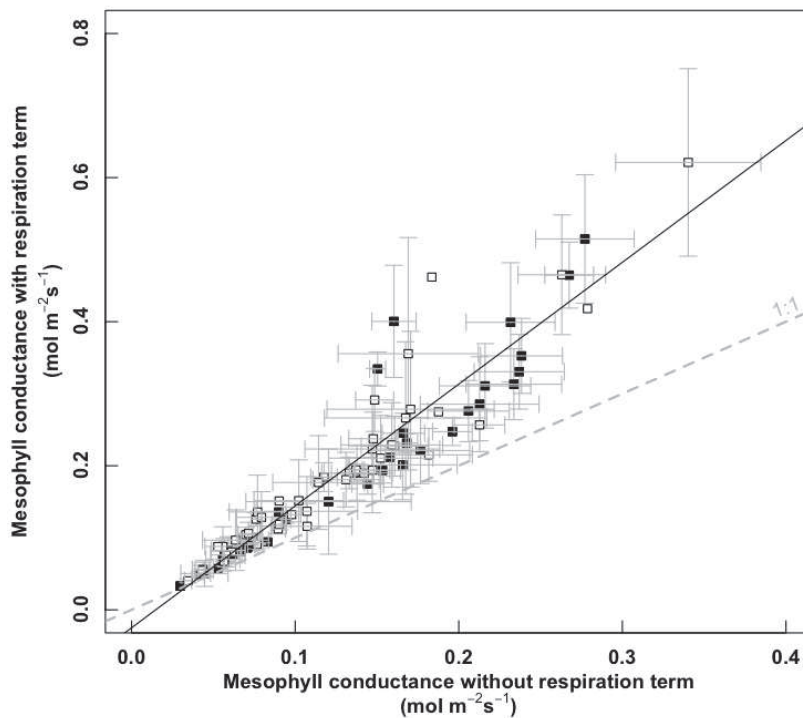


Figure 6: Mesophyll conductance g_m as computed by taking into account the contribution of respiration and photorespiration to $^{13}CO_2$ discrimination vs without taking them into account (i.e., fractionation factors e and f set to 0 in Eqn. 7). Results obtained under changing CO_2 (black squares) or irradiance (white squares). The dashed line represents

the 1:1 relationship. Each point represents the mean \pm SE of a given measurement ($n=3$).

Response of g_m to CO₂ mole fraction.

There was at maximum a 50% decrease in g_m with increasing CO₂ mole fraction (300 to 900 $\mu\text{mol mol}^{-1}$). This response was general, as all three species displayed a similar response to CO₂, with the exception of a single individual of *E. sieberi*. Our results contrast with earlier studies reporting no response of g_m to CO₂. This was the case in *Quercus ilex* and *Citrus aurantium* (chlorophyll fluorescence method, Loreto *et al.*, 1992), *Raphanus sativus* (isotopic discrimination, Von Caemmerer and Evans, 1991) and *Triticum aestivum* (isotopic discrimination, Tazoe *et al.*, 2009). Our results confirm several studies that reported a negative relationship between g_m and CO₂ (Flexas *et al.*, 2007b; Hassiotou *et al.*, 2009; Vrábl *et al.*, 2009; Bunce, 2010). We found the same magnitude of decrease of g_m with C_i than Flexas *et al.* (2007b) and Vrábl *et al.* (2009). Tazoe *et al.* (2011) found a $\approx 30\%$ decrease of g_m when C_i increased under 1% O₂ but no effect under 21% O₂ in two *Arabidopsis thaliana* genotypes or in *Nicotinia tabacum*, while we found a significant effect even under 21% O₂. The absence of a clear pattern of g_m responses among studies could be interpreted as a species-dependent response of g_m to C_i , but no common trait seems to be shared by the “non-responsive” vs. the “responsive” species.

There are a suite of methodological reasons and artifacts (e.g., choice or calculation of b , e , f , R_d or Γ^*) that might explain the discrepancy among studies. The case for e and f was discussed above. We used measured values of R_d and Γ (i.e., of its proxy C_i^*) for each species rather than arbitrary values taken from the literature. Despite some uncertainties regarding the choice of b or f (Lanigan *et al.*, 2008; Pons *et al.*, 2009), we conclude that the response of g_m that we recorded here is unlikely to be an artefact.

Rapid responses of g_m to CO₂ could be mediated by aquaporins that might impact the permeability of plasma and chloroplast membranes to CO₂ (Terashima and Ono, 2002), enhancing CO₂ diffusion in the liquid phase. Flexas *et al.* (2006) stated that NtAQP1 aquaporins expression can change g_m values by 20 to 50% in *Nicotiana tabacum*. These variations of g_m are of the same magnitude that in our study, but only direct measurements of aquaporin expression/activity could confirm the role of these proteins to the diffusion of CO₂ through membranes. Establishing a parallel between short term responses of g_m and of the expression and activities of aquaporins is still an

open area for research. Tholen *et al.* (2008) also found that chloroplast movements can induce a variation of g_m by 50% in *Arabidopsis thaliana*. But it is not known yet whether CO₂ variations can directly mediate a displacement of chloroplasts.

We observed a positive relationship between g_m and stomatal conductance g_s , as did Flexas *et al.* (2007c). Interestingly, such a relationship was also found by Flexas *et al.* (2006) when they compared plants over-expressing NtAQP1 aquaporin and controls. They suggested that the variation of g_m primarily induced by manipulating NtAQP1 expression, probably also lead to an adjustment of g_s and subsequently of A . This potentially indicates a physiological link between these two parameters (Flexas *et al.*, 2007c; Vrabl *et al.*, 2009). Nevertheless, the precise signalling cascade that could cause a coordinated response of stomatal and of mesophyll conductance remains to be elucidated.

Response of g_m to irradiance

Several studies observed an increase of g_m with increasing irradiance. Flexas *et al.* (2007b) reported that g_m increased in tobacco by ~40% when irradiance increased from 250 to 1000 $\mu\text{mol m}^{-2} \text{s}^{-1}$. Data from Gorton *et al.* (2003), reanalyzed by Flexas *et al.* (2008), also showed a positive effect of irradiance on g_m . Hassiotou *et al.* (2009) detected a ~22% increase in six *Banksia* species as irradiance was switched from 500 to 1500 $\mu\text{mol m}^{-2} \text{s}^{-1}$. Our study corroborates this positive effect of irradiance, with an increase of g_m by 60%, up to a plateau in irradiance reached between 500 and 1100 $\mu\text{mol m}^{-2} \text{s}^{-1}$, depending on the species. We found a slightly larger sensitivity of g_m to irradiance than earlier studies. Sensitivity to irradiance could be (i) species-dependent or (ii) due to different parameterisation of the model enabling g_m estimation. For instance, in our case, removing the respiratory and photorespiratory terms in the estimation of g_m led to a slightly smaller response of g_m to irradiance (table 2). A systematic analysis of the reported responses, with a standardised parameterisation, would be very helpful.

Like during the response to CO₂, g_m was positively correlated to g_s . This relationship seems to be independent of the method used to vary net CO₂ assimilation rates. A review by Flexas *et al.* (2008) insisted that g_s and g_m responded in parallel to irradiance, CO₂, temperature, and drought stress (Warren, 2008b). On the other hand,

Warren (2008b) reported that g_m was unaffected by increases in vapour pressure deficit while g_s decreased strongly, and Vrábl *et al.* (2009) reported that g_m was unaffected by feeding leaves with abscisic acid (ABA), whereas there was a clear decrease of g_s . In the two latter cases net CO₂ assimilation rate remained unaffected by VPD and ABA despite the severe reduction of g_s . The g_s - g_m relationship therefore may reflect a tight coordination between A and g_m . Thus it seems that g_m contributes to adjust the CO₂ supply to the sites of carboxylation in response to photosynthetic limitations like light availability, hydraulic constraints or biochemical limitations (Warren *et al.*, 2007). In our study, the coordinated variations of g_s and g_m apparently led to a very stable C_c (and C_i - C_c draw down) across irradiance levels, despite large variation in A . Such an homeostasis of C_c was already observed across a range of leaf morphologies (Hassiotou *et al.*, 2009), during leaf ageing (Ethier *et al.*, 2006; Warren, 2006), and such an adjustment seems to occur also during short-term fluctuations of irradiance.

CONCLUSION

This study with three *Eucalyptus* species confirmed that g_m estimated with the online ¹³C discrimination method, declines in response to short term increases of CO₂ mole fraction and increases with irradiance. The response to irradiance is saturated above 500 $\mu\text{mol m}^{-2} \text{s}^{-1}$ PPFD. The respiratory term in the ¹³C discrimination equation was found to be important to estimate absolute values of g_m but had little impact on the CO₂ and irradiance responses. During the responses to CO₂ and PPFD, g_s and g_m were tightly correlated and varied in parallel independently of the source of variation. Moreover, we observed that coordinated adjustments of CO₂ demand (A) and supply (g_s and g_m) led to a stability of C_c across irradiance variations. C_c homeostasis could be an advantage for the leaf to prevent large variation of the oxygenation/carboxylation ratio of the RubisCO, when the CO₂ demand increases.

APPENDIX I

Here we describe the procedure to calculate the standard deviation of Δ_{obs} ($Sd_{\Delta_{\text{obs}}}$) based on the standard deviation of the isotopic composition of reference and measured air ($Sd_{\delta^{13}\text{C}_e}$ and $Sd_{\delta^{13}\text{C}_o}$, respectively). In the equation of Evans et al (1986) to calculate Δ_{obs} , we substituted $\delta^{13}\text{C}_e$ and $\delta^{13}\text{C}_o$ by their respective standard errors $Sd_{\delta^{13}\text{C}_e}$ and $Sd_{\delta^{13}\text{C}_o}$ to obtain:

$$Sd_{\Delta_{\text{obs}}} \approx \frac{\xi(Sd_{\delta^{13}\text{C}_o} - Sd_{\delta^{13}\text{C}_e})}{1 + Sd_{\delta^{13}\text{C}_o} - \xi(Sd_{\delta^{13}\text{C}_o} - Sd_{\delta^{13}\text{C}_e})}$$

We replaced $(Sd_{\delta^{13}\text{C}_o} - Sd_{\delta^{13}\text{C}_e})$ and $Sd_{\delta^{13}\text{C}_o}$ by $\sqrt{Sd_{\delta^{13}\text{C}_o}^2 + Sd_{\delta^{13}\text{C}_e}^2}$ and $\sqrt{Sd_{\delta^{13}\text{C}_o}^2}$, respectively, as it is described in (Harris D.C., 1991) to obtain:

$$Sd_{\Delta_{\text{obs}}} \approx \frac{\xi \sqrt{Sd_{\delta^{13}\text{C}_o}^2 + Sd_{\delta^{13}\text{C}_e}^2}}{1 + \sqrt{Sd_{\delta^{13}\text{C}_o}^2} - \xi \sqrt{Sd_{\delta^{13}\text{C}_o}^2 + Sd_{\delta^{13}\text{C}_e}^2}}$$

Then, to calculate the cumulative effect of the upper term and the lower term, we summed their relative Sd to obtain the relative standard error of Δ_{obs} :

$$\frac{Sd_{\Delta_{\text{obs}}}}{\Delta_{\text{obs}}} = \left(\frac{\xi \sqrt{Sd_{\delta^{13}\text{C}_o}^2 + Sd_{\delta^{13}\text{C}_e}^2}}{\xi(\delta^{13}\text{C}_o - \delta^{13}\text{C}_e)} \right) + \left(\frac{1 + \sqrt{Sd_{\delta^{13}\text{C}_o}^2} - \xi \sqrt{Sd_{\delta^{13}\text{C}_o}^2 + Sd_{\delta^{13}\text{C}_e}^2}}{1 + \delta^{13}\text{C}_o - \xi(\delta^{13}\text{C}_o - \delta^{13}\text{C}_e)} \right)$$

$Sd_{\Delta_{\text{obs}}}$ is then equal to:

$$Sd_{\Delta_{\text{obs}}} = \left(\frac{\xi \sqrt{Sd_{\delta^{13}\text{C}_o}^2 + Sd_{\delta^{13}\text{C}_e}^2}}{\xi(\delta^{13}\text{C}_o - \delta^{13}\text{C}_e)} + \frac{1 + \sqrt{Sd_{\delta^{13}\text{C}_o}^2} - \xi \sqrt{Sd_{\delta^{13}\text{C}_o}^2 + Sd_{\delta^{13}\text{C}_e}^2}}{1 + \delta^{13}\text{C}_o - \xi(\delta^{13}\text{C}_o - \delta^{13}\text{C}_e)} \right) \Delta_{\text{obs}}$$

CHAPTER III

Is mesophyll conductance to CO₂ in leaves of three *Eucalyptus* species sensitive to short-term changes of irradiance under ambient as well as low O₂?

Is mesophyll conductance to CO₂ in leaves of three *Eucalyptus* species sensitive to short term changes of irradiance under ambient as well as low O₂?

Cyril DOUTHE^{1,2,3}, Erwin DREYER^{1,2*}, Oliver BRENDDEL^{1,2}, Charles R. WARREN³

1. INRA, Unité Mixte de Recherches 1147 "Ecologie et Ecophysiologie Forestières", F 54280 CHAMPENOUX, France

2. Nancy-Université, Unité Mixte de Recherches 1147 "Ecologie et Ecophysiologie Forestières", Faculté des Sciences, F 54500 VANDOEUVRE, France

3. University of Sydney, School of Biological Sciences, Heydon-Laurence Building, A08, The University of Sydney, NSW 2006, Australia.

Emails: Cyril.Douthé@nancy.inra.fr; dreyer@nancy.inra.fr; brendel@nancy.inra.fr, charles.warren@sydney.edu.au

*Correspondence and reprints

Short title: Changes of mesophyll conductance with irradiance and O₂

Additional Keywords: Photosynthesis, stomatal conductance, tuneable diode laser absorption spectrometry, photorespiration, ¹³C discrimination

Number of words in the main text: 6576.

Figures: 6

Tables: 5

ABSTRACT

Mesophyll conductance to CO₂ (g_m) limits the diffusion of CO₂ to the sites of carboxylation, and may respond rapidly (within minutes) to abiotic factors. We tested the rapid response of g_m to irradiance in three *Eucalyptus* species, under 21 and 1% O₂ in the atmosphere, with simultaneous measurements of leaf gas exchange and of on-line discrimination against ¹³CO₂ with a tuneable diode-laser absorption spectrometer (TDL-AS). 1% O₂ was used to specifically limit the uncertainties due to the ¹³C/¹²C fractionation occurring during photorespiration. Decreasing irradiance from 600 to 200 μmol m⁻² s⁻¹ led to a ≈60% decrease in g_m in all species under 21% O₂ while this effect was smaller but still significant under 1% O₂. The decrease of g_m was partly (17% at most) due to the increase of CO₂ in the chamber with nevertheless a dominant direct effect of irradiance alone. g_m apparently increased by ≈30% when O₂ was switched from 21 to 1%. Simulations showed that g_m estimates were only marginally sensitive to changes in most model parameters except in b (¹²C/¹³C fractionation during carboxylation), which in turn is dependent on β (the fraction of CO₂ assimilated by PEPc). Nevertheless, large irradiance or O₂-induced changes in β would be required to fully explain the observed changes in g_m . While the response of g_m to irradiance seems realistic, such a response to O₂ was never described before and remains questionable.

INTRODUCTION

Mesophyll conductance to CO₂ (g_m) induces a draw-down of CO₂ partial pressure (or mole fraction) between sub-stomatal cavities (C_i) and the sites of carboxylation in the chloroplast (C_c). When the biochemical model of photosynthesis of C₃ plants was first developed by Farquhar *et al.* (1980), it was considered that C_c was in equilibrium with C_i and thus mesophyll conductance was infinite. During the past two decades, accumulating evidence suggested that g_m is not infinite and C_c is substantially smaller than C_i (Evans *et al.* 1986; Lloyd *et al.* 1992; Terashima *et al.*, 2011). g_m varies among species from 0.05 to 0.5 mol m⁻² s⁻¹ and is often of a similar size than stomatal conductance g_s (see the review by Flexas *et al.* 2008). Variation of g_m among species is correlated with leaf anatomy, in particular leaf thickness, cell wall thickness, leaf mass per unit area or the cumulated chloroplast surface exposed to the intercellular air spaces (Flexas *et al.* 2008; Hassiotou *et al.* 2009; Terashima *et al.* 2006; Tholen *et al.* 2007, Terashima *et al.* 2011).

One of the open questions about mesophyll conductance is whether it changes rapidly (within minutes) in response to variations of environmental conditions. Support for rapid responses has come from the observation that g_m increased with increasing irradiance in three *Eucalyptus* species (Douthe *et al.* 2011) and *Nicotiana tabaccum* (Flexas *et al.* 2008) and decreased under increasing CO₂ concentration in trees and annual plants (Flexas *et al.* 2007), like for instance in three *Eucalyptus* species (Douthe *et al.* 2011), in seven *Banksia* species (Hassiotou *et al.* 2009), in three annuals (Tazoe *et al.* 2011) and in *Helianthus annuus* (Vrabl *et al.* 2009). However, some authors did not detect any response of g_m to CO₂ and/or irradiance like in *Triticum aestivum* (Tazoe *et al.* 2009) and *Nicotiana tabaccum* (Yamori *et al.* 2010). This discrepancy among studies is not yet fully elucidated.

Combined measurements of leaf gas exchange and discrimination against ¹³CO₂ during photosynthesis constitute one of the reference methods for estimating g_m (see Pons *et al.* 2009 and Warren 2006, for reviews). Overall discrimination against ¹³CO₂ (Δ , in ‰) is the result of fractionation during diffusion of CO₂ from atmosphere into chloroplasts, during carboxylation, photorespiration and respiration (Farquhar *et al.* 1982). The computation of g_m from gas exchange and online ¹³C discrimination is affected by a range of uncertainties related to the accuracy of the measurements and the uncertainty around parameter values (see Pons *et al.* 2009). Particular attention

has been devoted recently to discrimination during respiration and photorespiration (Gillon and Griffiths 1997; Lanigan *et al.* 2008; Tcherkez 2006; Tcherkez *et al.* 2011) and the fractionation factor associated to glycine decarboxylation and production of photorespired CO₂ has been estimated. In addition, decreasing O₂ in the air surrounding a leaf is a useful method to reduce uncertainties induced by photorespiration, since the oxygenase activity of RubisCO and therefore the emission of photorespired CO₂ decreases to almost zero under low O₂ in the chloroplast (Farquhar *et al.* 1980). Hence, g_m was sometimes recorded under low O₂ (Tazoe *et al.* 2009). Three studies estimated g_m under different O₂ concentrations and reported a lack of change of g_m from ambient to low O₂: Flexas *et al.* (2007) and Von Caemmerer and Evans (1991) used the isotopic method, and Loreto *et al.* (1992) used both isotopic and chlorophyll fluorescence methods. Nevertheless, Tazoe *et al.* (2011) observed that g_m was less responsive to changes in CO₂ under 21 than 1% O₂ which suggests that the computation of g_m might be affected by photorespiration.

Surprisingly, to the best of our knowledge, no study ever considered the occurrence of potential, irradiance or O₂-induced changes in some parameters of the model (besides the obvious change of Γ^* , directly related to O₂ as predicted by the model of Farquhar *et al.* 1980); in particular, changes in the ratio carboxylation by rubisco to carboxylation by PEPc may occur as a response to changing irradiance or O₂. Given that such rapid changes could have important consequences for the estimation of g_m , this is an important shortcoming in our knowledge of short term responses of g_m .

The first objective of our study was to detect rapid responses of g_m to irradiance. Discrimination against ¹³CO₂ by the leaf was assessed by measuring leaf gas exchange with a custom built gas-exchange chamber coupled to a tuneable diode-laser absorption spectrometer (TDL-AS) which allows high frequency measurements of ¹³CO₂ and ¹²CO₂ during photosynthesis. Three *Eucalyptus* species differing in photosynthetic capacity were used to investigate the inter-specific stability of the g_m response to irradiance. The single point method was used to estimate g_m (Pons *et al.* 2009). Measurements were performed under 21 and 1% O₂ to modulate photorespiration and its influence on ¹³C discrimination. Our second objective was to check *via* simulations if the rapid response of g_m to irradiance and possibly O₂ could not be attributed to an artefact due to uncertainties in parameters of the $\Delta^{13}\text{C}$ model

(non-photorespiratory respiration, R_d ; fractionation during non photorespiratory respiration, e or during photorespiration f , and during carboxylation, b and finally CO_2 compensation point Γ^*). We first used a range of biologically relevant values for each parameter, to check whether a response of g_m was still detectable under different parameter sets. During a second step, we checked whether rapid variations of these parameters during changes in irradiance or O_2 could cause or at least contribute to the apparent variations of g_m with irradiance and O_2 .

MATERIAL AND METHODS

Plant material

We used three *Eucalyptus* species: *E. globulus* Labill., *E. saligna* Sm. and *E. sieberi* L. A. S. Johnson. Plants were grown for 5 months in a greenhouse under natural light at an average daily temperature of 25°C in 8L pots filled with compost-based substrate. They were watered with automatic drip irrigation. At the time of the experiment they were ~70 cm high.

Photosynthesis and isotopic measurements

We used the experimental set-up described in Douthe *et al.* (2011). It includes a LI-6400 portable gas exchange system (LI-COR, Lincoln, NE, USA) equipped with a 18 cm² custom built chamber, and coupled to a TDL-AS (TGA100A, Campbell Scientific, Logan, UT, USA). Air flow into the chamber was set at 400 $\mu\text{mol s}^{-1}$, and air temperature at 25°C, leading to leaf temperatures of 25.5°C \pm 0.58°C (n=90). Irradiance was provided by a LI-COR RGB light source (6400-18, LI-COR), which covered the entire chamber surface. A sub-sample of air was diverted from the sample (at chamber outlet) and from the reference gas line of the LI-6400, into the TDL-AS. The TDL-AS measured sequentially gas from two calibration cylinders, the LI-6400 reference gas and finally the LI-6400 sample gas. Each intake was measured for 45 s. The data from the first 15 s were ignored to minimise carryover and enable stabilisation between intakes when switching sources. The total time for a sequence of measurements was therefore 180 s.

Total CO₂ concentration in the two calibration cylinders was given by the cylinder supplier and checked with a recently factory-calibrated LI-8100 IRGA (LI-COR, Lincoln, NE, USA) while $\delta^{13}\text{C}$ was analysed *via* the gas-bench inlet of an IRMS (Delta S, Finningan, Bremen) at INRA Nancy (n= 10 glass exetainers/tank, Labco, Buckinghamshire, UK). Absolute values of ¹²CO₂ and ¹³CO₂ were respectively 414.5 and 4.487 $\mu\text{mol mol}^{-1}$ for cylinder 1 and 286.89 and 3.104 $\mu\text{mol mol}^{-1}$ for cylinder 2, which corresponds to CO₂ mole fraction and $\delta^{13}\text{C}$ of 419 \pm 10 $\mu\text{mol mol}^{-1}$, -36.6 \pm 0.08‰ and 290 \pm 7, -36.9 \pm 0.2‰, for cylinder 1 and 2, respectively (means \pm sd). A linear interpolation between the two points for each isotopologue was used for calculating $\delta^{13}\text{C}_e$ and $\delta^{13}\text{C}_o$. All CO₂ mole fractions used

during our measurements remained within this calibration range.

Measurements were made under photosynthetic photon flux densities (PPFD) of 1000, 600 and 200 $\mu\text{mol m}^{-2} \text{s}^{-1}$ under 21 and 1% O_2 , on a single leaf of five individuals per species (i.e., 3 levels of irradiance x 2 O_2 mole fractions x 5 replicate leaves x 3 species). All measurements were made on the youngest fully expanded leaf.

For measurements under 21% O_2 , ambient air was pumped at approximately 2 l min^{-1} to the LI-6400 inlet via a “T” junction and vent (to prevent over-pressurisation). CO_2 was removed with the LI-6400 soda lime and then the desired CO_2 was added with the LI-6400 CO_2 -controller. For measurements under 1% O_2 , ambient air at 0.1 l min^{-1} was mixed with high purity nitrogen (99.99%, Air Liquide) at 1.9 l min^{-1} to feed the LI-6400. In this latter case, the LI-6400 configuration was adjusted to account for the effect of O_2 on calibration (Bunce 2002). When O_2 was switched from 21 to 1%, a constant offset of +1.287‰ was detected in $\delta^{13}\text{C}$ at the inlet due to changes in sensitivity of the TDLAS. All records of inlet and outlet $\delta^{13}\text{C}$ under low O_2 were thereafter recomputed with this constant offset.

The measurement sequence was 1000, 600 and 200 $\mu\text{mol m}^{-2} \text{s}^{-1}$, each irradiance step being measured sequentially under 21 and 1% O_2 . We waited at least fifteen minutes at each PPFD / O_2 step to homogenise the air inside the measurement circuit and let the leaf reach a steady state. CO_2 mole fraction at the inlet of the chamber was set at $C_e=400 \mu\text{mol mol}^{-1}$. Controlling CO_2 at inlet rather than in the chamber improved the stability of CO_2 and $\delta^{13}\text{C}$ in the chamber. As a result, small but significant changes of CO_2 were recorded in the chamber (C_a , see supplementary table 1): C_a decreased with increasing irradiance due to changes in net CO_2 assimilation rates. This decrease was taken into account by including C_a as a cofactor in the statistical analysis of the results. During each irradiance and O_2 step we recorded three measurements at 180 s intervals.

Estimation of mesophyll conductance (g_m)

g_m was estimated from the difference between the observed discrimination by the leaf (Δ_{obs}) and the discrimination computed from the simple form of the discrimination model of Farquhar:

$$\Delta_i = a + (b - a) \frac{C_i}{C_a} \quad (\text{eq.1})$$

where a is discrimination by diffusion in air and b the discrimination during carboxylation. This model assumes mesophyll conductance to be infinite, and a lack of impact of decarboxylation processes (R_d and photorespiration) on discrimination.

Δ_{obs} was quantified by comparing the $\delta^{13}\text{CO}_2$ of the air entering and leaving the chamber, following Evans *et al.* (1986):

$$\Delta_{\text{obs}} = \frac{\xi(\delta^{13}C_o - \delta^{13}C_e)}{1000 + \delta^{13}C_o - \xi(\delta^{13}C_o - \delta^{13}C_e)} \quad (\text{eq. 2})$$

where:

$$\xi = \frac{C_e}{C_e - C_o} \quad (\text{eq. 3})$$

ξ is the ratio of CO_2 entering the chamber over the CO_2 drawdown induced by the leaf. g_m is then estimated as:

$$g_m = \frac{(b - e_s - a_i) A / C_a}{(\Delta_i - \Delta_{\text{obs}}) - \frac{eR_d / k + f\Gamma^*}{C_a}} \quad (\text{eq. 4})$$

We used values of $e_s=1.1\text{‰}$ (CO_2 dissolution in the liquid phase) and $a_i=0.7\text{‰}$ (CO_2 diffusion in liquid phase, O'Leary 1981). The value of f (fractionation during photorespiration) was considered to be 11‰ , based on theoretical calculations by Tcherkez (2006), subsequently confirmed by direct measurements (Lanigan *et al.*, 2008). The value of b was set at 28‰ , considering that:

$$b = \beta b_4 + (1 - \beta) b_3 \quad (\text{eq.5})$$

with b_3 the fractionation factor by RubisCO ($\approx 30\text{‰}$), b_4 the fractionation factor by PEPc (-5.7‰), and $\beta \approx 0.055$ the fraction of leaf carbon fixed by PEPc (Farquhar *et al.*, 1982).

We used the apparent CO_2 photorespiratory compensation point (C_i^*) as a proxy for Γ^* (von Caemmerer *et al.* 1994). We estimated R_d and C_i^* with the Laisk method (Viil *et al.* 1977) for the three species from the intersection of three A - C_i curves (C_e of 125, 100 and $50 \mu\text{mol mol}^{-1}$) measured at three irradiance levels (100, 50 and $25 \mu\text{mol m}^{-2} \text{s}^{-1}$). C_i^* did not differ between species (t-test >0.05), so we used the mean (C_i^*

$=38.7 \pm 0.51 \mu\text{mol mol}^{-1}$, $n=11$) as a common value for the three species. When measurements were performed under low O_2 , we used $C_i^* = 1.85 \mu\text{mol mol}^{-1}$ (Von Caemmerer *et al.* 1994). As we expected g_m to vary with irradiance, we did not attempt to compute actual values of Γ^* . Moreover, we showed during simulations that errors on the estimate of Γ^* had only a limited impact on the estimates of g_m which shows that using C_i^* instead of actual Γ^* had only limited consequences on our results. R_d was $0.41 \pm 0.09 \mu\text{mol m}^{-2} \text{s}^{-1}$ in *E. globulus*, 0.31 ± 0.09 ($n=4$) in *E. saligna* and 0.68 ± 0.07 ($n=2$) in *E. sieberi* ($n=5$), and we assumed that these estimates correctly assessed respiration in the light, assuming no or very little changes in R_d with irradiance (Peisker and Apel, 2011).

As the isotopic signature of the reference gas provided by cartridges differed from that used by the leaves for earlier photosynthesis, and since respiration R_d probably uses partly carbon pools assimilated before the gas exchange measurements (Tcherkez *et al.* 2011), e was replaced by $e' = e + \delta^{13}\text{C}_{\text{tank}} - \delta^{13}\text{C}_{\text{atmosphere}}$ following Wingate *et al.* (2007). This procedure is not perfect as the fraction of recently fixed carbon probably increased during the measurement sequence, but there is no satisfactory alternative to take such changes into account. For e , we used 1‰ as suggested by Farquhar *et al.* (1982) and as done by Tazoe *et al.* (2009). The LI-6400 was fed with compressed CO_2 cartridges with $\delta^{13}\text{C}$ varying between -5.91‰ and -5.51‰. This resulted in $e' \approx 3.24 \pm 0.08$ ‰ across all measurements.

We estimated the uncertainty (standard deviation) of Δ_{obs} due to the finite precision of $\delta^{13}\text{C}$ measurements. This was achieved by propagating uncertainty (standard deviations) of $\delta^{13}\text{C}_e$ and $\delta^{13}\text{C}_o$ through the equations estimating Δ_{obs} (see Douthe *et al.* 2011 for computation):

$$Sd_{\Delta_{\text{obs}}} = \left(\frac{\xi \sqrt{Sd_{\delta^{13}\text{C}_o}^2 + Sd_{\delta^{13}\text{C}_e}^2}}{\xi(\delta^{13}\text{C}_o - \delta^{13}\text{C}_e)} + \frac{1 + \sqrt{Sd_{\delta^{13}\text{C}_o}^2} - \xi \sqrt{Sd_{\delta^{13}\text{C}_o}^2 + Sd_{\delta^{13}\text{C}_e}^2}}{1 + \delta^{13}\text{C}_o - \xi(\delta^{13}\text{C}_o - \delta^{13}\text{C}_e)} \right) \Delta_{\text{obs}} \quad (\text{eq.6})$$

The propagated uncertainty in Δ_{obs} (i.e. $Sd_{\Delta_{\text{obs}}}$) was used as the basis for a filter to remove unreliable estimates of Δ_{obs} . As the computation of g_m is based on $\Delta_i - \Delta$, we set that g_m estimates were unreliable if $\Delta_i - \Delta$ was smaller than $Sd_{\Delta_{\text{obs}}}$. Consequently we rejected all values where $\Delta_{\text{obs}} + Sd_{\Delta_{\text{obs}}} > \Delta_i$. We applied this filter to individual data

points.

Assessment of the sensitivity of mesophyll conductance estimates via numerical simulations

Given the uncertainties around several parameters of the discrimination model (eq. 4), we performed several simulations to check to what extent they could influence the computed values of g_m and the observed responses to irradiance.

In a first analysis, we considered that values of fractionation factors and fluxes remained constant across the range of irradiance and O_2 values. We used different but still realistic values for R_d , e , f , Γ^* and b to check whether recomputed g_m remained sensitive to irradiance as compared to the values obtained with the initial parameter set ($R_d \approx 0.5 \mu\text{mol m}^{-2} \text{s}^{-1}$, $e = 3.24\%$, $f = 11\%$, $\Gamma^* = C_i^* = 38.7 \mu\text{mol mol}^{-1}$ and $b = 28$). We used values for R_d from 0 to $3 \mu\text{mol m}^{-2} \text{s}^{-1}$ which largely covers the range of values recorded under similar temperature (Atkin *et al.* 2000, Ghashghaie *et al.* 2003). We varied e between -15 to +15%, which covers the range of variation reported by Ghashghaie *et al.* (2003) in a number of species and experimental conditions. The values of f ranged from 0 to 15% (Ghashghaie *et al.* 2003). In the case of b , we used values found in the literature that range from 26 to 30% (Lanigan *et al.* 2008; Von Caemmerer and Evans 1991). Γ^* was changed between 30 and 50 to reflect the range of variations reported by Evans and Loreto (2000) and to take into account the potential error made while considering $\Gamma^* = C_i^*$. We tested with a mixed effect model whether the effect of irradiance and O_2 remained significant despite the changes in each parameter, one parameter being changed at a time.

In a second analysis, we tested what would be the effect of potential changes in e , R_d , f , Γ^* and b with irradiance on the observed response of g_m . We used the data set describing the change of g_m induced by switching irradiance from 600 to $200 \mu\text{mol m}^{-2} \text{s}^{-1}$ under 21% O_2 in *E. sieberi* and *E. globulus*, as these two species represented the two extremes of absolute assimilation and g_m in our data set. We simulated the impact of a change of each parameter on the g_m value measured under $200 \mu\text{mol m}^{-2} \text{s}^{-1}$ PPFD, and checked to what extent such a change was able to alleviate the observed decrease of g_m . The same approach was used with the whole data set to investigate the impact of the change in β under changing O_2 . In the latter case, we restricted the

analysis to β , because it is the most likely change induced by switching O₂ from 21 to 1%. Moreover, β was detected in our analysis as having the largest potential impact on g_m estimates.

Statistical analyses

All statistical analyses were performed with R (R Development Core Team 2010, <http://www.R-project.org>). Mixed-effect linear models were performed to assess species and treatment effect on A , g_s , C_i , the drawdown $C_i - C_c$ and g_m . Irradiance, Species and O₂ were set as fixed factors and C_a as a cofactor, to take into account the fact that C_a was not homogenous among irradiance levels. Normality and heteroscedasticity were graphically checked with QQ-Plots. In case of heteroscedastic data we weighted the means as a function of their variance. In case of non-normal distributions, variables were log-transformed. All interactions were tested for each procedure, and were removed from the model when not significant. To compare slopes of the g_m -irradiance response, we set irradiance as a covariate and species and O₂ as fixed factors. Significance was accepted at $P < 0.05$. Post-hoc tests were then performed to compare simultaneously the different slopes within each species and O₂. We used mean least squares regressions to assess the correlation between variables (R^2 and P -value).

RESULTS

Observed response of mesophyll conductance (g_m) to irradiance treatments and to O_2

Under 21% O_2 , when irradiance was decreased from 600 to 200 $\mu\text{mol m}^{-2} \text{s}^{-1}$, A declined from 15 to 5 $\mu\text{mol m}^{-2} \text{s}^{-1}$ and g_s from 0.7 to 0.1 $\text{mol m}^{-2} \text{s}^{-1}$ while C_i increased slightly in *E. globulus* and *E. saligna* (Table 1 and Figure 1).

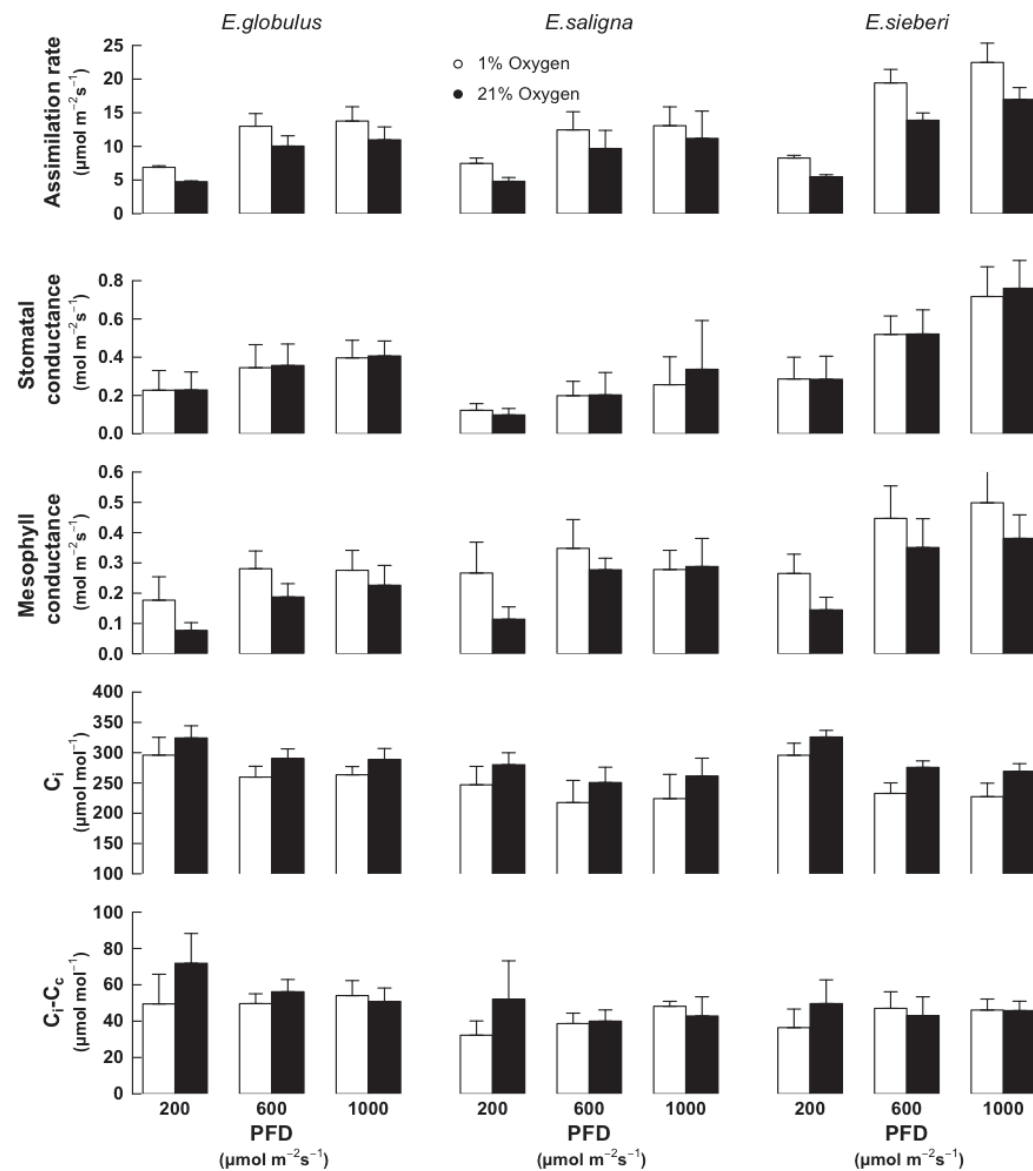


Figure 1: Net CO_2 assimilation rate (A), stomatal conductance to water vapour (g_s), mesophyll conductance to CO_2 (g_m), CO_2 mole fraction in the intercellular airspace (C_i) and difference of CO_2 mole fraction between intercellular airspace and chloroplasts ($C_i - C_c$) as recorded under three levels of irradiance (PPFD) in seedlings of *Eucalyptus globulus*, *E. saligna* and *E. sieberi*. Measurements conducted under 21 (black bars) or 1 % O_2 (white bars). Means and standard deviations ($n=5$).

Table 1: Effects of irradiance, species and O₂ on net CO₂ assimilation rate (A), stomatal conductance to water vapour (g_s) and mesophyll conductance to CO₂ (g_m) computed with standard and stable parameters with irradiance (b, e, f, R_d and Γ^*). Irradiance, species and O₂ effects were incorporated into the model as fixed effects, and *individual plant* as a random effect. In case of heteroscedastic data the mean was weighted as a function of the variance. Degrees of freedom are indicated as subscripts.

		A	g_s	g_m
Irradiance	F _(2,60) P	773.42 <.0001	89.54 <.0001	100.62 <.0001
Species	F _(2,12) P	11.49 0.001	7.89 0.007	10.86 0.002
O ₂	F _(1,60) P	397.45 <.0001	NS NS	62.15 <.0001
Irradiance x Species	F _(4,60) P	14.66 <.0001	16.22 <.0001	4.17 0.004
Irradiance x O ₂	F _(2,60) P	8.15 0.0007	NS NS	3.60 0.03
Species x O ₂	F _(2,60) P	3.89 0.002	NS NS	NS NS

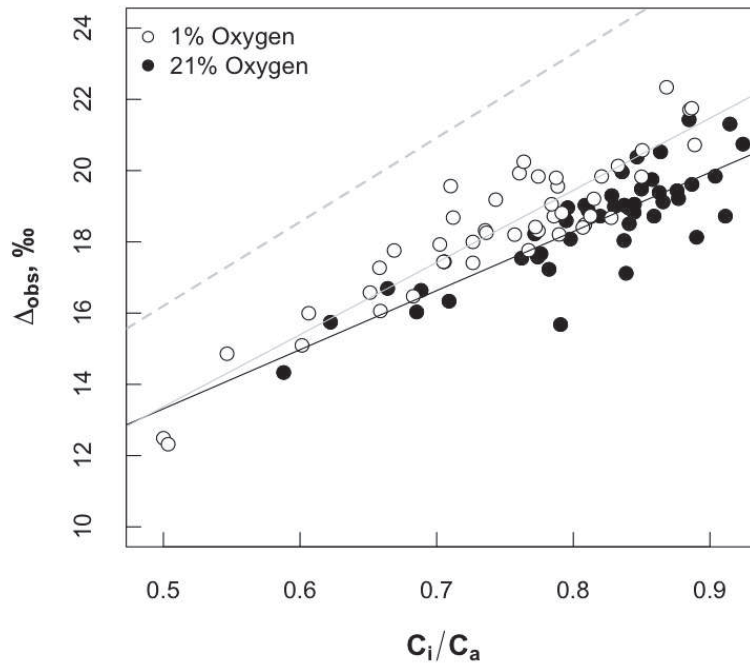


Figure 2: Variations of observed discrimination against ¹³CO₂ (Δ_{obs} , ‰) with the ratio of intercellular/atmospheric mole fraction (C_i/C_a) ratio under 21 (black points) and 1 % O₂ (white points) in three Eucalypt species. Each point is the mean of three measurements at 180s intervals. The dotted line represents the discrimination computed from the simple form of Farquhar's model (Δ_i , Eq.1).

E. sieberi displayed a larger photosynthetic capacity than the two other species, with 50% higher values of A and g_s . The slope of the Δ_{obs} -irradiance relationship was not different from 0 in any species ($P>0.05$, data not shown). Nevertheless, we

observed a significant and positive correlation between Δ_{obs} and C_i/C_a across species (Figure 2). Δ_{obs} varied between 14 and 21‰ and C_i/C_a between 0.6 and 0.9. The difference between the predicted (Δ_i) and observed discrimination Δ_{obs} did not change with irradiance in any species.

Table 2: Effects on mesophyll conductance (g_m) of switching irradiance from 600 to 200 $\mu\text{mol m}^{-2} \text{s}^{-1}$ under 21 and 1% O_2 : t-test comparisons.

Species	O_2 (%)	t-value	p-value
<i>Eucalyptus globulus</i>	21	3.93	0.001
	1	2.90	0.067
<i>Eucalyptus saligna</i>	21	5.01	< 0.001
	1	2.13	0.43
<i>Eucalyptus sieberi</i>	21	5.62	< 0.001
	1	4.22	< 0.001

Under 21% O_2 , the mean value of g_m across species significantly declined from 0.40 to 0.07 $\text{mol m}^{-2} \text{s}^{-1}$ with the drop in irradiance ($F_{(2,60)} = 100$, $P < 0.0001$). In all three species, g_m declined when irradiance dropped from 600 to 200 $\mu\text{mol m}^{-2} \text{s}^{-1}$ (Table 2), but not when it was switched from 1000 to 600 $\mu\text{mol m}^{-2} \text{s}^{-1}$. This pattern matches closely the one detected for A and g_s . g_m was positively correlated with A ($R^2 = 0.77$, $P < 0.0001$) and g_s ($R^2 = 0.39$, $P < 0.0001$) (Figure 3). We checked whether the observed responses were due to the sensitivity of g_m to irradiance or to changing C_a in the measurement chamber with a covariance analysis (Table 3). The analysis indeed detected a significant effect of C_a , which did not alleviate the much larger effect of irradiance. In the following, we present responses to the irradiance treatments that include a small but significant response to CO_2 .

Switching from 21 to 1% O_2 increased A on average by 30% whereas stomatal conductance remained unaffected (Figure 1, Table 1). There was still a positive relationship between A and g_s ($R^2 = 0.65$, $P < 0.001$) under low O_2 , but the slope differed from that under 21% O_2 ($P = 0.02$, Figure 3). As a consequence, C_i was 10% lower under low O_2 . The C_i - C_c draw-down was not significantly affected by O_2 (Figure 1). C_c was not affected by the change in O_2 under low irradiance, but was under higher levels of 600 and 1000 $\mu\text{mol m}^{-2} \text{s}^{-1}$. C_c was $\approx 20\%$ lower under 1 than 21% O_2 in all

species (not shown).

Table 3: Effects of irradiance, species, O₂ and C_a on mesophyll conductance to CO₂ (g_m). Irradiance, species and O₂ effects were incorporated into the model as fixed effects, C_a as a covariant, and *individual plant* as a random effect. In case of heteroscedastic data the mean was weighted as a function of the variance. Degrees of freedom are indicated as subscripts.

		g_m
Irradiance	F _(2,69)	106.46
	P	<.0001
Species	F _(2,12)	25.06
	P	0.002
O ₂	F _(1,69)	74.49
	P	<.0001
C _a	F _(1,69)	58.38
	P	<.0001
Irradiance x Species	F _(4,60)	4.17
	P	0.004
Irradiance x O ₂	F _(2,60)	7.00
	P	0.001

Decreasing O₂ also impacted Δ_{obs} that was still positively correlated with C_i/C_a, but $\approx 1\%$ higher under 1 than 21% O₂ (Figure 2). A significant interaction between irradiance and O₂ can be seen in table 1: under low O₂, the response of g_m to irradiance was still clearly significant in *E. sieberi*, marginally significant in *E. globulus* but no longer significant in *E. saligna* (Table 2).

Surprisingly, the computed values of g_m were on average $\approx 30\%$ larger under 1% than under 21% O₂ (Figure 1, Table 1). The respective changes of g_m and A with O₂ were tightly coordinated, as we detected a unique A/g_m regression under ambient and low O₂ (Figure 3). g_m was significantly increased by the decrease in O₂ under 200 $\mu\text{mol m}^{-2} \text{s}^{-1}$, but less so under 600 and 1000 $\mu\text{mol m}^{-2} \text{s}^{-1}$ PPFD (Figure 1). The covariance analysis showed that the difference of g_m between 21 and 1% O₂ remained significant even after taking into account the impact of the small changes in C_a (Table 3).

Table 4: Effects on mesophyll conductance (g_m) of decreasing irradiance from 600 down to 200 $\mu\text{mol m}^{-2} \text{s}^{-1}$ under 21 and 1% O_2 . The “Initial” column refers to the effect observed on g_m with the initial parameterization ($R_d \approx 0.5 \mu\text{mol m}^{-2} \text{s}^{-1}$, $e \approx +3\text{‰}$, $\Gamma^* = 38.7$ or $1.85 \mu\text{mol mol}^{-1}$ (for 21% or 1% O_2 , respectively), $f = 11\text{‰}$ and $b = 28\text{‰}$), the other columns indicate whether the effect remained significant once the indicated parameter was changed. For Γ^* with used the first value indicate under 21% O_2 while the second under 1% O_2 . *** $P < 0.001$, ** $P < 0.01$, * $P < 0.05$, † $P < 0.1$, NS not significant.

Species	% O_2	Initial	$R_d=0$	$R_d=2$	$R_d=3$	$e=-15$	$e=-5$	$e=+15$	$f=0$	$f=5$	$f=15$	$\Gamma^*=30$ or 1.42	$\Gamma^*=35$ or 1.66	$\Gamma^*=50$ or 2.38	$b=26$	$b=27$	$b=30$
<i>E. globulus</i>	21	***	***	†	NS	***	***	†	***	***	**	***	***	**	***	**	***
	1	†	*	NS	NS	***	**	NS	*	*	NS	NS	†	NS	*	**	***
<i>E. saligna</i>	21	***	***	***	**	***	***	**	***	***	***	***	***	***	***	***	***
	1	NS	NS	NS	NS	***	NS	NS	NS	NS	NS	NS	NS	NS	*	*	**
<i>E. sieberi</i>	21	***	***	***	*	***	***	***	***	***	***	***	***	***	NS	*	***
	1	***	***	†	NS	***	***	NS	**	**	**	***	***	**	*	†	***

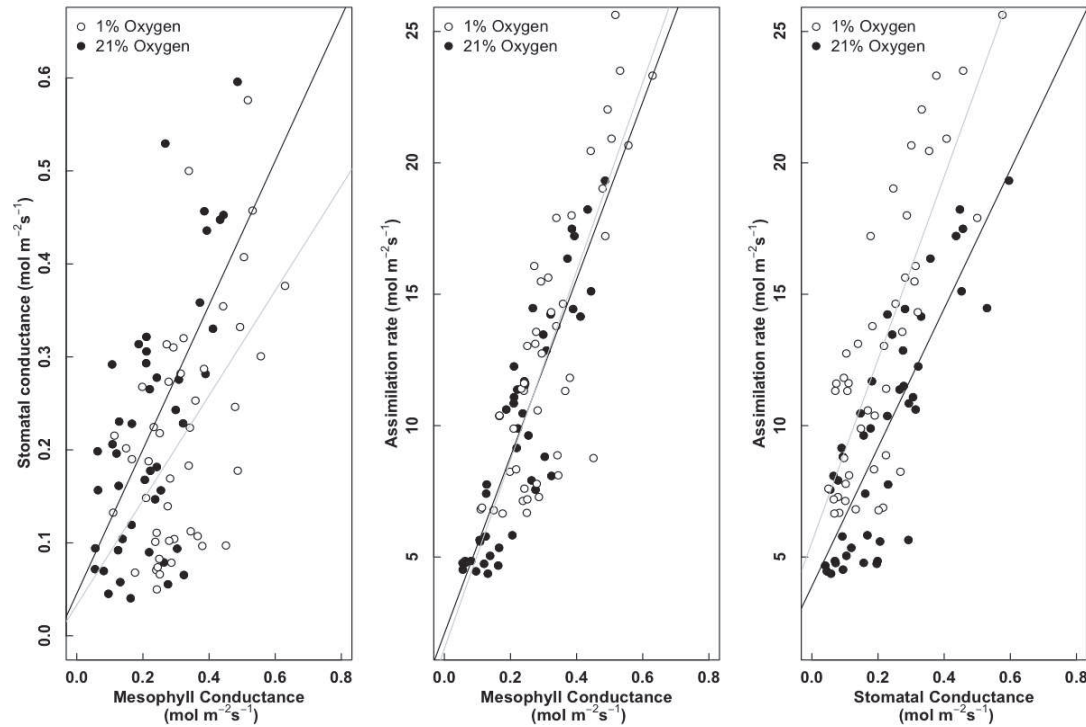


Figure 3: Relationships between mesophyll conductance to CO_2 (computed with standard and stable fractionation factors) and stomatal conductance (left), between mesophyll conductance and net CO_2 assimilation rate (center) and between net CO_2 assimilation rate and stomatal conductance (right). Measurements conducted under 21 (black points) or 1% O_2 (white points).

Uncertainties on g_m values due to model parameters

The same mixed effect model was used with different sets of parameters to check whether the observed response of g_m to irradiance and O_2 was still significant (Suppl. Table 2). No change was detected for the main effects irradiance, species, O_2 compared to the model established with the initial set of parameters. To investigate minor changes in more detail, we performed separate analyses for each species, concentrating on the most important decrease of g_m , i.e., the one observed between 600 and 200 $\mu\text{mol m}^{-2} \text{s}^{-1}$ (Table 4).

According to the mixed effect model, g_m remained responsive to irradiance under the full range of values of R_d and e . Increasing R_d or e resulted in increased absolute values of g_m (Figure 4). This effect was particularly large when g_m was small: below 0.1 $\text{mol m}^{-2} \text{s}^{-1}$ we observed up to 50% increase in g_m , but this represents a limited increase of absolute values (0.05 $\text{mol m}^{-2} \text{s}^{-1}$). However, the responses of g_m to irradiance were still significant in the majority of cases, except when R_d took the extreme value of 3 $\mu\text{mol m}^{-2} \text{s}^{-1}$ or $e=15\%$ for two species (see Table 4).

With respect to photorespiration, increasing Γ^* and f increased the absolute value of g_m (Figure 4). However, the response of g_m to irradiance remained significant, independently of values taken by Γ^* (30, 35 and 50 versus 38.7 $\mu\text{mol mol}^{-1}$ in the original model) or f (0, 5 and 15%, compared to 11%) (Suppl. Table 1 and Table 4).

Parameter b had clearly a larger impact on estimates of g_m compared to all other parameters (Figure 4). g_m was increased on average by 86% with $b=26\%$ and 37% with $b=27\%$, and decreased by 28% when $b=30\%$ compared to the initial value ($b=28\%$). Using $b=26\%$ resulted in very high values of g_m , up to 1.2 $\text{mol m}^{-2} \text{s}^{-1}$. The g_m response to irradiance within each species nevertheless remained significant under 21% O_2 (Table 4), with an exception for *E. sieberi* at $b=26\%$ and 1% O_2 irrespective of b . In summary, the absolute value of g_m is clearly dependent of the value used for b , but the response of g_m to irradiance remained significant with all b value used.

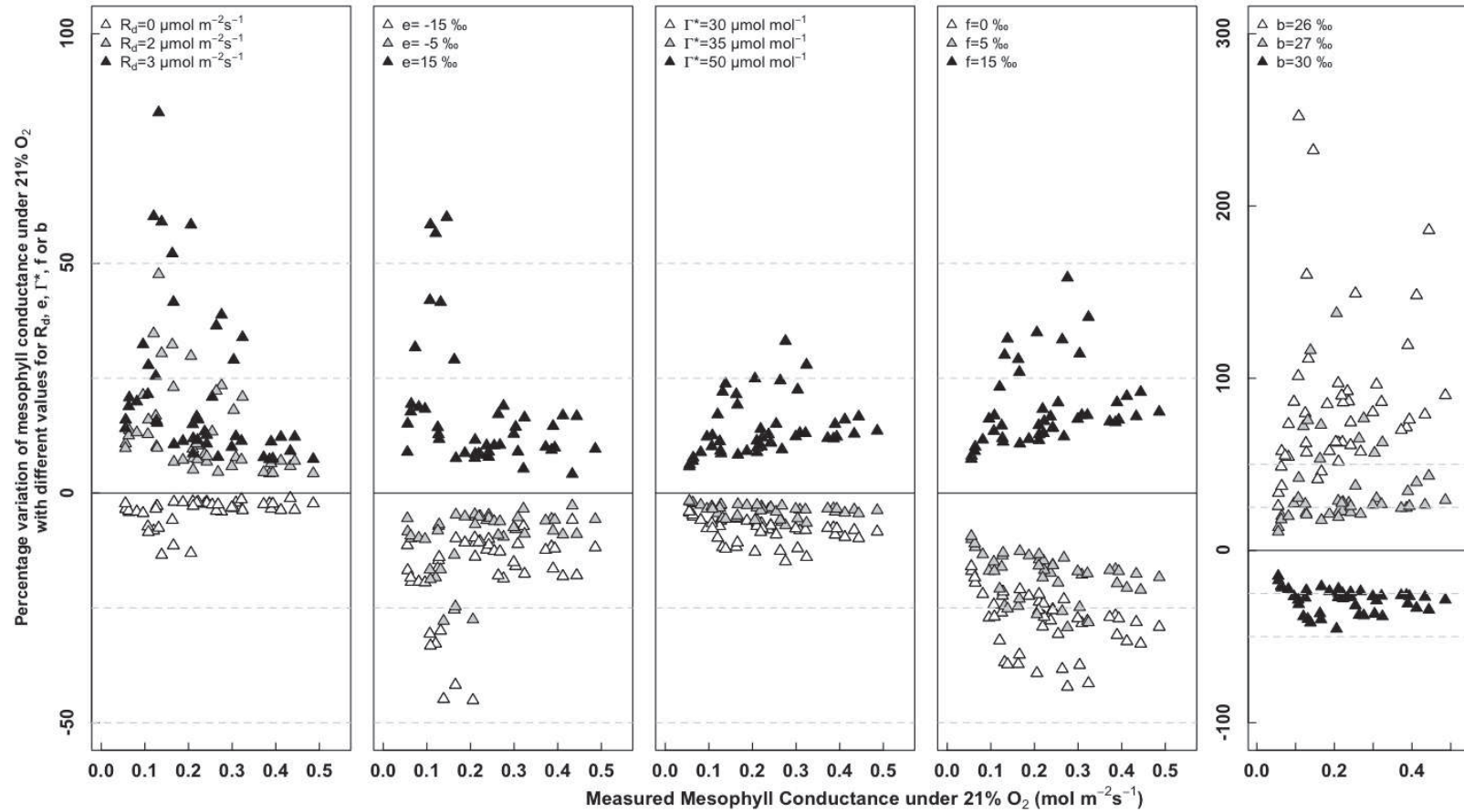


Figure 4: Relative deviation of g_m (in %) recalculated with different values of (from the left to the right) R_d , Γ^* , f and b , and compared to values of g_m computed with the initial parameterisation (horizontal axis). Each symbol corresponds to a different value used for the analysis (see legend for details). The original values are: R_d 0.41, 0.31 and 0.68 $\mu\text{mol m}^{-2}\text{s}^{-1}$ for *E. globulus*, *E. saligna* and *E. sieberi*, respectively, $e \approx +3\text{‰}$, $\Gamma^* = 38.7 \mu\text{mol mol}^{-1}$, $f = 11\text{‰}$ and $b = 28\text{‰}$. The scale of the left panel (b parameter) was modified to fit with the range of values.

Uncertainties in the responses of g_m due to potential changes in parameters due to changing irradiance or O_2 .

We tested the effect of a potential change of these parameters with irradiance on the response of g_m . The results are very clear in the two species used for the simulation (Figure 5): none of the simulated changes in e , R_d , f or Γ^* was able to alleviate the observed response of g_m to irradiance. The only parameter that could potentially alleviate it would be b , but this would require a change from 28 to 25.1‰ under decreasing irradiance. Such variations of b could occur via variations of β (relative amount of carbon fixed by PEPc, see Eq. 5): an increase from 0.055 to 0.14 with decreasing irradiance would be required (considering $b_3=30\text{‰}$ and $b_4=-5.7\text{‰}$).

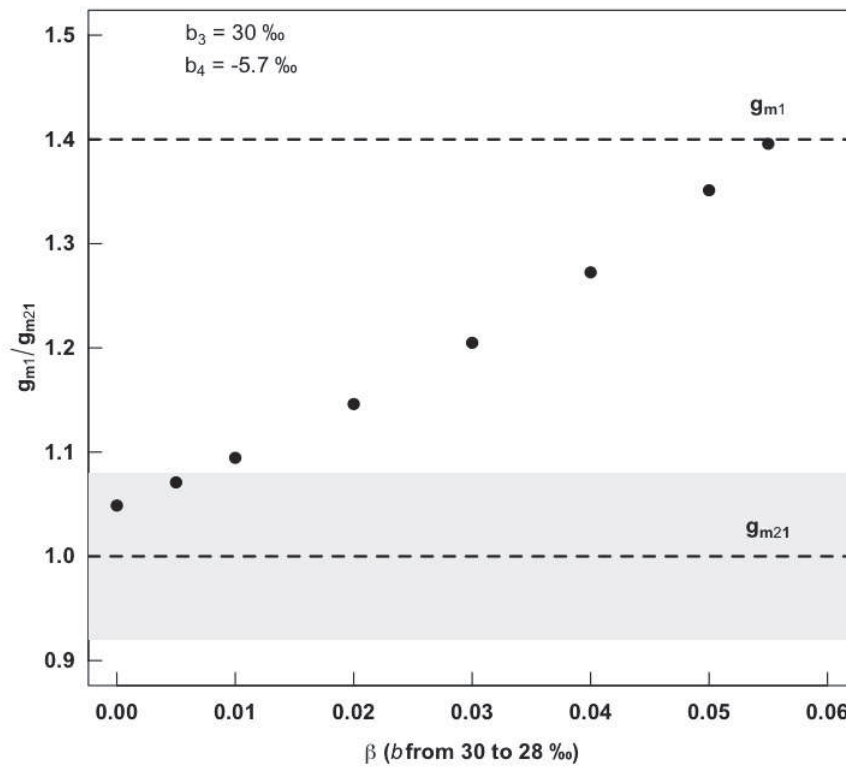


Figure 6: Impact of switching β in equation 3 from 0.055 under ambient O_2 to a variable value under low O_2 on the ratio g_m under low vs. under ambient O_2 (g_{m1} and g_{m21} , respectively). Values of decreasing β resulted in a convergence of the ratio towards 1. The grey area represents the uncertainty of absolute values of g_m recorded under ambient O_2 . Values of β below 0.01 resulted in non significant differences between g_m recorded under ambient and low O_2 .

Figure 6 similarly shows the changes in β that would be required to alleviate the apparent 30% increase of g_m when switching from 21 to 1% O₂. In this case, β would need to drop from 0.055 to 0 to cancel the apparent response of g_m to O₂. In Table 5 we specifically compared the effects of the different O₂ treatments when β was kept stable, or when it was switched from 0.055 under 21% O₂ to 0.00 under 1% O₂. The results show that the O₂ effect was no longer visible in the latter case.

Table 5: Mixed effect model for the effects of irradiance, species and O₂ mole fraction on computed values of g_m under the hypothesis of (i) a constant value of the parameter β (fraction C fixed by PEPc) with O₂ mole fraction ($\beta=0.055$, thus $b=28\%$), and (ii) an O₂-sensitive value of β ($\beta=0.055$ at 21% O₂ and 0 at 1% O₂, thus b varied from 28% to 30%). Non-significant interactions were removed from the model.

		g_m (constant β with O ₂)	g_m (O ₂ -sensitive β)
irradiance	F _(2,60)	100.62	132.26
	<i>P</i>	<.0001	<.0001
Species	F _(2,12)	10.86	10.67
	<i>P</i>	0.002	0.002
O ₂	F _(1,60)	62.15	NS
	<i>P</i>	<.0001	NS
irradiance x Species	F _(4,60)	4.17	6.36
	<i>P</i>	0.004	0.0002
irradiance x O ₂	F _(2,60)	3.60	5.38
	<i>P</i>	0.03	0.006

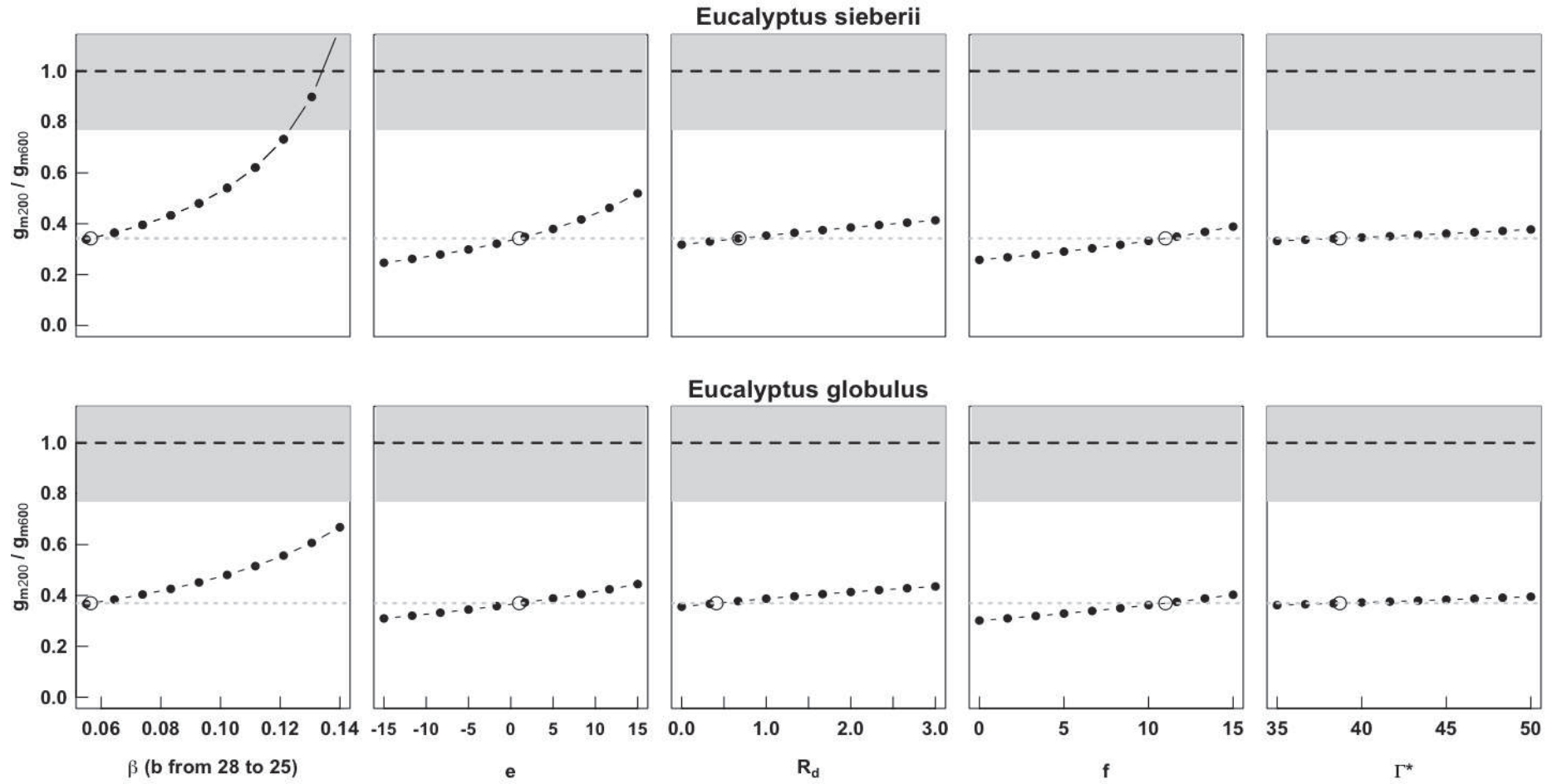


Figure 5: Ratio of mesophyll conductance (g_{m200}/g_{m600}) recorded under low (200) and medium (600 $\mu\text{mol m}^{-2} \text{s}^{-1}$ PPFD) irradiance. Empty circles represent the measured ratio. Black dots are recalculated ratios resulting from a change of the model parameter (see equation 4) when switching irradiance from 200 to 600 $\mu\text{mol m}^{-2} \text{s}^{-1}$. We used as

starting point (i) the data (A , c_i , g_s , ...) observed under 21% O_2 in the species with the largest (*E. sieberi*) and the smallest (*E. globulus*) absolute change of g_m (and A) and (ii) the standard parameters ($R_d \approx 0.5 \mu\text{mol m}^{-2} \text{s}^{-1}$, $e \approx +3\%$, $\Gamma^* = 38.7 \mu\text{mol mol}^{-1}$, $f = 11\%$ and $\beta = 0.055$, i.e., $b = 28\%$) under $600 \mu\text{mol m}^{-2} \text{s}^{-1}$ and computed what would be the value of g_m under $200 \mu\text{mol m}^{-2} \text{s}^{-1}$ due solely to a change in the parameter. The data were normalised to 1 with respect to g_m under $600 \mu\text{mol m}^{-2} \text{s}^{-1}$ PPFD. The figure shows that even the full range of parameter values is unable to explain the observed change in g_m , except for β , for which switching from 0.55 to 0.14 could explain a large fraction of the apparent change in g_m with irradiance. The grey area represents the uncertainty of the ratio between g_m under 200 vs. $600 \mu\text{mol m}^{-2} \text{s}^{-1}$.

DISCUSSION

Rapid response of mesophyll conductance to irradiance under 21 and 1% O₂

We observed a rapid decrease (within minutes) of g_m with a decrease of irradiance in 3 *Eucalyptus* species under 21% O₂, as has been previously reported (Flexas *et al.* 2007; Hassiotou *et al.* 2009; Douthe *et al.* 2011). A fraction of the g_m response may have been induced by the small increase in CO₂ in the chamber (C_a) as irradiance decreased. We used the CO₂-induced decrease in g_m reported by Douthe *et al.* (2011) for the same species to compute the potential contribution of the response to CO₂ to the overall change in g_m . A maximal contribution of about 17% was estimated. Such a computation assumes that the effects of CO₂ and irradiance are additive, while there is currently no information available in the literature about potential interactions between the two factors. Moreover, C_a and irradiance were tightly correlated in our experiment, and we are therefore unable to further disentangle the individual effects of each of the two factors. In the following discussion, the response to irradiance integrates a probably minor but still significant CO₂ effect.

We found a larger sensitivity of g_m than reported in earlier studies, with an average change of $\approx 60\%$ between high and low irradiance, compared to $\approx 40\%$ under the same range of irradiance levels (Flexas *et al.* 2007), and to $\approx 22\%$ (Hassiotou *et al.* 2009). In the latter case, irradiance varied between 1500 and 500 $\mu\text{mol m}^{-2} \text{s}^{-1}$. In contrast, two studies claimed that g_m was insensitive to a range of irradiance from 200 to 1500 $\mu\text{mol m}^{-2} \text{s}^{-1}$ in *Triticum aestivum* and *Nicotiana tabacum* (Tazoe *et al.* 2009; Yamori *et al.* 2010). The reason for the discrepancy between studies is still unclear but may be related to species-specific differences, as recently suggested for the response of g_m to CO₂ (Tazoe *et al.* 2011). It nevertheless appears that the range of irradiance used could also influence the conclusion about the response of g_m to irradiance. If the response of g_m to irradiance is non-linear, and further if it even declines under high irradiances ($>1000 \mu\text{mol m}^{-2} \text{s}^{-1}$, Tazoe *et al.* 2009; Yamori *et al.* 2010), then the range of irradiance levels used may impact the final outcome of the tests.

In summary, our results suggest that g_m is truly responsive to irradiance as

suggested earlier (Flexas *et al.* 2008), and that the uncertainties due to fractionation during photorespiration can not cause the apparent response of g_m to irradiance since g_m remains responsive under 21 as well as 1% O_2 (with a small exception). Nevertheless, these conclusions remain valid only if the parameters b , e , R_d , f and Γ^* used in the computations are close to reality and remain stable with irradiance. We address these questions below.

Sensitivity of g_m estimates to changes of model parameter values

Could the observed responses be caused by a mis-estimation of model parameters?

Since (i) our simulations indicated that only extreme values of R_d ($>2 \mu\text{mol m}^{-2} \text{s}^{-1}$) could alleviate the response of g_m to irradiance and (ii) our estimations of R_d from the Laisk method provided values close to those found in the literature (Atkin *et al.* 2000 for *Eucalyptus pauciflora* and Warren 2008 for *Eucalyptus regnans*, under similar temperature and irradiance), we may safely conclude that the observed response of g_m to irradiance was not due to the use of erroneous values of R_d . Similarly, the response of g_m to irradiance remained significant independently of the value taken by e (except specific cases and $e=15\text{‰}$, see Table 4). Such extreme values of R_d and e are expected to occur only under large variations of temperature and/or respiratory substrate (Atkin *et al.* 2000; Ghashghaie *et al.* 2003). Thus, we also concluded that the response of g_m to irradiance was not due to the use of poorly estimated values of R_d and e .

The precise value of f , discrimination due to the decarboxylation of glycine during photorespiration was a matter of debate during many years (Gillon and Griffiths 1997; Igamberdiev *et al.* 2001; Ivlev *et al.* 1996) but recent theoretical as well as experimental studies showed that it is close to 10‰ (Tcherkez 2006; Lanigan *et al.* 2008). Our simulations indicated that even with a large shift in the estimate of f (from 0 to 15‰), the response of g_m to irradiance remains significant. The actual value of Γ^* is not yet well established and may change with species and environment (Evans and Loreto, 2000). In addition, we recognise that using C_i^* as a proxy of Γ^* could bias the g_m estimates. Nevertheless, the simulations showed that under the range of Γ^* tested, the response of g_m to irradiance remained significant, suggesting that potential errors in the parameterization of Γ^* (and thus the absence of correction of

C_i^*) cannot be at the origin of the observed response to irradiance.

Similarly, g_m was responsive to irradiance independently of the value taken by b , except in specific cases (for *E. sieberi* when $b=26\text{‰}$ under 21% O_2). Such a range of b is still likely, regarding the uncertainty observed for b_3 (fractionation by RubisCO, between 28.5 and 30‰, see McNevin *et al.* 2007) and for β (relative amount of carbon fixed by PEPc, between ≈ 0 and 0.15, see Saurer *et al.* 1995 and Vu *et al.* 1985 for extreme values). Combining such extreme values in Eq. 5 led to a range of b from 30 to 23‰, but the lowest value used in the literature is $b=26\text{‰}$ (Lanigan *et al.* 2008, from a statistical approach). The dramatic effect of changing b on the absolute value of g_m highlights the pressing need to improve our estimates of b and even more β , but our simulations nevertheless showed that the possible error in b unlikely underpins the apparent response of g_m to irradiance.

Was the observed response caused by a potential shift of model parameters in response to changes in irradiance or O_2 ?

To the best of our knowledge, this question was never explicitly addressed in g_m studies, or expressed differently, the exclusive cause of the divergence of observed and modelled discrimination was considered to be changes in g_m and complete stability of other parameters. Figure 5 clearly showed that variations of e , R_d , f and Γ^* with irradiance were unlikely to explain the variation of g_m when irradiance dropped from 600 to 200 $\mu\text{mol m}^{-2} \text{s}^{-1}$: the variations of e , R_d , f or Γ^* required to level out changes of g_m with irradiance are clearly out of the range of commonly accepted values (Ghashghaie *et al.*, 2003; Evans and Loreto 2000; Atkin *et al.* 2000; Tcherkez 2006). Such large variations are unlikely to happen. R_d is usually significantly down-regulated in the presence of light, but the intensity of inhibition is rather stable above 200 $\mu\text{mol m}^{-2} \text{s}^{-1}$ (Atkin *et al.* 2000; Peisker and Apel 2001, Yin *et al.* 2011). The required change of e would mean a severe change of respiratory substrate (Tcherkez *et al.* 2005). f as well as Γ^* should be stable with irradiance as long as O_2 and temperature remain stable. This clearly indicates that rapid variations of e , R_d , f or Γ^* with irradiance are unlikely to occur, and should be of a much too large amplitude to be really considered as a potential cause for the rapid response of apparent g_m to irradiance.

On the other hand, b would have to vary from 28‰ to 25.07‰ with decreasing

irradiance to alleviate the observed change of g_m . Such a variation of b would require a variation of β from 0.055 to 0.15, under the likely hypothesis that b_3 remains constant and close to 30‰ (McNevin *et al.* 2007) and b_4 to -5.7‰ (O'Leary 1981). This would imply a very large increase of the relative contribution of PEPc to total carbon fixation. β is usually assumed to vary between 0.05 (Melzer and O'Leary 1987; Von Caemmerer and Evans 1991) and 0.1 (Farquhar and Richards 1984), but a higher value of 0.13 was found in *Citrus sinensis* (Vu *et al.* 1985). Is such an increase realistic? Decreased irradiance affects C fixation by rubisco, but possibly not the fixation by PEPc. Therefore, a temporary increase of β cannot be excluded, although we have no experimental basis for further discussing this option. Clearly, an improved assessment of the absolute value of β and its genetic and environmental variability is a prerequisite to further studies in this field.

A last line of arguments is that rapid responses of g_m to irradiance have also been detected when using chlorophyll fluorescence instead of isotopic discrimination (Flexas *et al.* 2008; Hassiotou *et al.* 2009), as the fluorescence method is not dependent on β . We conclude that β is unlikely to give rise to an artefactual response of g_m to irradiance, but a clear confirmation that β is only little affected by irradiance will be necessary to definitively make this point.

Are the observed variations of g_m with O_2 realistic?

The observation of a 30% increase of g_m under 1% O_2 was a surprise. As the simulations described above showed that changes in b were the most likely to impact the computation of g_m , we concentrated our analyses on this parameter. Indeed, it is very unlikely that e or f varied with O_2 (Tcherkez *et al.* 2004).

With respect to β , we showed that the difference of g_m between 21 and 1% O_2 disappeared when $\beta=0.055$ under 21% O_2 and approaches 0 under 1% O_2 . There is no experimental evidence that β could change with O_2 , and to our knowledge no study has ever tested this hypothesis. Nevertheless, a realistic hypothesis could suppose that because only carboxylation by RubisCO is directly affected by the drop of O_2 in the chloroplast (*via* the balance with the oxygenase activity, Farquhar *et al.* 1980), it could result in an increase of the relative amount of carbon fixed by RubisCO, i.e., in a decrease of β . Indeed, our results do not allow to conclude definitively whether g_m or β (or both) change with O_2 , which highlights the need to better understand possible

changes of β with environmental conditions (here O_2). Interestingly, Tholen and Zhu (2011) recently presented a three-dimensional model of photosynthesis including g_m , that predicts that a decrease of O_2 would increase g_m due to the spatial distribution of CO_2 emission (in mitochondria) and carboxylation (in the chloroplasts). This tends to confirm our observations, but further studies are needed to definitively assess whether β or g_m really change with O_2 .

CONCLUSION

In this study we found that mesophyll conductance (g_m) responds positively to increasing irradiance in three *Eucalyptus* species under ambient O_2 , and under low O_2 for *E. sieberi* and *E. globulus*. We explored several ways to have an improved view of the influence of the different parameters in the model linking $\Delta^{13}C$ and g_m . Firstly, recalculating g_m values with different values for R_d , e , Γ^* , f and b still resulted in significant response of g_m to PPFD under 21% O_2 and did not fundamentally change the smaller response observed under 1% O_2 . The parameter b had the largest influence on the estimation of g_m , and dramatically affected the estimation of the absolute value of g_m . As b is influenced by the ratio PEPc/rubisco carboxylation (β), it would be useful to obtain additional estimations of β for more species, and assess whether it varies among species and with environmental conditions.

The response of g_m to irradiance cannot be explained alone by rapid variations of e , R_d , f or Γ^* with irradiance. We highlighted that only extreme variations of b with irradiance, via variations of β , could alleviate the apparent response of g_m to irradiance. Future studies should focus on such potential variations of β . Similarly, the unexpected response of g_m to O_2 would be reconsidered if β dropped temporarily to zero, which has never been tested.

Supplementary material

Supplementary table 1. Mean values of CO₂ mole fraction in the measurement chamber (C_a) according to the different treatments of irradiance and O₂ availability (mean ± SD, n=15).

Irradiance (PPFD)	21% O ₂	1% O ₂
1000 $\mu\text{mol m}^{-2} \text{s}^{-1}$	335.5 ± 18.1 $\mu\text{mol mole}^{-1}$	320.4 ± 23.0 $\mu\text{mol mole}^{-1}$
600 $\mu\text{mol m}^{-2} \text{s}^{-1}$	344.1 ± 12.9 $\mu\text{mol mole}^{-1}$	327.5 ± 17.9 $\mu\text{mol mole}^{-1}$
200 $\mu\text{mol m}^{-2} \text{s}^{-1}$	373.2 ± 3.5 $\mu\text{mol mole}^{-1}$	361.9 ± 3.6 $\mu\text{mol mole}^{-1}$

Supplementary table 2: Effects of irradiance (PPFD, 3 levels), species (3 *Eucalyptus* species) and O₂ (21 and 1%) on g_m computed with different values of the model parameters R_d , f , Γ^* and b (see equation 4). Parameter values were kept stable across irradiance and O₂ levels, except for Γ^* which was recalculated under low O₂. Irradiance, species and O₂ effects were incorporated into the model as fixed effects, and *individual plant* as a random effect. In case of heteroscedastic data the mean was weighted as a function of the variance. Degrees of freedom are indicated as subscript of F value.

		$R_d=0$	$R_d=2$	$R_d=3$	$e=-15$	$e=-5$	$e=+15$	$f=0$	$f=5$	$f=15$	$\Gamma^*=30$	$\Gamma^*=35$	$\Gamma^*=50$	$b=26$	$b=27$	$b=30$
PPFD	$F_{(2,60)}$	95.84	48.37	30.88	149.53	126.35	39.12	138.53	116.03	74.20	92.58	107.70	79.84	83.03	73.90	195.40
	P	<.0001	<.0001	<.0001	<.0001	<.0001	<.0001	<.0001	<.0001	<.0001	<.0001	<.0001	<.0001	<.0001	<.0001	<.0001
Species	$F_{(2,12)}$	9.45	10.36	10.28	8.19	6.80	11.89	10.08	10.76	10.81	10.64	10.90	10.75	10.28	16.39	8.84
	P	0.003	0.004	0.002	0.007	0.01	0.001	0.002	0.002	0.0042	0.002	0.002	0.0042	0.002	0.001	0.004
O ₂	$F_{(1,60)}$	62.14	42.82	36.54	104.71	71.88	41.66	185.75	136.40	16.68	89.59	75.85	24.36	32.40	22.55	109.09
	P	<.0001	<.0001	<.0001	<.0001	<.0001	<.0001	<.0001	<.0001	<.0001	<.0001	<.0001	<.0001	<.0001	<.0001	<.0001
PPFD x Species	$F_{(4,60)}$	4.78	NS	NS	7.48	6.23	4.77	4.51	4.36	3.10	4.04	4.34	3.41	NS	NS	8.87
	P	0.001	NS	NS	<.0001	0.0001	0.01	0.002	0.003	0.02	0.005	0.003	0.01	NS	NS	<.0001
PPFD x O ₂	$F_{(2,60)}$	NS	3.82	4.67	15.21	NS	NS	NS	NS	5.12	NS	3.24	4.86	NS	NS	NS
	P	NS	0.027	0.012	<.0001	NS	NS	NS	NS	0.008	NS	0.04	0.01	NS	NS	NS

CHAPTER IV

Mesophyll conductance of poplar leaves varies rapidly with changes in CO₂ and irradiance: an assessment from on line ¹³CO₂ discrimination records with TDL-AS.

Mesophyll conductance of poplar leaves varies rapidly with changes in CO₂ and irradiance: an assessment from on line ¹³CO₂ discrimination records with TDL-AS.

Cyril DOUTHE^{1,2,3}, Daniel EPRON^{1,2}, Oliver BRENDEL^{1,2}, Charles R. WARREN³,
Erwin DREYER^{1,2*}

Addresses

1. INRA, Unité Mixte de Recherches 1147 "Ecologie et Ecophysiologie Forestières", F 54280 CHAMPENOUX, France
2. Nancy Université, Unité Mixte de Recherches 1147 "Ecologie et Ecophysiologie Forestières", Faculté des Sciences, F 54500 VANDOEUVRE, France
3. University of Sydney, School of Biological Sciences, Heydon-Laurence Building A08, The University of Sydney, NSW 2006, Australia.

Emails: Cyril.Douthe@nancy.inra.fr; daniel.epron@scbiol.uhp-nancy.fr ;
charles.warren@sydney.edu.au ; brendel@nancy.inra.fr, dreyer@nancy.inra.fr

*Correspondence and reprints

Short title: Rapid changes of mesophyll conductance in poplar leaves

Additional Keywords: Photosynthesis, stomatal conductance, *Populus*, tunable diode laser absorption spectrometry, isotopic discrimination, ¹³C

Number of words: 6 Figures: 3 Tables:

ABSTRACT

An increasing number of studies estimate mesophyll conductance to CO₂ diffusion into leaves (g_m) due to its large effect on photosynthesis via CO₂ availability in the chloroplast. g_m was initially considered to be dependant only on leaf structure, and thus stable in the short-term. Several studies have now shown that g_m can change rapidly (within minutes) in response to CO₂ or irradiance, while other studies reported g_m was unaffected by these sources of variations. The absence of a clear consensus means that the rapid response of g_m to CO₂ and irradiance still needs confirmation. We estimated dynamic changes of g_m from combined leaf gas exchange measurements and on-line records of ¹³CO₂ discrimination on poplar leaves by modulating successively irradiance and then CO₂ on the same leaf. We observed a clear increase of g_m with increasing irradiance and a decrease with increasing CO₂. Under irradiance variations, g_m was positively correlated with assimilation rate and stomatal conductance. We performed a simulation analysis to test the impact on the assimilation rate of a variable g_m (measured data) *versus* a stable g_m with irradiance. Simulations have shown that at low irradiance different in g_m values have a negligible impact on photosynthesis, while as under high irradiance photosynthesis was drastically reduced by a low g_m but not increased by a high g_m .

INTRODUCTION

Similar to stomatal conductance (g_s), which is the conductance between the atmosphere (at $[\text{CO}_2]=C_a$) and intercellular air space (at $[\text{CO}_2]=C_i$), mesophyll conductance to CO_2 (g_m) can be seen as an equivalent conductance between intercellular air spaces and the site of carboxylation, in the chloroplast (at $[\text{CO}_2]=C_c$). As a result, net CO_2 assimilation rate (A) can be expressed, following Fick's law, as:

$$A = g_s(C_a - C_i) = g_m(C_i - C_c)$$

(Eq. 1)

g_m was identified as a potential resistance to CO_2 diffusion in the leaf by the pioneering work of Gaastra (Gaastra, 1959) on photosynthesis, but has long been very difficult to estimate. Estimations of g_m were greatly facilitated by establishment of methods combining gas exchange measurements and chlorophyll fluorescence (Epron *et al.*, 1995; Harley *et al.*, 1992; Loreto *et al.*, 1992) or isotopic discrimination against $^{13}\text{CO}_2$ (Evans *et al.*, 1986; Lloyd *et al.*, 1992; Von Caemmerer and Evans, 1991).

Nowadays, g_m has been estimated in many species and functional groups (Flexas *et al.*, 2008), and there is some support for the ability of mesophyll conductance to vary rapidly (within minutes) to changes in environmental conditions. Several studies reported that g_m was negatively correlated with $[\text{CO}_2]$ (Doutte *et al.*, 2011; Flexas *et al.*, 2007; Flexas *et al.*, 2008; Tazoe *et al.*, 2011; Vrabl *et al.*, 2009), or g_m was positively correlated with irradiance (Doutte *et al.*, 2011; Flexas *et al.*, 2008; Hassiotou *et al.*, 2009). Nevertheless, other studies reported g_m was unaffected by CO_2 or irradiance (see Tazoe *et al.*, 2009), showing that rapid responses of g_m to changes in irradiance and CO_2 are still a matter of discussion.

An important question emerges with the possibility of variable g_m in the short term: what is the impact of such variable g_m *versus* a stable g_m on the assimilation rate, and thus on C_i and C_c ? A simulation analysis have shown that a low g_m will decrease photosynthesis, a direct consequence of reducing CO_2 availability in the chloroplast (Farquhar *et al.*, 1980), and increase the CO_2 draw-down ($C_i - C_c$) (Niinemets *et al.*, 2009). But this simulation was set in constant CO_2 , irradiance and with a constant g_m (i.e several leaves simulated with for each a constant value of g_m with a varying A). The next step could be to perform a simulation of assimilation rate where g_m is constant *versus* stable and confront it with measured data from a living leaf. Since variations of CO_2 around the leaf will obviously vary C_i and C_c by forcing CO_2

diffusion inside the leaf, irradiance variations appears as good solution to vary assimilation rate, and let the leaf modulate C_i and C_c via g_s and g_m . This could help to better understand possible rapid variations of g_m as a rapid functional adjustment in a context of varying environmental conditions.

The aim of this study was to test the rapid response of g_m under varying CO_2 and irradiance, using online discrimination against $^{13}CO_2$ during photosynthesis, in poplar leaves. We used a custom-built gas exchange system equipped with a large photosynthesis chamber ($\approx 200\text{ cm}^2$ allowing measurement of a whole leaf), coupled to a TDLAS. For each leaf g_m was estimated for $\approx 8\text{h}$ while irradiance and then CO_2 were varied. Finally, we performed a simulation of the assimilation rate under varying irradiance for a low and high but stable g_m , and compared with the measured data based on the hypothesis of a variable g_m , to assess how a variable g_m *versus* a stable g_m influences the assimilation rate under varying irradiance.

MATERIAL & METHODS

Plant material

The experiment was carried out on four-month-old cuttings of *Populus deltoides* x *nigra* (clones “Soligo” and “I-214”) and *Populus deltoides* x *trichocarpa* (clone “Raspalge”). Cuttings were planted in October 2008 in 7L pots containing a 50/50 (v/v) mixture of peat and sand with fertilizer added at the beginning of the growth (Nutricote 100, 13/13/13 with oligoelements, 40 g per pot) and maintained in a growth chamber at Champenoux (France) under a controlled temperature of 25°C and relative air humidity of 50%, with an optimal irrigation regime and a photoperiod of 16/8 hours day/night. One week before measurements started, plants were moved to the site of measurement (University of Nancy, Vandoeuvre-les-Nancy) and put in a climate chamber with the same conditions as during growth.

Gas exchange measurements

Measurements of leaf photosynthesis were carried out on fully expanded leaves in a custom-built leaf chamber of 13x26cm designed to enclose a whole leaf. The working air flow through the chamber was 5L min⁻¹ controlled by a mass flow controller (Bronkorst). Leaf temperature (T_{leaf}) was measured with a nickel-chrome thermocouple, and T_{leaf} was maintained constant at 22.1 °C ± 0.7 (mean ± SD) using Peltier elements to control air temperature within the leaf chamber. Photosynthetic photon flux density (PPFD, $\mu\text{mol photons m}^{-2} \text{ s}^{-1}$) was monitored with a quantum sensor (LI90SA; Li-Cor, Inc., Lincoln, NE, USA) inside the chamber. Irradiance was provided by two 20cm x 20cm LED panels (P.S.I. Photon System Instruments, Brno, Czech Republic). Chamber air was well stirred with fans to homogenise gas composition and temperature inside the chamber. Boundary layer conductance, estimated with a filter paper leaf replica, was 1-2 mol m⁻² s⁻¹, calculated for each leaf as a function leaf area from estimations based on the filter paper method (Jones 1989). Air pressure inside the chamber was measured with pressure sensors and maintained slightly above atmospheric pressure at $\approx 18.7 \pm 3$ mbar (mean ± SD) to avoid influx into the chamber. Water vapour at the inlet of the chamber was controlled with a dew-point generator equipped with Peltier elements and air pressure sensor. All measured variables were recorded with a datalogger (CR23X; Campbell Scientific Inc.) every second and averaged every three minutes. Water vapour in the sample circuit was measured with a calibrated gas analyser (Li-7000, LI-COR, Lincoln, NE, USA). After

recalculating the air flow leaving the photosynthesis chamber to account for the efflux of water by the leaf (Ball, 1987 Eq.11b), transpiration rate (E) was assessed by mass balance and stomatal conductance to water vapour (g_{sw}) was calculated from Fick's law based on leaf temperature (Ball, 1987) and accounting for boundary layer conductance and a stomatal ratio of 0.7 for Poplar (Le-Thiec, personal communication) with equations from Li-6400 manual (eq. 1-9 and 17-9). Stomatal conductance to CO₂ (g_s) was calculated with $g_s = g_{sw}/1.6$. CO₂ entering the circuit was provided by ambient air (for PPFD variations, $\delta^{13}\text{C} \approx -8 \text{ ‰}$) or by mixing ambient air with pure CO₂ from a compressed tank (Air Liquide, with $\delta^{13}\text{C} \approx -30 \text{ ‰}$) for CO₂ variations. CO₂ concentration in inlet (C_e) and outlet (C_a) was measured with a TDLAS (TGA100A; Campbell Scientific, Inc.). Because air flow was dried before entering the TDLAS, the measured CO₂ concentration was different from that in the reference and the sample circuits because of dilution in water vapour. C_e and C_a were then recalculated following Ball (1987):

$$C_e = \frac{C_{TDLAS}(1 - W_e)}{1 - W_{TDLAS}}$$

(Eq. 2)

where C_{TDLAS} is CO₂ concentration measured by TDLAS in dried air, W_e and W_{TDLAS} are water vapour concentration in reference (dew point) and in air flow after drying, respectively, with W_{TDLAS} assumed to be zero. The same calculation was applied to C_a , using W_o , the water vapour concentration in the sample. Knowing C_e and C_a , net assimilation (A) was assessed by mass balance, and C_i , the CO₂ concentration in intercellular air spaces was calculated following (Ball, 1987).

The TDLAS was frequently calibrated during the experiment with three calibration tanks (see Table 1). The cycle of measurements consisted in successively measuring inlet/outlet/inlet/tank3/tank1/tank2, each during thirty seconds, with the fifteen first seconds skipped to prevent measuring concentration resulting from the actual air flow with the remaining air from the previous sampled gas in the sequence. The two inlet measurements were averaged to determine air composition at the inlet of the leaf chamber. This sequence allowed measurements with a three-minute resolution.

Table 1: Total CO₂ mole fraction (CO_{2tot}, in $\mu\text{mol mol}^{-1}$), isotopic composition ($\delta^{13}\text{C}$, in ‰), and mole fraction of each isotopologue ($\mu\text{mol mol}^{-1}$) in the three calibration gases used to calibrate the TDLAS during the experiment. $\delta^{13}\text{C}$ for each tank was measured with mass spectrometer.

Tank	CO _{2tot}	$\delta^{13}\text{C}$	¹² CO ₂	¹³ CO ₂
T1	300.4	-38.3	297.20	3.20
T2	703.3	-35.2	695.79	7.51
T3	401.5	-35.2	397.22	4.28

Five out of eight measured plants (see Table 2 for details) were subjected successively to an increasing irradiance from ≈ 150 to $\approx 800 \mu\text{mol m}^{-2} \text{s}^{-1}$ PPFD, and then to an increasing C_e from ≈ 400 to $\approx 900 \mu\text{mol mol}^{-1}$. PPFD variations were carried out under constant C_e, with C_e slightly varying between plants (between 390 and 420 $\mu\text{mol mol}^{-1}$, see Table 2). C_e variations were performed under constant PPFD, but differing between plants, from 560 to 960 $\mu\text{mol m}^{-2} \text{s}^{-1}$ PPFD (Table 2).

Table 2: For each plant, the irradiance used during the CO₂ variations, and CO₂ concentration entering the chamber (C_e) during the irradiance variations. Irradiance and CO₂ responses are shown in Figures 2 and 3.

Clone	Plant	CO ₂ experiment	PPFD experiment
		PPFD during C _e experiment ($\mu\text{mol m}^{-2} \text{s}^{-1}$)	C _e during PPFD experiment ($\mu\text{mol mol}^{-1}$)
I-214	I1		409.4 \pm 0.84
	I2	965.6 \pm 2.7	398.3 \pm 2.9
Soligo	S1	794.6 \pm 0.6	419.2 \pm 1.2
	S2	843.7 \pm 0.3	391.7 \pm 1.5
	S3	617.8 \pm 1.2	
Raspalje	R2	863.4 \pm 0.8	419.86 \pm 0.3
	R3	938.8 \pm 1.6	397.2 \pm 4.02
	R4	563.5 \pm 1.6	

Estimation of mesophyll conductance (g_m)

The mesophyll conductance to CO₂ was estimated from the difference between the simple equation of discrimination and the observed discrimination by the leaf (Δ_{obs}). The simple equation of discrimination (Farquhar *et al.*, 1982) is expressed as:

$$\Delta_i = a + (b - a) \frac{C_i}{C_a}$$

(Eq. 3)

where a is discrimination by diffusion in air and b discrimination by carboxylation, which assumes mesophyll conductance as infinite and a lack of impact of decarboxylation processes (R_d – respiration rate in the light and photorespiration), and the observed discrimination by the leaf (Δ_{obs}). Δ_{obs} can be quantified by comparing the $\delta^{13}\text{CO}_2$ of the air entering and leaving the chamber, following Evans *et al.* (1986):

$$\Delta_{obs} = \frac{\xi(\delta^{13}C_o - \delta^{13}C_e)}{1000 + \delta^{13}C_o - \xi(\delta^{13}C_o - \delta^{13}C_e)}$$

(Eq. 4)

where:

$$\xi = \frac{C_e}{C_e - C_o}$$

(Eq. 5)

ξ is the ratio of CO_2 entering the chamber over the CO_2 drawdown induced by the leaf. g_m is then estimated as by taking into account respiration and photorespiration using the complete Farquhar model for isotopic discrimination (Farquhar *et al.*, 1982) as:

$$g_m = \frac{(b - e_s - a_i) A / C_a}{(\Delta_i - \Delta_{obs}) - \frac{eR_d / k + f\Gamma^*}{C_a}}$$

(Eq. 6)

where k is the carboxylation efficiency ($k=(A+R_d)/(C_i-\Gamma^*)$), following (Farquhar *et al.*, 1980). We used values of $e_s=1.1\text{‰}$ (CO_2 dissolution in liquid) and $a_i=0.7\text{‰}$ (CO_2 diffusion in liquid phase), following (O'leary, 1981). The value of f (fractionation during photorespiration) was set at 11‰ , based on theoretical calculations of Tcherkez (2006), that were subsequently confirmed from empirical measurements (Lanigan *et al.*, 2008). To the best of our knowledge, the only study having estimated g_m in poplar with the isotopic method is (Hanba *et al.*, 2003), using a common value of $b=30\text{‰}$ for poplar and others species measured in that study. We choose to use the same value in the absence of a direct estimate of b in poplar. Respiration in the dark (R_n) was measured before starting measurements of g_m . Respiration rate in the light (R_d) was set at 66% of R_n , following estimation of Piel (these 2002) performed on

Populus koreana x trichocarpa cv "Peace", leading to R_d between 0.58 and 0.90 $\mu\text{mol m}^{-2} \text{s}^{-1}$. We used estimation of $\Gamma^* = 37.43 \mu\text{mol mol}^{-1}$ from Bernacchi *et al.* (2002) at 25°C. We corrected this value for the leaf temperature during our experiment ($T_{\text{leaf}}=22.1^\circ\text{C}\pm 0.7(\text{mean}\pm\text{SD})$) following the same authors, leading to Γ^* varying between 35.7 and 39.3 $\mu\text{mol mol}^{-1}$.

Mixing ambient air with pure CO_2 from a compressed tank changed the isotopic composition of the CO_2 used during the experiment, with variations from -8.4 to -27.9‰. e , fractionation during respiration was replaced by $e' = e + \delta^{13}\text{C}_{\text{source}} - \delta^{13}\text{C}_{\text{atmosphere}}$ (Wingate *et al.*, 2007), leading to e' varying from 0.53‰ to -18.93‰.

Estimation of assimilation rate for a stable g_m

To test the effect of a variable *versus* stable g_m on assimilation rate under varying PPFD, we recalculated the assimilation rate (A) with the hypothesis that g_m remained stable during the irradiance variation. We based this simulation on plant I2 which showed a variable g_m from 0.05 to 0.25 $\mu\text{mol m}^{-2} \text{s}^{-1}$ with increasing irradiance (Figure 2) and tested stable g_m values of $g_m=0.05$ (g_m is minimal and stable with irradiance), 0.1 (intermediary), 0.3 (g_m is maximal and stable with irradiance), and 0.8 (g_m is very high and stable) $\mu\text{mol m}^{-2} \text{s}^{-1}$. We used an iterative approach with $A_{\text{Fick}} = f(g_{tc}, C_a, C_i, E)$ (which is the assimilation rate calculated from the Ficks law accounting for the interaction between H_2O diffusing outward and CO_2 diffusing inward, see (Ball, 1987) eq. 31), $C_c = C_i - A_{\text{Fick}}/g_{m\text{fixed}}$ and $A_{\text{bioch}} = \min\{A_c, A_j\}$, with

$$A_j = \frac{J(C_c - \Gamma^*)}{(4C_c + 8\Gamma^*)} - R_d$$

(Eq. 7)

and

$$A_c = \frac{V_{c\text{max}}(C_c - \Gamma^*)}{C_c + K_c(1 + O/K_o)} - R_d$$

(Eq. 8)

where J is electron transport rate, $V_{c\text{max}}$ the maximal CO_2 fixation velocity and O the O_2 partial pressure in the chloroplast, K_c and K_o the Michaelis-Menten constant for carboxylase and oxygenase, respectively. K_c and K_o from Bernacchi *et al.* (2002) and recalculated for T_{leaf} were used. J was estimated with the empirical non-rectangular hyperbola equation of Von Caemmerer (2000) based on PPFD and J_{max} . Values of $J_{\text{max}}=110 \mu\text{mol m}^{-2} \text{s}^{-1}$ and $V_{c\text{max}}=60 \mu\text{mol m}^{-2} \text{s}^{-1}$ fitted well with measured A

($R^2=0.99$) thus we used these values to calculate A_{bioch} . We used Solver add-in in Microsoft Excel to determine C_i to have $A_{Fick}=A_{bioch}$. In summary, measured data (A , C_a , C_i , C_c , g_s , and g_m) were used to determine V_{cmax} and J_{max} . Then, we simulated C_i and A , fixing g_m and knowing C_a , g_s , V_{cmax} and J_{max} .

Statistical analysis

All statistical analyses were performed with R (R Development Core Team 2010, <http://www.R-project.org>). A linear mixed-effect model was used to assess effect of PPFD and CO₂ variations on A , g_s , C_c , C_i - C_c draw-down and g_m . For PPFD variations, clone and PPFD (as factor) were set as fixed effect and individual plants within each PPFD as random effect. For CO₂ variations, clone and C_i (as covariate) were set as fixed effect. During CO₂ experiment PPFD was different between each individual plant (see Table 2), thus PPFD was set as random effect. We assessed variations of mesophyll conductance for each plant and within each experiment with ANOVA, where PPFD was set as factors and C_i as covariate following the source of variation used (CO₂ or PPFD). Normality and heteroscedasticity were graphically checked with QQ-Plots. In case of heteroscedastic data we choose to weight the mean as a function of the variance. In case of non-normal distribution, variables were log-transformed. Significance was accepted at $P<0.05$. We used mean least squares regression to assess the correlation between variables (R^2 and P -value).

RESULTS

Photosynthesis and g_m under changing irradiance and CO_2

An example of the time course of measurements is presented in Figure 1 where irradiance is firstly increased, and then CO_2 on the same leaf.

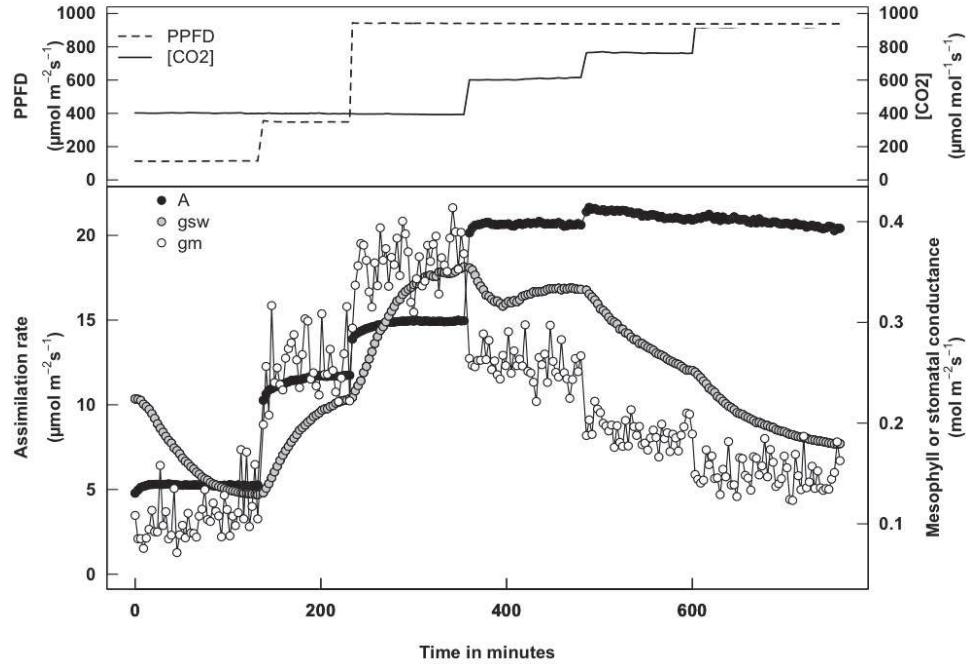


Figure 1: Time course of net CO_2 assimilation rate (A , black dots), stomatal (g_s grey dots) and mesophyll (g_m open dots) conductance to CO_2 during stepwise changes of irradiance (PPFD) followed by CO_2 . The upper panel shows variations of irradiance (dashed line) and CO_2 entering the chamber (continuous line). Each point is a single measurement by the tunable diode laser absorption spectrometer (TDLAS, integration of thirteen seconds) and the gas exchange system, at 3 min. intervals.

When irradiance was increased from 110 to 950 $\mu\text{mol m}^{-2} \text{s}^{-1}$ PPFD in three steps, we observed a significant increase of net assimilation rate (A) from 5 to 14 $\mu\text{mol m}^{-2} \text{s}^{-1}$, stomatal and mesophyll conductance to CO_2 (g_s and g_m) from 0.1 to 0.35 $\text{mol m}^{-2} \text{s}^{-1}$. We observed that during each irradiance step, g_m changed faster than g_s and reached a stable value after only 10-15 minutes whereas stabilization of g_s required sometimes 1 hour. When irradiance was maintained constant and CO_2 mole fraction of the air entering the chamber (C_e) increased from 400 to 910 $\mu\text{mol mol}^{-1}$ in four steps, we induced an increase of A up to a plateau above 600 $\mu\text{mol mol}^{-1}$. g_s and g_m decreased linearly from 0.35 to 0.15 $\text{mol m}^{-2} \text{s}^{-1}$ as C_e increased. For all plants, variations of A , g_s and g_m are presented in Figures 2 and 3 for irradiance and CO_2 variations,

respectively. A mixed-effect model accounting all plants measured in this study showed that A , g_s and g_m were affected by irradiance and CO_2 (Table 3).

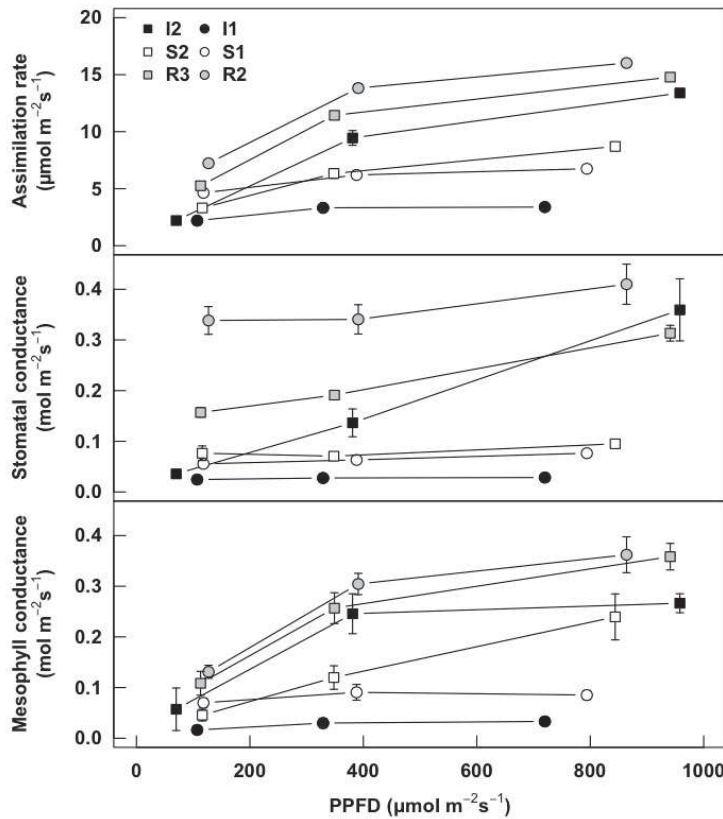
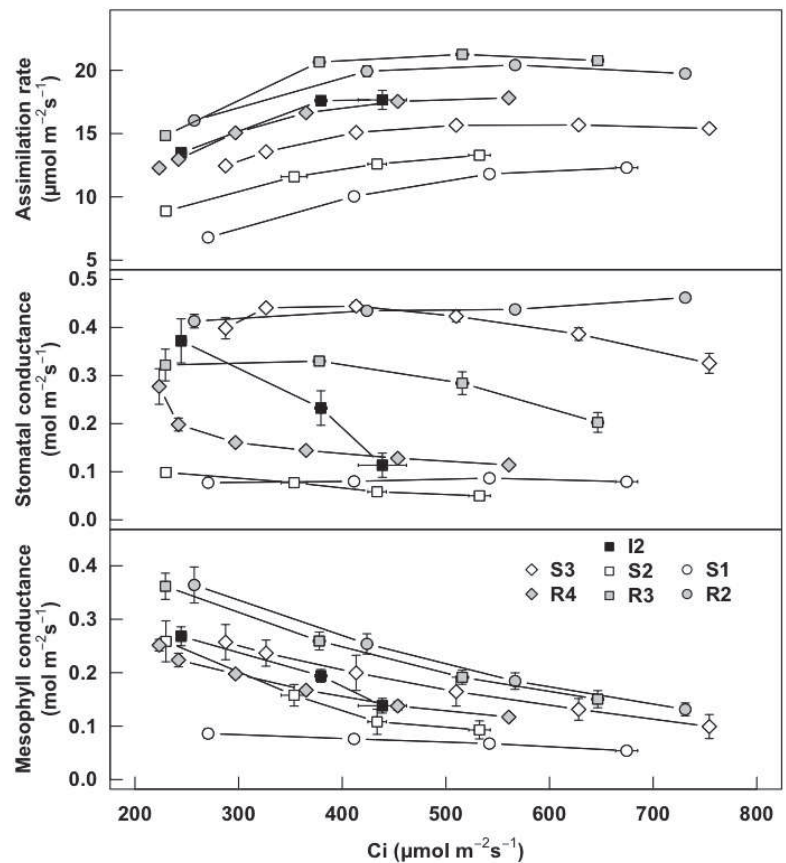


Figure 2: Variations of net CO_2 assimilation rate (upper panel), stomatal conductance to CO_2 (middle panel) and mesophyll conductance to CO_2 (lower panel) during changes of irradiance (PPFD). Each point is a mean of measurements during one irradiance step (30~40 single measurements), errors bars are standard deviations. I is for clone “I-214”, S for clone “Soligo” and R for clone “Raspalje”.

Figure 3: Variations of net CO_2 assimilation rate (upper panel), stomatal conductance to CO_2 (middle panel) and mesophyll conductance to CO_2 (lower panel) during step-wise CO_2 changes. Each point is a mean of measurement during one step of CO_2 (30~40 single measurements), error bars are standard deviation. I is for clone “I-214”, S for clone “Soligo” and R for clone “Raspalje”.



We did not observe any significant clonal difference, but a C_i x clone interaction for CO_2 variations. Taken individually, all plants displayed significant variations of A , g_s and g_m with increasing irradiance and CO_2 , but the range of variation differed among replicates. In 6 out of 8 plants there were large responses to irradiance and CO_2 , whereas in 2 plants responses were small. All responsive plants exhibited the typical variations showed in Figure 1.

Table 3: Mixed-effects model for A , g_s , C_c , C_i - C_c draw-down and g_m under changing irradiance (PPFD) and CO_2 (C_i). For irradiance changes, the irradiance x clone interaction was not significant and therefore removed from the model. irradiance was set as factor and individual plant was as random effect within each level of irradiance. For C_i variations, C_i was set as covariate and irradiance as random effect because each plant was measured under a different irradiance (see M&M).

Experiment			A	g_s	C_c	$C_i - C_c$	g_m
Irradiance variations	Irradiance	$F_{(2,10)}$	16.91	4.72	28.55	NS	12.78
		P	<.001	0.03	0.0001	NS	0.002
	Clone	$F_{(2,3)}$	NS	NS	NS	NS	NS
		P	NS	NS	NS	NS	NS
CO_2 variations	C_i	$F_{(1,669)}$	2473.4	372.8	36773.7	6663.3	3420.9
		P	<.0001	<.0001	<.0001	<.0001	<.0001
	Clone	$F_{(2,4)}$	13.6	NS	NS	NS	NS
		P	0.01	NS	NS	NS	NS
	C_i x Clone	$F_{(2,669)}$	29.42	253.1	82.3	73.2	70.6
		P	<.0001	<.0001	<.0001	<.0001	<.0001

Under changing irradiance, we observed a positive correlation between g_m and g_s ($R^2=0.69$, $P<0.001$, $g_m=0.73g_s+0.04$) (not significant intercept), and g_m and A ($R^2=0.94$, $P<0.001$, $g_m=0.02A-0.04$) (see Figure 4). To explore how the different CO_2 mole fractions inside the leaf varied with variations of CO_2 demand (A), we compared variations of C_a , C_i and C_c when A varied with irradiance (Figure 5) considering data from all the plants. Since we controlled CO_2 mole fraction entering the chamber (C_e) in our experiment, we observed slight decrease of C_a along the increasing CO_2 uptake by the plant. With A varying from 2 to 14 $\mu\text{mol m}^{-2} \text{s}^{-1}$, C_i decreased by 60 $\mu\text{mol mol}^{-1}$

(significant negative slope), but C_c was maintained constant (slope not significantly different from zero), all plants considered together (Figure 5). The C_i - C_c draw-down was slightly decreased by $\approx 50 \mu\text{mol mol}^{-1}$ with increasing A . Within each plant, C_c dropped in average by $50 \mu\text{mol mol}^{-1}$ with the increase in A (not shown).

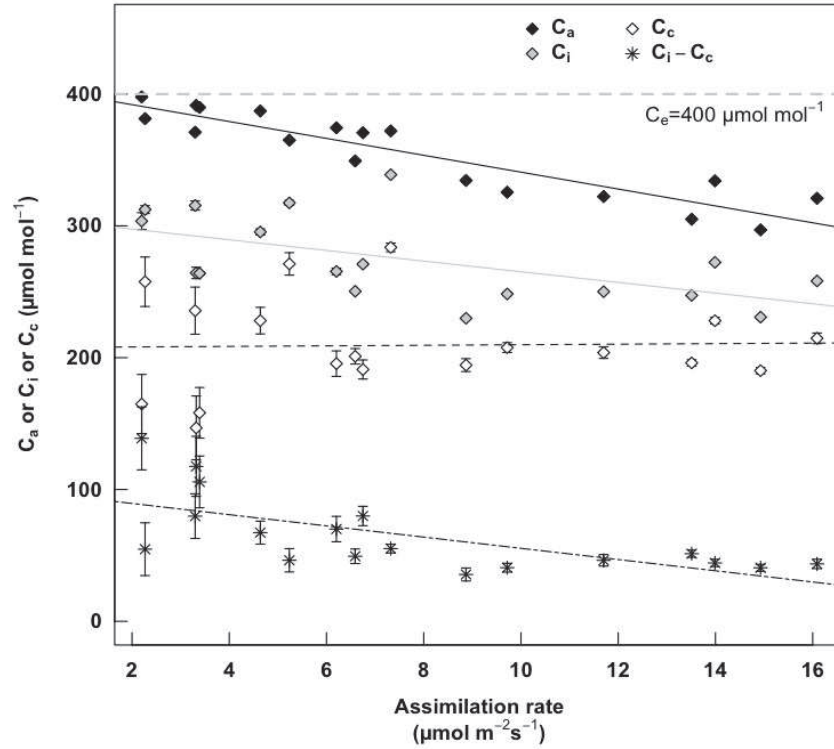


Figure 5: During the PPFD experiment, variations of CO_2 mole fraction in the atmosphere (C_a , black diamonds and black continuous line), intercellular airspace (C_i , grey diamonds and grey continuous line) and chloroplast (C_c , empty diamonds and black dashed line) versus assimilation rate (A). Each point is mean (30~40 single measurements), error bar are standard deviation.

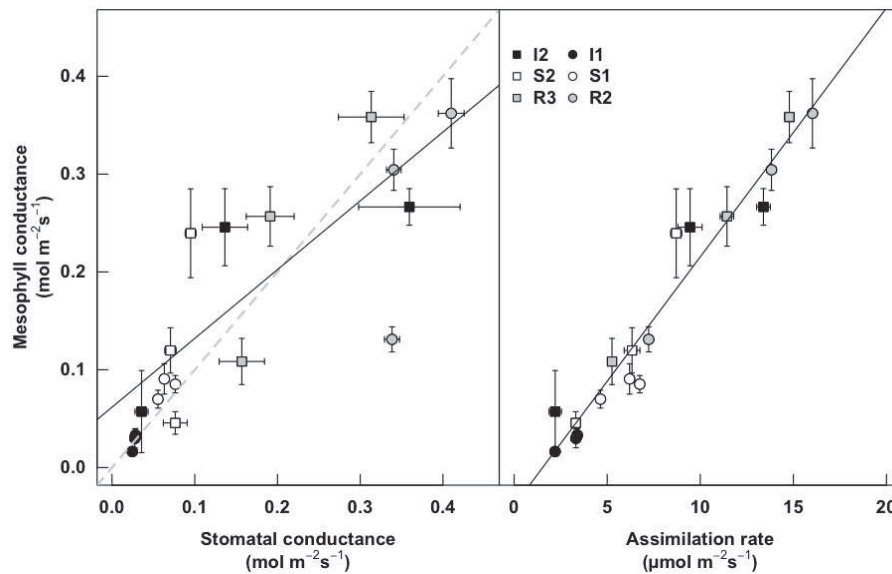


Figure 4: Relationship between mesophyll conductance to CO₂ and stomatal conductance to CO₂ (left) and net assimilation rate (right) during PPFD experiment. Each point is a mean of measurement during one irradiance step (30~40 single measurements), errors bars are standard deviation. Dashed grey line in the left panel in the 1:1 relationship. I is for clone “I-214”, S for clone “Soligo” and R for clone “Rasplje”.

How would A be affected if g_m was unaffected by irradiance?

We estimated the effect of a stable g_m on A under varying irradiance using a simulation approach performed on data from the plant I2 which showed a large variation of $A > 10 \mu\text{mol m}^{-2} \text{s}^{-1}$, (black dots in Figure 6). Under low PPFD=70 $\mu\text{mol m}^{-2} \text{s}^{-1}$ (low A and g_s), the impact of different g_m values on A was very small ($<0.5 \mu\text{mol m}^{-2} \text{s}^{-1}$). At medium PPFD =380 $\mu\text{mol m}^{-2} \text{s}^{-1}$, using $g_m=0.8 \text{ mol m}^{-2} \text{s}^{-1}$ increased A by only $\approx 0.5 \mu\text{mol m}^{-2} \text{s}^{-1}$, meanwhile low g_m (0.05 $\text{mol m}^{-2} \text{s}^{-1}$) decreased A by $\approx 3 \mu\text{mol m}^{-2} \text{s}^{-1}$. Comparison between A calculated with J limitation and V_{max} limitation showed that A was J limited at this part of the curve i.e under low and medium PPFD. The impact of g_m was much higher at high PPFD=960 $\mu\text{mol m}^{-2} \text{s}^{-1}$, with $g_m=0.1$ and $0.05 \text{ mol m}^{-2} \text{s}^{-1}$ (while measured $g_m=0.25 \mu\text{mol m}^{-2} \text{s}^{-1}$) decreased A by 3 and 6 $\mu\text{mol m}^{-2} \text{s}^{-1}$ (i.e 25 and 50%). On the other hand, a high $g_m=0.8 \text{ mol m}^{-2} \text{s}^{-1}$ only increased A by 1 $\mu\text{mol m}^{-2} \text{s}^{-1}$. Under high PPFD, assimilation was V_{max} limited. Finally, we used $g_m=0.3 \text{ mol m}^{-2} \text{s}^{-1}$ which correspond to the maximum (high PPFD) measured g_m . We observed no change of A with a stable g_m compared to the variable (measured) g_m . With the measured g_m , the C_i-C_c draw down was 50 $\mu\text{mol mol}^{-1}$ and constant with PPFD (and thus A) variations. For a stable and low $g_m = 0.05 \text{ mol m}^{-2} \text{s}^{-1}$, C_i-C_c draw down increased from 50 to 150 $\mu\text{mol mol}^{-1}$ during PPFD and A variations, while for a high $g_m= 0.8 \text{ mol m}^{-2} \text{s}^{-1}$ C_i-C_c varied from 3 to 17 $\mu\text{mol mol}^{-1}$ (not shown).

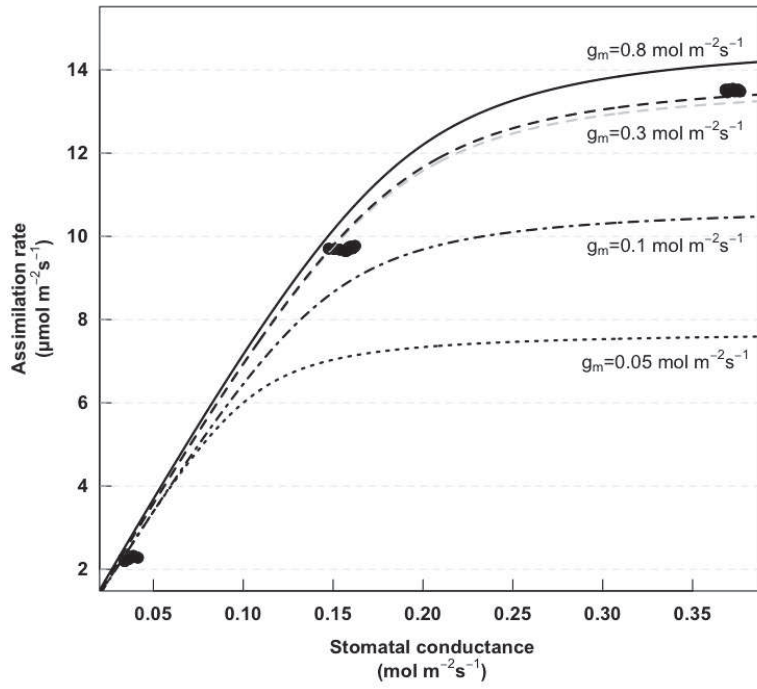


Figure 6: Relationship between net assimilation rate versus stomatal conductance for different values of mesophyll conductance (g_m). Black dots are measured values (g_m is variable between 0.05 and 0.26 $\text{mol m}^{-2} \text{s}^{-1}$) and the grey dashed line is the fitted hyperbola non-rectangular with $J_{max}=110 \text{ } \mu\text{mol m}^{-2} \text{s}^{-1}$ and $V_{cmax}=60 \text{ } \mu\text{mol m}^{-2} \text{s}^{-1}$. We selected points where g_s was stable (variations $< 0.05 \text{ mol m}^{-2} \text{s}^{-1}$) for the individual plant I2. Continuous black line is recalculated A for $g_m=0.8 \text{ mol m}^{-2} \text{s}^{-1}$, dashed black line is recalculated A for $g_m=0.3 \text{ mol m}^{-2} \text{s}^{-1}$, and dot-dashed black line is recalculated A for $g_m=0.1 \text{ mol m}^{-2} \text{s}^{-1}$, and dotted black line is recalculated A for $g_m=0.05 \text{ mol m}^{-2} \text{s}^{-1}$.

DISCUSSION

We found a rapid response of mesophyll conductance (g_m) to PPFD and CO₂ in poplar clones. In response to PPFD or CO₂ g_m respectively increased and decreased in an experiment conducted over several hours. Under PPFD variations, g_m was of the same range of g_s (i.e from 0.05 to 0.4 mol m⁻² s⁻¹) and positively correlated to g_s and A . These variations led to a rather constant C_c across all PPFD all plants considered together. Recalculation of A using a stable g_m showed (i) since PPFD in low and thus A is J_{max} limited g_m had no impact on A and (ii) that under high irradiance A can be reduced by up to 50 % if $g_m=0.05$ mol m⁻² s⁻¹ compared to measured, but was practically not affected by a high g_m .

Rapid variations of g_m with PPFD and CO₂

We confirm that g_m changes rapidly (within minutes) to change in PPFD or CO₂. The positive response of g_m to PPFD in poplar clones is consistent with previous studies on *Arabidopsis thaliana* (Flexas *et al.*, 2007), *Eucalyptus* species (Douthe *et al.*, 2011) and in *Banksia* species (Hassiotou *et al.*, 2009). However, in wheat (Tazoe *et al.*, 2009) and *Nicotiana tabacum* (Yamori *et al.*, 2010) g_m was found to be stable with irradiance.

The reason(s) for the discrepancy between studies is not known. We can firstly think that different parameterizations (i.e. different values chosen for b , e or f) could possibly induce different g_m -response to PPFD. The estimation of rapid-response of g_m is based on the assumption that other fractionation factors are not affected by PPFD. There is little probability that e (fractionation during R_d) was PPFD sensitive because this parameter is generally affected by variation the respiratory substrate, which is unlikely to happen under a variation of PPFD, and the temperature (Ghashghaie *et al.*, 2003) which varied by only 2°C on the overall dataset. It is a similar story for f (fractionation during photorespiration), which is unlikely to have varied during our experiment because temperature and O₂ were constant. There are no studies comparing the parameter b (fractionation by Rubisco and PEPc), at various PPFD. The relative amount of carbon fixed by PEPc, (denoted β) could change with PPFD if the amount of carbon fixed by RubisCO increases with PPFD (because the availability of ATP, NADPH and RuBP increases), but not that of PEPc. We tested such hypothesis, considering g_m constant at maximum measured value ($g_m=0.25$ mol

$\text{m}^{-2} \text{s}^{-1}$). We recalculated b to explain all the variability of $\Delta^{13}\text{C}$ measured. In such cases, b has to take a value of 26‰ at low PPFD and increase to 30‰ at high PPFD. These values cover the overall range of b found in the literature. Assuming $b_3=31‰$, $b_4=-5.7‰$ and both are unaffected by PPFD, the large range in b requires $\beta=0.025$ at high PPFD (for $b=30‰$) and 0.14 at low PPFD (for $b=26‰$) (assuming $b=(1-\beta)b_3+\beta b_4$). A value of $\beta=0.14$ is high but still possible regarding estimations provided by (Vu *et al.*, 1985) with $\beta=0.13$ estimated from enzyme activities. Nevertheless, it is not sure that enzyme activities really reflect the amount of carbon fixed by each enzyme. Moreover, it has been never shown that β could change with irradiance. Hence, we could consider that variation in β or b should not lead to the apparent variation in g_m with PPFD. Nevertheless, due to the dramatic influence of β on estimations of g_m , there is a pressing need for better estimates of β and its possible response to environmental factors, especially irradiance.

With the exception of one recent paper (Tazoe *et al.*, 2009), all studies have observed a decrease of g_m with increasing CO_2 (Bunce, 2010; Centritto *et al.*, 2003; Douthe *et al.* 2011; Flexas *et al.*, 2007; Flexas *et al.*, 2008; Hassiotou *et al.*, 2009; Tazoe *et al.*, 2011; Vrabl *et al.*, 2009). The average decrease of g_m with increasing CO_2 is about 50%, but varies between studies from 20% (Tazoe *et al.*, 2011) to 60% (Flexas *et al.*, 2008), with C_i from 200 to 700 $\mu\text{mol mol}^{-1}$. Here we found g_m decreased by an average of 60% over the same range of C_i , strengthening the hypothesis that g_m is truly responsive to CO_2 . As is the case for PPFD, these conclusions depend directly on the hypothesis that fractionation factors are stable with CO_2 .

Impact of a stable g_m on net CO_2 assimilation rate under PPFD variations

To examine the implications of the PPFD response of g_m for photosynthesis, we simulated rates of photosynthesis for a hypothetical plant in which g_m does not vary with PPFD. At low PPFD ($<100 \mu\text{mol m}^{-2} \text{s}^{-1}$) A was not affected by the different values taken by g_m , higher or lower than estimated by $\Delta^{13}\text{C}$ method (Figure 6). On the other hand, at high PPFD and with open stomata, A was strongly decreased compared to measured when g_m is low and stable. This effect is especially important when A is V_{cmax} limited. This highlights the fact that g_m has to be important under high PPFD, i.e. when CO_2 availability become very limiting for A , but not necessarily under low

PPFD (limitation by J). On the other hand, a very high g_m ($0.8 \text{ mol m}^{-2} \text{ s}^{-1}$, more than three times maximum measured g_m) is not necessarily an advantage regarding the low gain in A ($\approx 1 \text{ } \mu\text{mol m}^{-2} \text{ s}^{-1}$). This approach suggests that a variable g_m appears to be an advantage for the leaf, only high when CO_2 is limiting. This suggests that a possible cost could be induced by such apparatus, which is in accordance with the hypothesis that biochemical processes (which probably represents a metabolic cost) are involved in the rapid variations of g_m like carbonic anhydrase or aquaporins (Flexas *et al.*, 2006; Terashima and Ono, 2002; Uehlein *et al.*, 2008).

We observed that all plants treated together, C_c is maintained quite constant for A variations between 2 and $16 \text{ } \mu\text{mol m}^{-2} \text{ s}^{-1}$ under PPFD variations, all plants considered together. This appears to be a direct consequence of rapid adjustments of g_s and g_m during PPFD changes because with an increasing CO_2 demand (A) if the CO_2 supply would remain constant (g_s , g_m), then C_c should drop severely. A large drop in C_c would decrease the CO_2/O_2 ratio and then disadvantage the carboxylation compared to oxygenation activity of RubisCO. These results suggest that rapid-change of g_m could be an advantage for the leaf to prevent C_c drop and the following limitation (estimated to be 50% decreased with $g_m=0.05 \text{ } \mu\text{mol m}^{-2} \text{ s}^{-1}$ at high PPFD) of photosynthesis with increasing irradiance.

CONCLUSION

We observed that g_m increases with PPFD and decreases with CO_2 , which bring support for the hypothesis that g_m is able to rapidly change (within minutes) to environmental conditions. Under varying PPFD, the range of g_m value was very close to that of g_s , g_m was well correlated with g_s and A , leading to a constant C_c despite increasing CO_2 demand. This suggests a coupling between CO_2 demand and supply at the minutes scale, and thus that some mechanism can modify g_m rapidly to prevent large decreases in C_c . We tested the possible effect of a stable g_m on A and showed that a very high (three times higher than maximal g_m measured) and stable g_m should not be an advantage for the plant. On the other hand, a low (minimal g_m measured under low PPFD) and stable g_m could decrease A up to 50% under high irradiance. These results suggest that a variable g_m could be an optimal solution to adapt CO_2 supply with rapid changes in CO_2 demand, assuming a possible cost for maintaining a high g_m related to candidates like aquaporins or carbonic anhydrase.

CONCLUSIONS and PERSPECTIVES

Influence of the different parameters in the $\Delta^{13}\text{C}$ model

This work was focused on the use of the discrimination model of Farquhar and colleagues (Farquhar *et al.*, 1982), which predicts the discrimination against ^{13}C ($\Delta^{13}\text{C}$) during plant photosynthesis following the leaf gas exchange. Since this model is widely used to estimate water use efficiency at different scale, it appeared important to better understand the parameter able to influence the $\Delta^{13}\text{C}$ -WUE relationship. In Chapter I we provided a literature review of studies comparing leaf bulk tissue $\Delta^{13}\text{C}$ and measured gas exchange, highlighting a large variability in the observed $\Delta^{13}\text{C}$ -WUE relationship. We pointed that such variability is partially caused by the use of leaf bulk tissue to measured $\Delta^{13}\text{C}$, which induce (i) difference in time scale integration between $\Delta^{13}\text{C}$ and WUE and (ii) an additional variability of $\Delta^{13}\text{C}$ caused by the different $\delta^{13}\text{C}$ of each leaf component (Bowling *et al.*, 2008). Moreover, our simulations showed that not accounting for mesophyll conductance (g_m) or setting different values of g_m dramatically affects the estimation of WUE from $\Delta^{13}\text{C}$ measurements. It was the same conclusion for b . This clearly shows that the estimation of WUE (or more generally leaf gas exchange) from $\Delta^{13}\text{C}$ measurements have to be used with caution. If possible, g_m should be estimated and incorporated in the $\Delta^{13}\text{C}$ model, or in other words, preferentially use the complete form rather than the simple form of the $\Delta^{13}\text{C}$ of Farquhar *et al.* (1982) to estimate leaf gas exchange from $\Delta^{13}\text{C}$. This can be difficult, regarding the possible variations of g_m with environmental conditions (see below). That is why we decided to focus the next part of our work on the estimations of g_m , its influence on the complete form of the $\Delta^{13}\text{C}$ model and its possible ability to change with environment.

Estimating g_m from isotopic measurements: the importance of the parameterization

By rearranging the equation linking leaf gas exchange and $\Delta^{13}\text{C}$, it is possible to estimate g_m , the mesophyll conductance to CO_2 (Evans *et al.*, 1986; Farquhar *et al.*, 1982). A sensitivity analysis of the g_m estimation to the parameters in the first chapter showed that b , the fractionation during the carboxylation, affects dramatically the g_m estimation. Taken individually, fractionation factors during decarboxylations (e and f) are less influent, and finally R_d and Γ^* (non-photorespiratory respiration and photorespiration, respectively) are weakly influents on the estimation of g_m (see Chapter I). On the other hand, accounting or not for the respiratory term can change g_m by up to 50% (Chapter II). Finally, the sensitivity analysis showed some

interactions between the parameters in the g_m estimation: the effect of a given parameter on g_m will change with the value taken by another parameter. For example, combining high f (fractionation during photorespiration) and low b can double the value of g_m . These findings evidence that the absolute value of g_m assessed by isotopic method is dependant of the choice of parameters. On the other hand, the range of g_m values is likely to be of the same order as g_s (stomatal conductance), because both isotopic and chlorophyll fluorescence methods give approximately the same range of values (see Centritto *et al.*, 2009; Loreto *et al.*, 1992; Vrabl *et al.*, 2009).

The response of g_m to varying CO_2

This work took place in the context of the rapid response of g_m to changing irradiance and CO_2 . CO_2 variation was the most used source of variations among the literature, but no consensus was reached yet when this thesis was started. We clearly showed that g_m was responsive to CO_2 variations when estimated with the isotopic method, and confirmed it in four different tree species (one poplar and three eucalypts). We especially accorded attention to the importance of the respiratory term (Chapter II), and observed that g_m was still responsive to CO_2 including or not the influence of decarboxylations. We nevertheless recommend to include this term when g_m is estimated from the isotopic method, regarding the decrease up to 50% of the g_m absolute value when estimated without the respiratory term (Chapter II). When compared to the literature, we found the same negative response of g_m under increasing CO_2 , and approximately the same relative decrease, by $\approx 50\%$, when C_i increased from 300 to 900 $\mu\text{mol mol}^{-1}$. This is a comparable range that found by recent studies using the isotopic method (Tazoe *et al.*, 2011), the chlorophyll fluorescence method (Hassiotou *et al.*, 2009), or both of them (Vrabl *et al.*, 2009). In chapters I and III, we discussed about the possibility that rapid variations of other parameters in the model could make the g_m rapid response artifactual under varying irradiance (this point is detailed below). We did not performed this analysis on the CO_2 g_m response because g_m was found to clearly vary with CO_2 using two different methods (see Vrabl *et al.*, 2009). Indeed, if rapid variations of, for example, b would occur during CO_2 variations (meaning that g_m would remain stable with CO_2), there is little chance that g_m would be found to vary using the chlorophyll fluorescence method. This fact, combined with our results repeated on several species and a careful parameterization, clearly evidence that the g_m response to CO_2 is not artifactual.

The g_m response to irradiance variations

Compared to CO₂ variations, this source of variations was less studied since g_m is suspected to vary rapidly. Our work strongly brought support for g_m varies rapidly with irradiance in tree species. We confirmed results from Flexas *et al.* (2007) who observed a positive relationship between g_m and irradiance in tobacco using the chlorophyll fluorescence method. On the other hand, two studies found g_m stable with irradiance (Tazoe *et al.*, 2009; Yamori *et al.*, 2010). To ensure our results, we firstly checked whether such response was not an artifact induced by the parameterization. To do that we firstly observed a positive g_m response to irradiance including or not the respiratory component (Chapter II), we provided detailed irradiance responses on three eucalypts under two different O₂ mole fractions (Chapter III) to evidence that the presence/absence of photorespiration does not cancel g_m response to irradiance, and we finally eliminated possible rapid variations of other parameters in the model susceptible to vary instead of g_m by simulation. These simulations evidenced that non-realistic variations of each parameters are needed to fully explain $\Delta^{13}\text{C}$ variations instead of g_m , confirming that g_m effectively varies with irradiance. We found exception for the b parameter, able to vary in a realistic range with varying irradiance. Moreover, we reasoned that an increase of b with irradiance, as simulated, was plausible since only the RubisCO fixation is directly dependent of irradiance (via electron transport rate), but not that of PEPc. This suggests a possible variation of β with irradiance, with less relative amount of carbon fixed by PEPc (thus smaller β and higher b) at high irradiance. Our results evidenced that g_m is very likely to vary with irradiance, but a final confirmation is needed concerning the possible variations of b . This information could be approached using ratio of PEPc over RubisCO activities or by the labelling of metabolites under rapid variations of irradiance.

Possible interest of a varying g_m with changing CO₂ or irradiance

Our results confirm rapid response of g_m under varying CO₂ and irradiance, and we explore here possible explanation such rapid response.

Under varying CO₂, we observed a decrease of g_m with increase CO₂, thus when photosynthesis is high. A decrease of g_m could be explained by a reduction of a possible cost while the photosynthesis is still maintained. This hypothesis was pointed by Hassiotou *et al.* (2009), and follows the same rationale proposed for the g_s negative response to CO₂ (Brodribb *et al.*, 2009). Under varying irradiance, we

showed by simulation that there is not interest for the plant to maintain a high g_m at low irradiance (Chapter IV). Concomitantly, g_m is very limiting for photosynthesis at high irradiance. An optimization of the possible cost-induced by a high g_m would induce such investment only when the return benefit on photosynthesis is high (higher gain on assimilation rate). Such conditions occur at low CO₂ or high irradiance. This point of view could fit with the fact that g_m is apparently related to proteins facilitating CO₂ transport through membranes, the aquaporins. This implies that a cost should be induced to have higher aquaporins content or a higher proportion of activated aquaporins. The cost hypothesis is not elucidated, since the regulation of aquaporins activity at the short-term is not clear yet.

Another approach can be used to understand rapid g_m variations, not focused on a cost/benefit point of view, but based on the repetitive g_s - g_m correlations. The possible role of aquaporins is, again, an attractive hypothesis. It has been shown that aquaporins gating property significantly affect conductivity to water at the cell scale (Kim and Steudle, 2009) and at the leaf scale (Cochard *et al.*, 2007), in response to short-term variations of irradiance (within minutes) (see for review Heinen *et al.*, 2009). In both studies, increasing irradiance increased cell or leaf conductivity to water. Since PIP family aquaporins are involved in both water and CO₂ transport (Maurel *et al.*, 2008), we can suppose that irradiance-induced variations in water conductivity should be accompanied by variations of CO₂ conductance (g_m). It has been shown that the same NtAQP1 aquaporin is present in both plasma membrane and in chloroplast envelope in tobacco (Uehlein *et al.*, 2008). Interestingly, the authors concluded that the NtAQP1 aquaporins was more involved in water transport when present in the plasma envelope, but more involved in CO₂ transport when present in the chloroplast envelope. Thus, if changes in the leaf hydraulic status affects aquaporins content or activation, this would have an impact on the CO₂ diffusion. Since high irradiance is known to increase g_s and thus the transpiration rate, which as consequence increases the hydraulic demand, a higher water conductance through aquaporins is needed to prevent drop in bulk leaf water potential, as discussed by Cochard *et al.* (2007). This fact combined with findings by Uehlein *et al.* (2008) suggest that changes in leaf hydraulic status will affect both water and CO₂ transport through aquaporins, and explain well the higher g_m found under high irradiance. This also fit with the decrease of g_s and g_m at high CO₂. It is well known that high CO₂ decreases g_s , and this decrease probably decrease the overall hydraulic demand. Thus,

as discussed by Cochard *et al.* (2007), in conditions of low hydraulic demand the water pathway mediated by aquaporins should be lowered, probably related to an energetic cost associated, which in turn decrease CO₂ diffusion. As we proposed in the Discussion of Chapter IV, it could be more pertinent to consider g_m variations in the context of both water and carbon fluxes. This could explain the repetitive correlations between g_s and g_m at the instantaneous scale.

Sensitivity of g_m to others source of variations

Some studies found a disconnection between g_s and g_m , especially under abscissic acid treatment (ABA; Vrabl *et al.*, 2009), while g_s was decreased with ABA but not g_m . This experiment can highlight the fact that specific factors can affect g_s , but not g_m . The same g_s - g_m disconnection was observed by varying VPD (Warren, 2008), with again g_s affected by VPD but not g_m . We repeated the same VPD experiment on poplar, and observed the same pattern as Warren (2008) (see Figure D1).

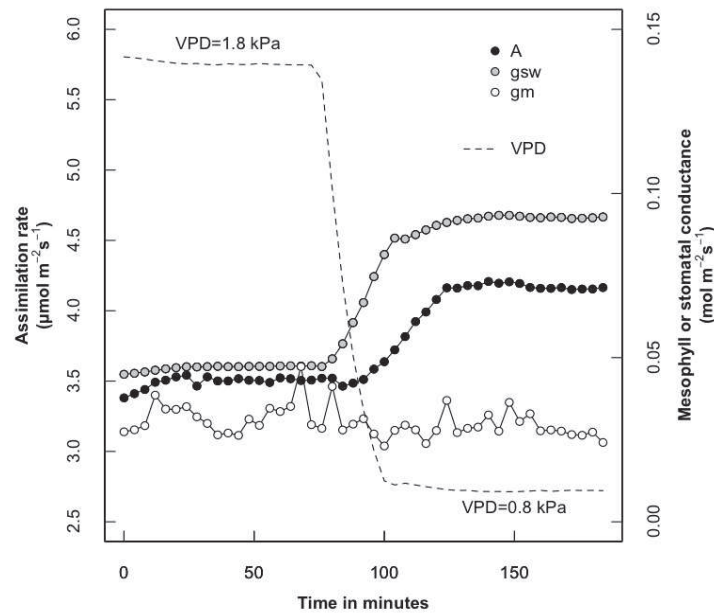


Figure D1: Temporal course of net assimilation rate (blacks dots, A, in $\mu\text{mol m}^{-2} \text{s}^{-1}$), stomatal conductance to CO₂ (grey dots, g_s , in $\mu\text{mol m}^{-2} \text{s}^{-1}$) and mesophyll conductance to CO₂ (empty circles, g_m , in $\mu\text{mol m}^{-2} \text{s}^{-1}$) in response to varying VPD from 1.8 to 0.8 kPa (dashed lines) in poplar leaf exposed to CO₂ concentration around the leaf of $380 \mu\text{mol mol}^{-1}$ and irradiance of $700 \mu\text{mol m}^{-2} \text{s}^{-1}$ PPFD.

Thus, the g_s - g_m relationship is clearly effective under some conditions (CO₂ and irradiance) but not systematically. This evidences the complexity of the short-term regulation of g_m , and probably different sensing mechanisms between g_s and g_m . This address an unresolved questions at the moment: by which mechanism external

conditions (irradiance, CO₂ etc..) affect g_m , thus probably aquaporins regulation? The g_s - g_m disconnection (i.e the presence / absence of a relationship) is a promising topic, which should help us to identify and separate the different sensing mechanisms behind rapid regulations of g_s and g_m .

In conclusion, this work was focused on the relationship between $\Delta^{13}\text{C}$ and leaf gas exchange. We highlighted the importance of mesophyll conductance on the $\Delta^{13}\text{C}$ signal, especially to estimating water use efficiency. We secondly focused on the ability of g_m to change rapidly under varying irradiance and CO₂. We extended the range of species where g_m was found to change with both sources of variation, demonstrate that these responses were not artifactually caused by neither the respiratory term, the presence of photorespiration or rapid variations of other parameter in the $\Delta^{13}\text{C}$ model. We found exception for the b parameter under irradiance variations, highlighting the need to better estimate this parameter and its possible rapid variations. We finally showed that the limitation imposed by g_m changes with irradiance, suggesting that a variable g_m should be more advantageous for the plant. The role of aquaporins appeared to be an attractive hypothesis to explain rapid g_m changes, and its relationship with g_s , suggesting the need to consider both water and carbon fluxes under varying environment to better under g_m regulation.

In consequence, we suggest that future studies can be focused on the following topics:

- Perform g_m estimations using simultaneously both isotopic and fluorescence methods,**
- Estimate the parameter b and especially β under different irradiance conditions, using enzyme activities, or pulse carbon labeling,**
- Verify if short-term variations g_m variations are accompanied to variations of aquaporins content or activation,**
- Finally, we suggest that an effort should be done on the modelling of g_m rapid variations, using a mechanistic approach, probably based on its relationship with A and/or g_s . Beyond the simple fact to know how g_m varies rapidly, a mechanistic comprehension of such variations should allow to incorporate rapid g_m changes in photosynthesis models at the plant or ecosystem scale, and prediction models of $\Delta^{13}\text{C}$ signal.**

ANNEX I

Annex I

The aim of this section is to describe the gas exchange systems coupled to a Tunable Diode Laser Absorption Spectrometer (TDLAS) (TGA100A, Campbell Scientific, Logan, UT, USA) used to measure discrimination against $^{13}\text{CO}_2$ during photosynthesis ($\Delta^{13}\text{C}$), and the subsequent estimations of mesophyll conductance to CO_2 (g_m). For each of the two circuits used, we then describe the tests performed to assess the potential influence of leaks, a crucial points to valid our measurements. The first part is focused on a commercial portable gas exchange system (LI-COR, Lincoln, NE, USA) used in Sydney based on a classical leaf clamp system. The second part will describe the system used at the Université de Nancy, based on a custom-built chamber which allowed us to enclose a whole leaf.

Part 1: Using a LI-COR 6400 coupled to a TDLAS

Measuring gas composition

We used a LI-6400 portable gas exchange system to measure all photosynthesis parameters (A , g_s , C_i etc..), while the TDLAS – for tunable diode laser absorption spectrometer was used to measure isotopic composition of air entering and leaving the photosynthesis chamber. Infra-Red Gas Analyzer (IRGA) are based on absorption of infra-red (IR) signal by CO_2 and water vapor molecules in the measured gas. The main problem is that CO_2 and water vapor absorb in the same wavelength. IRGA uses a broad-band source (non specific) emitting in a large range of wavelength, and a detector sensitive to only CO_2 absorbed wave-length allows to calculate absorbed energy by CO_2 only (*idem* for water vapor).

The TDLAS is based on the same principle but emits in specific absorption lines to focus IR absorption by $^{12}\text{CO}_2$ and $^{13}\text{CO}_2$ only. This requires a laser source with a temperature regulation with liquid nitrogen and a controlled-current to obtain a stable wavelength focused on the desired absorption line. Changing the current of the laser source allows to select different absorption lines and scan alternatively $^{12}\text{CO}_2$ and $^{13}\text{CO}_2$ at a frequency of 10Hz.

Description of the gas exchange circuit

The system is described in Figure A1. The LI-6400 allows to control air flow, CO_2 and water vapour mole fractions in the air entering the photosynthesis chamber, as well as irradiance and leaf temperature. The LI-6400 was equipped with a custom-built chamber of 18 cm^2 using a classical leaf clamp system. The CO_2 mixer control

of the LI-COR 6400 was used vary CO₂ mole fraction in the circuit. Water vapour mole fraction entering the circuit was varied following the needs by scrubbing the air through a desiccant (drierite). Once air composition was set correctly, the TDLAS was plugged to the LI-COR 6400 circuit to sample a part of the air flow to analyse isotopic composition. The TDLAS was connected through a “T” tubing to the reference tube of the LI-6400 between the console and the IRGA. In the same way, the TDLAS intake of sample gas was connected in-between the LI-6400 chamber exhaust and the match valve. The TDLAS was set to continuously withdraw 150 mL min⁻¹ (~111 μmol s⁻¹) from sample and reference fluxes of the LI-6400. This withdrawal of air was smaller than the flow through the LI-6400 chamber (400 μmol s⁻¹), which means that the TDLAS could sample air from the LI-6400 while maintaining a positive pressure in the LI-6400 chamber. Existence of a positive pressure inside the LI-6400 chamber was checked through the curvature of the propafilm covering the top of the chamber. Ambient air (at a flow rate of 0.1 L min⁻¹) was diluted with pure nitrogen (N₂, at a flow rate of 1.9 L min⁻¹) to perform measurements under 1% O₂. For 1% O₂ measurements, the LI-6400 configuration was adjusted to account for the effect of O₂ on calibration (Bunce 2002).

Calibration and measurement sequence

A manifold was used to switch continuously between the three calibrations tanks, the reference and the sample intake, each intake being measured during 45 seconds with 15 first seconds not accounted to prevent any mix with the previous gas measured. The TDLAS was calibrated with two tanks (T1 and T2) with CO₂ concentrations of respectively 419 ± 10 and 290 ± 7 μmol mol⁻¹ (mean ± CI) given by the provider and checked with a recently factory-calibrated LI-8100 IRGA (LI-COR, Lincoln, NE, USA). Isotopic composition of the each tank was measured by sampling air into 12-mL exetainers (Labco Limited, Buckinghamshire, UK) and analysed via the gas-bench inlet of an IRMS (Delta S, Finningan, Bremen) at INRA Nancy (n= 10 exetainers / tank). For T1 and T2, δ¹³C was $-36.6 \pm 0.08\text{‰}$ and $-36.9 \pm 0.2\text{‰}$ (mean ± S_d, n=10), respectively. Absolute values of ¹²CO₂ and ¹³CO₂ were respectively 414.51 and 4.487 μmol mol⁻¹ for T1 and 286.89 and 3.104 μmol mol⁻¹ for T2, considering the CO₂ mole fraction indicated by the provider took into consideration both isotopologues.

The isotopic composition ($\delta^{13}\text{C}$) is expressed relative to the Vienna Pee Dee belemnite (VPDB) standard as:

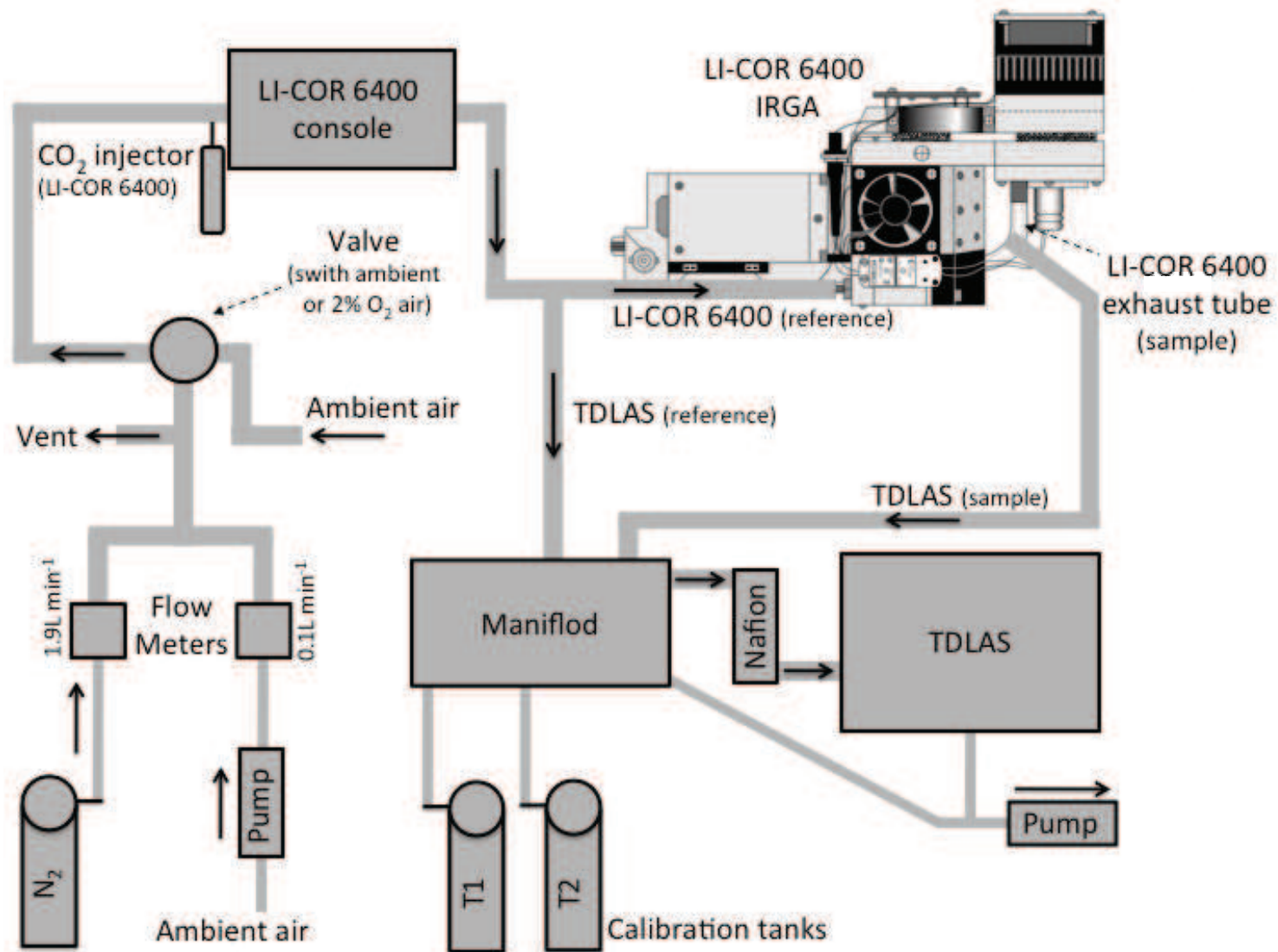
Erreur ! Des objets ne peuvent pas être créés à partir des codes de champs de mise en forme.

where R_s and R_{VPDB} are the isotopic ratio (computed as $R = {}^{13}\text{CO}_2 / {}^{12}\text{CO}_2$) of the sample and the standard, respectively. To estimate total CO_2 concentration from measurements of ${}^{12}\text{CO}^{16}\text{O}^{16}$ and ${}^{13}\text{CO}^{16}\text{O}^{16}$ it is necessary to account for the concentration of other isotopologues

Erreur ! Des objets ne peuvent pas être créés à partir des codes de champs de mise en forme.

where f_{other} is 0.00474 following Griffis *et al.* (2004).

The sequence of TDL measurements included two calibration gases and these were used for calibration of each measurement sequence. This involved calculation of the deviation between the measured values of calibration tanks and the known values to determine a gain and offset for each isotopologue in each tank being measured (Bowling *et al.* 2003). The gain and offset were used to calculate ${}^{12}\text{CO}_2$ and ${}^{13}\text{CO}_2$ of LI-6400 sample and reference gases in each measurement sequence.



exchange system used in Sydney to record online discrimination against ¹³CO₂ during photosynthesis. Upstream the LI-6400 console, the circuit was to produce air with 21% O₂ with 1 % O₂ by dilution air with pure N₂. The LI-6400 console, air is diluted by the TDLAS before being in the Li-6400 clamp

Estimating leaks of the gas exchange system

It is known that classical clamping systems allow CO₂ to diffuse through chamber gaskets (Rodeghiero *et al.*, 2007). Thus, it is important to quantify these CO₂ leaks during experiments to check if they can affect our estimation of photosynthesis parameters (A , C_i etc...), and the measurements of $\delta^{13}\text{C}$ used to estimate g_m . The CO₂ leaks are enhanced whenever the CO₂ mole fraction in the chamber differs from that in the air surrounding the chamber (i.e. ambient air in the lab). We performed measurements of the difference in CO₂ mole fraction entering (C_e) and leaving (C_o) in an empty chamber (without leaf) to estimate the impact of CO₂ leaks. We repeated this experiment under 21% O₂ and 1% O₂. Source CO₂ was provided with compressed CO₂ cartridges fixed on the CO₂ injector of the LI-6400, with $\delta^{13}\text{C} = -5.88\text{‰}$ (estimation from TDLAS at $C_e = 300 \mu\text{mol mol}^{-1}$).

Results are presented in Figure A2. Under 21% O₂, the $C_o - C_e$ difference was comprised between $-0.1 \mu\text{mol mol}^{-1}$ at $C_e = 200 \mu\text{mol mol}^{-1}$ and $1 \mu\text{mol mol}^{-1}$ at $C_e = 1000 \mu\text{mol mol}^{-1}$ (Figure A2, upper panel), the same range of C_e used in the CO₂ variations experiment presented in Chapter II. At $C_e = 2000 \mu\text{mol mol}^{-1}$, the $C_o - C_e$ difference increased up to $3 \mu\text{mol mol}^{-1}$. We observed the same pattern under 1% O₂, but with slightly lower $C_o - C_e$ difference for the same C_e (Figure A2, upper panel). The $\delta^{13}\text{C}_o - \delta^{13}\text{C}_e$ difference was not affected by the changes of C_e and remained constant between -0.5‰ and 0.5‰ (except noisy points, see Figure A2, lower panel). No difference was observed between 21 and 1% O₂.

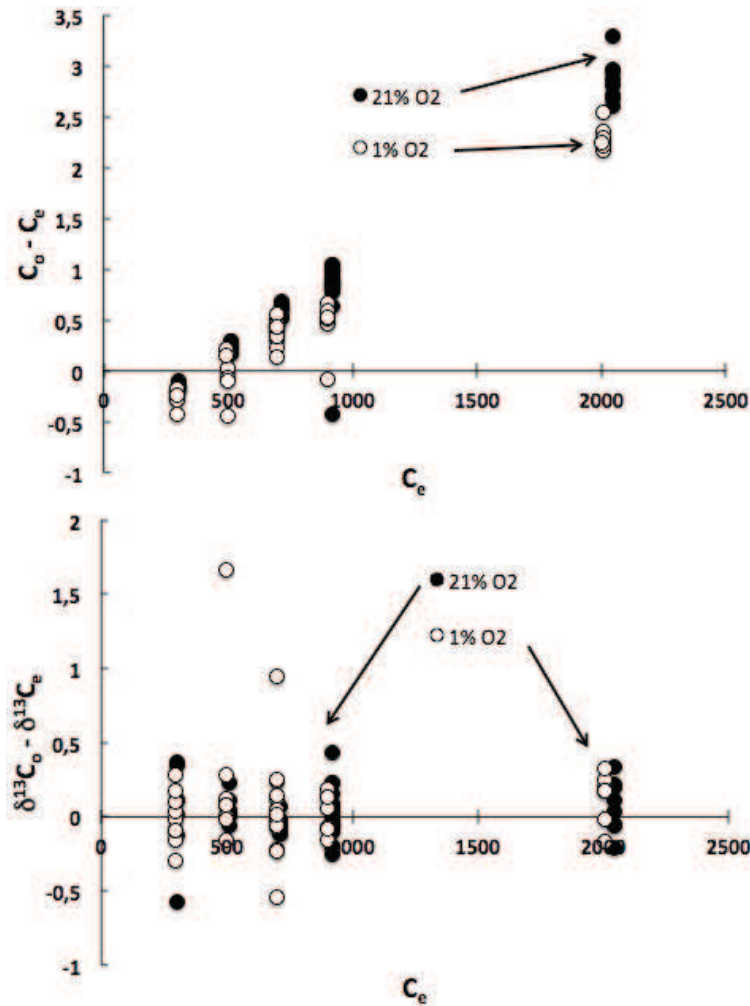


Figure A2: Upper panel: Difference between CO₂ molar fraction entering and leaving the photosynthesis chamber (C_e and C_o , respectively in $\mu\text{mol mol}^{-1}$) versus CO₂ mole fraction entering the chamber (C_e). Measurements were performed under 21 (black dots) and 1% O₂ (empty circles).

Lower panel: Difference between isotopic composition of air entering and leaving the photosynthesis chamber ($\delta^{13}C_e$ and $\delta^{13}C_o$, respectively in ‰) plotted versus CO₂ molar fraction entering the chamber (C_e). Measurements were performed under 21 (black dots) and 1% O₂ (empty circles).

The derivation of $\delta^{13}C$ with variations of C_e

We observed that the absolute value of $\delta^{13}C$ increased exponentially with the value of C_e , with $\delta^{13}C = -5.88\text{‰}$ at $C_e = 300 \mu\text{mol mol}^{-1}$, and $\delta^{13}C = -1.66\text{‰}$ at $C_e = 1000 \mu\text{mol mol}^{-1}$ (Figure A3), for measurements under 21% O₂. The same pattern was observed for measurements under 1% O₂. Since calibration tanks covered a range between 290 and 419 $\mu\text{mol mol}^{-1}$, that ensures a linearity of the $\delta^{13}C$ signal, but not above $C_e = 419 \mu\text{mol mol}^{-1}$. We applied a correction to compensate for the observed deviation based on the deviation from reference values. Reference values were those measured at $C_e = 300 \mu\text{mol mol}^{-1}$, which is within the range of calibration tanks. The equation to

compute the corrected $\delta^{13}\text{C}$ was $\delta^{13}\text{C}_{\text{eobs}} - (0,000004 \cdot C_e^2 + 0,0024C_e - 1,3397)$ with $\delta^{13}\text{C}_{\text{eobs}}$ the not corrected $\delta^{13}\text{C}$, leading to corrected values showed in Figure A3.

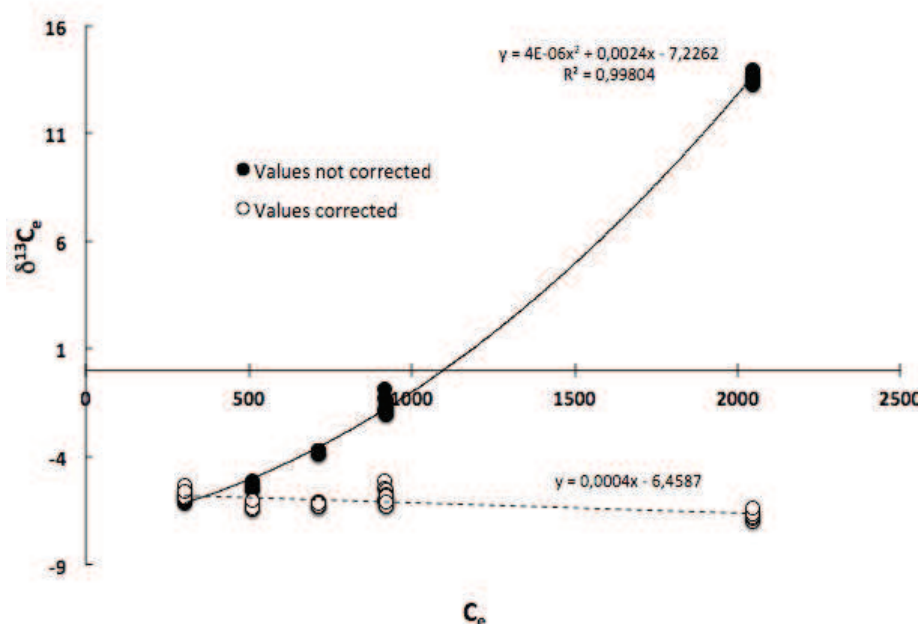


Figure A3: Observed isotopic composition of CO_2 entering the photosynthesis chamber ($\delta^{13}\text{C}_e$, black dots) plotted versus CO_2 molar fraction entering the chamber (C_e). Corrected values to compensate the deviation are shown in empty circles. The same CO_2 compressed cartridge was used along this experiment with $\delta^{13}\text{C} = -5.88\text{‰}$ (estimation from TDLAS at $C_e = 300 \mu\text{mol mol}^{-1}$). Since calibration tanks covered a range between 290 and $419 \mu\text{mol mol}^{-1}$, the derivation is due to the lack of calibration tanks above $C_e = 419 \mu\text{mol mol}^{-1}$.

The effect of changing O_2 on the observed $\delta^{13}\text{C}$ value

We observed that, with the same $\delta^{13}\text{C}$ of source CO_2 , $\delta^{13}\text{C}$ of air measured under $1\% \text{O}_2$ was systematically 1.37‰ higher than under $21\% \text{O}_2$ (Figure A4). We suspected that an interaction between O_2 and the TDLAS detector induced such shift in the measured $\delta^{13}\text{C}$, since calibrations tanks had air only with $21\% \text{O}_2$. We thus corrected values by subtracting the observed shift on the measured $\delta^{13}\text{C}$, leading to corrected values shown in Figure A4.

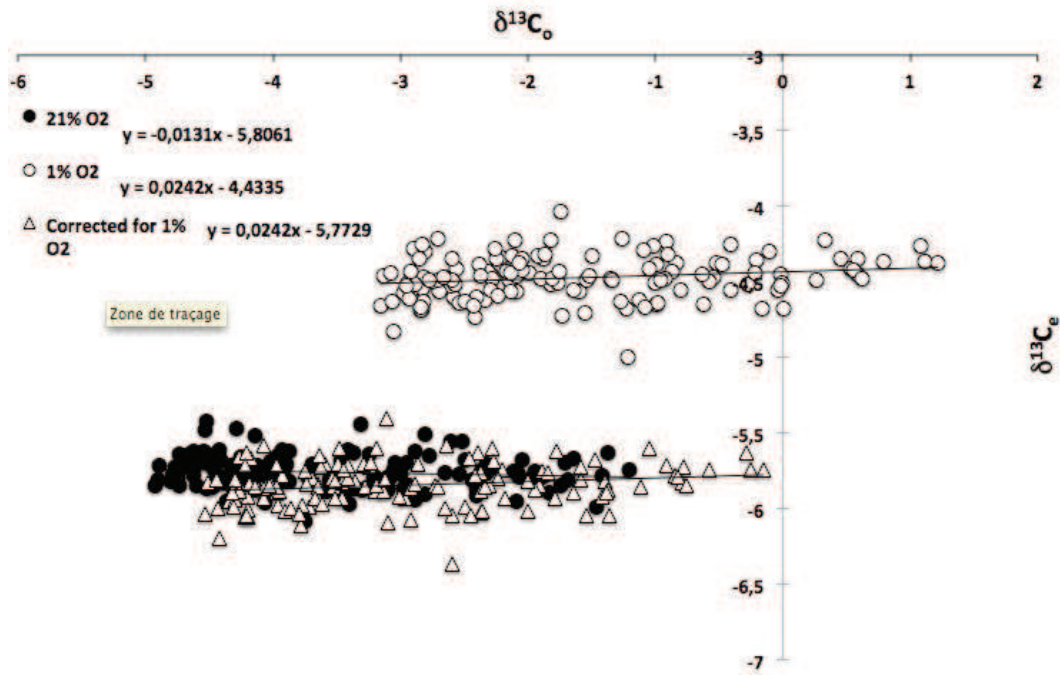


Figure A4: Observed $\delta^{13}\text{C}_e$ in 21% O_2 (black dots) and the shifted $\delta^{13}\text{C}_e$ values observed in 1% O_2 (empty circles) plotted versus $\delta^{13}\text{C}_o$. The shift was calculated from the intercepts of $\delta^{13}\text{C}_e$ under 21% and 1% O_2 (shift=1.3726‰). Corrected values under 1% O_2 are represented by empty triangles. Each point is a single measurement with TDLAS from 30s integrated signal.

Conclusions

We concluded that this gas exchange circuit provided satisfying precision data since (i) CO_2 leaks influence at maximum the C_e - C_o difference by $1 \mu\text{mol mol}^{-1}$, and (ii) the measurements of $\delta^{13}\text{C}$ had a precision below 0.5‰. We also compensated the deviation of $\delta^{13}\text{C}$ with the variations of C_e and O_2 , ensuring no artifactual data of $\delta^{13}\text{C}$.

Part 2: Using a custom-built photosynthesis chamber coupled to a TDLAS

Description of the gas exchange circuit

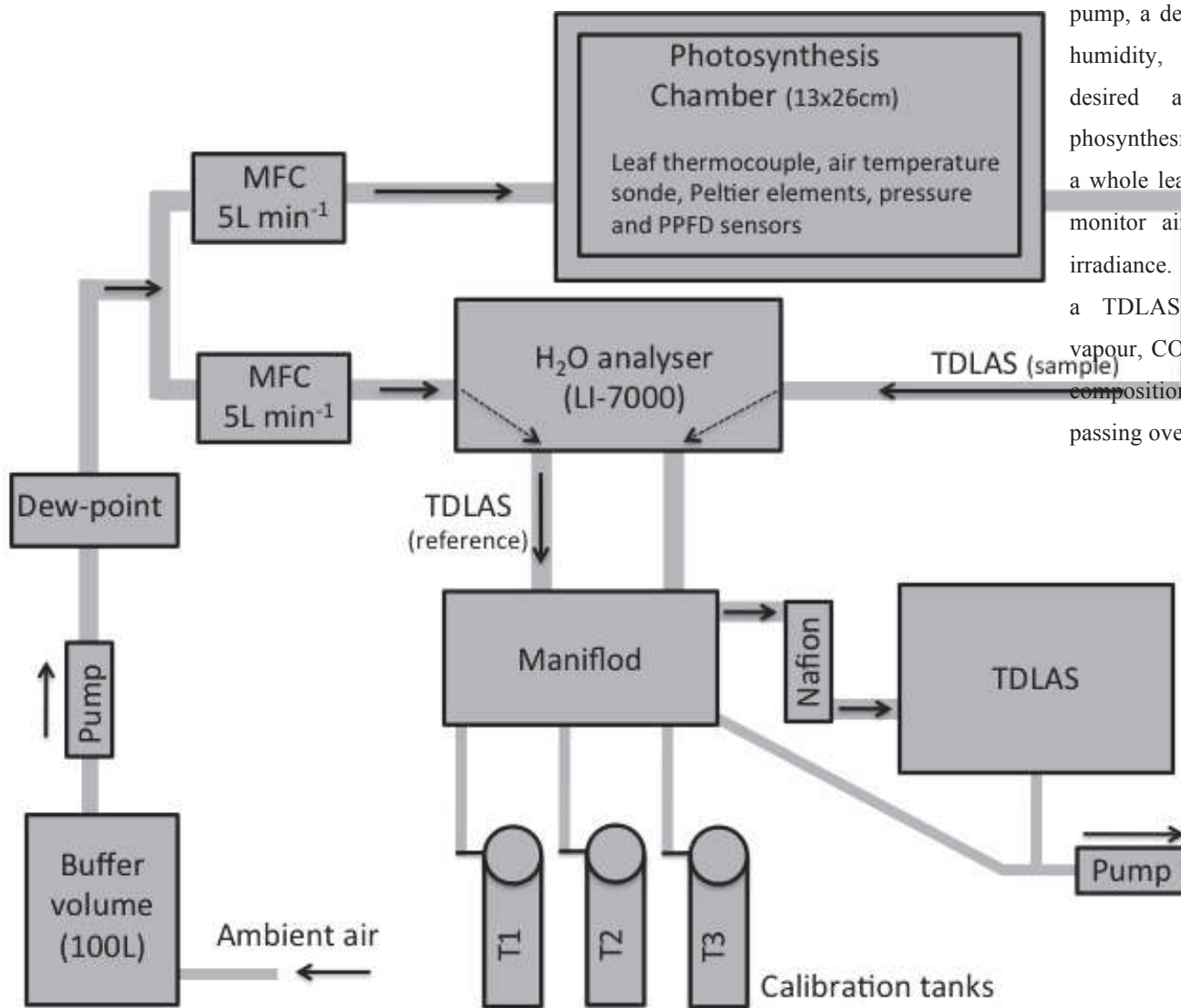
For measurements of leaf photosynthesis conducted at the Université de Nancy, we used an aluminium custom-built leaf chamber of 13x26cm. The main advantage to use such a photosynthesis chamber are: (i) to enclose a whole leaf and thus exclude problems induced by clamping systems (mechanical stress on the leaf and photosynthesis recorded on only a part of the leaf) and (ii) to considerably reduce leaks since the custom-built chamber was equipped with “O” rings sealed with ten bolts. The complete gas exchange circuit is presented in Figure A5.

The working air flow through the chamber was 5L min^{-1} controlled by a mass flow controller (Bronkorst). Leaf temperature (T_{leaf}) was measured with a nickel-

chrome thermocouple, and T_{leaf} was maintained constant at $22.1 \text{ }^{\circ}\text{C} \pm 0.7$ (mean \pm SD) using Peltier elements to control air temperature within the leaf chamber. Photosynthetic photon flux density (PPFD, $\mu\text{mol photons m}^{-2} \text{ s}^{-1}$) was monitored with a quantum sensor (LI90SA; Li-Cor, Inc., Lincoln, NE, USA) inside the chamber. Irradiance was provided by two 20cm x 20cm LED panels (P.S.I. Photon System Instruments, Brno, Czech Republic). Chamber air was well stirred with four fans to homogenise gas composition and temperature inside the chamber. Boundary layer conductance, estimated with a filter paper leaf replica, was $1\text{-}2 \text{ mol m}^{-2} \text{ s}^{-1}$, calculated for each leaf as a function leaf area from estimations based on the filter paper method (Jones 1989). Air pressure inside the chamber was measured with pressure sensors and maintained slightly above atmospheric pressure at $\approx 18.7 \pm 3 \text{ mbar}$ (mean \pm SD) to avoid influx into the chamber. Water vapour at the inlet of the chamber was controlled with a dew-point generator equipped with Peltier elements and air pressure sensor. All measured variables were recorded with a datalogger (CR23X; Campbell Scientific Inc.) every second and averaged every three minutes. Water vapour in the sample circuit was measured with a calibrated gas analyser (Li-7000, LI-COR, Lincoln, NE, USA). After recalculating the air flow leaving the photosynthesis chamber to account for the efflux of water by the leaf (Ball, 1987 Eq.11b), transpiration rate (E) was assessed by mass balance and stomatal conductance to water vapour (g_{sw}) was calculated from Fick's law based on leaf temperature (Ball, 1987) and accounting for boundary layer conductance and a stomatal ratio of 0.7 for Poplar (Le-Thiec, personal communication) with equations from Li-6400 manual (eq. 1-9 and 17-9). Stomatal conductance to CO_2 (g_s) was calculated with $g_s = g_{sw}/1.6$. CO_2 entering the circuit was provided by ambient air (for PPFD variations, $\delta^{13}\text{C} \approx -8 \text{ ‰}$) or by mixing ambient air with pure CO_2 from a compressed tank (Air Liquide, with $\delta^{13}\text{C} \approx -30 \text{ ‰}$) for CO_2 variations. CO_2 concentration in inlet (C_e) and outlet (C_a) was measured with a TDLAS (TGA100A; Campbell Scientific, Inc.). Because air flow was dried before entering the TDLAS, the measured CO_2 concentration was different from that in the reference and the sample circuits because of dilution in water vapour. C_e and C_a were then recalculated following Ball (1987):

$$C_e = \frac{C_{\text{TDLAS}}(1 - W_e)}{1 - W_{\text{TDLAS}}} \quad (\text{Eq. A1})$$

where C_{TDLAS} is CO_2 concentration measured by TDLAS in dried air, W_e and W_{TDLAS} are water vapour concentration in reference (dew point) and in air flow after drying, respectively, with W_{TDLAS} assumed to be zero. The same calculation was applied to C_a , using W_o , the water vapour concentration in the sample. Knowing C_e and C_a , net assimilation (A) was assessed by mass balance, and C_i , the CO_2 concentration in intercellular air spaces was calculated following Ball (1987).



exchange system used in Nancy to record online discrimination against ¹³CO₂ during photosynthesis. Air flow pass through buffer volume and then a pump, a dew-point generator control air humidity, mass flow controllers set desired air flow. A customized photosynthesis chamber allows to enclose a whole leaf with the needed sensors to monitor air pressure, temperature and irradiance. A water vapour analyser and a TDLAS allow to monitor water vapour, CO₂ mole fractions and isotopic composition of air before and after passing over the leaf.

Test of the circuit

To test the presence of leaks in the gas exchange circuit, we firstly flushed the chamber with pure nitrogen (Air Liquide) and recorded the CO₂ molar fraction with a LI-7000 H₂O/CO₂ analyzer placed after the chamber. We did not detected CO₂ leaks since the measured CO₂ molar fraction in the chamber was $< 0.2 \mu\text{mol mol}^{-1}$, thus below the detection threshold of the LI-7000 (not shown). We then flushed the photosynthesis chamber with CO₂ molar fraction at $1000 \mu\text{mol mol}^{-1}$ provided by calibration tanks (Air Liquide). Again, the recorded CO₂ molar fraction in the photosynthesis chamber was not different from $1000 \mu\text{mol mol}^{-1}$ (not shown).

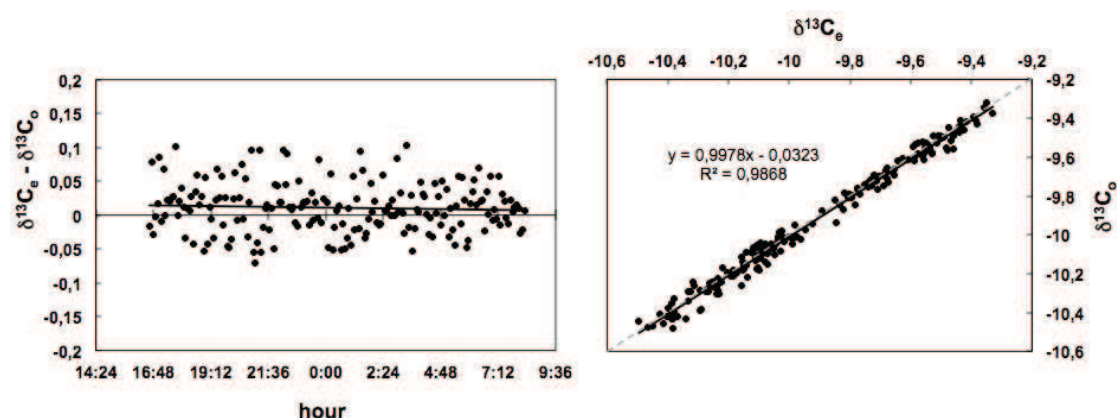


Figure A6: On the left panel, recorded difference between $\delta^{13}\text{C}_e - \delta^{13}\text{C}_o$ (isotopic composition of air entering and leaving the photosynthesis chamber) with an empty chamber during 15h. On the right panel, the corresponding correlation between $\delta^{13}\text{C}_e$ and $\delta^{13}\text{C}_o$, the grey dashed line represent the 1:1 relationship. The variation of $\delta^{13}\text{C}_e$ (from -9.3‰ to -10.6‰) was due to changes in the atmospheric $\delta^{13}\text{C}$ at the Université de Nancy on Julian day 112, 2009.

To test if isotopic composition of a gas entering the chamber was not modified when passing through the circuit (i.e. if any discrimination was induced by the circuit's components), we recorded $\delta^{13}\text{C}_e$ and $\delta^{13}\text{C}_o$ in the empty chamber (no leaf inside) during 15 hours. The $\delta^{13}\text{C}_e - \delta^{13}\text{C}_o$ difference was comprised between -0.1 and 0.1‰ (Figure A6).

Conclusions

This circuit equipped with a custom-built photosynthesis chamber provided data not influenced by CO₂ leaks, due to the absence of a clamping system and an “O” ring with high sealing power. The discrimination by the circuit was considered as null, since the precision measurement was about 0.1‰.

REFERENCES

- Atkin OK, Evans JR, Ball MC, Lambers H, Pons TL.** 2000. Leaf respiration of snow gum in the light and dark. interactions between temperature and irradiance. *Plant Physiology* **122**, 915-23.
- Bagard M, Le Thiec D, Delacote E, Hasenfratz-Sauder M-P, Banvoy J, Gérard J, Dizengremel P, Jolivet Y.** 2008. Ozone-induced changes in photosynthesis and photorespiration of hybrid poplar in relation to the developmental stage of the leaves. *Physiologia Plantarum* **134**, 559-74.
- Ball JT.** 1987. Calculations related to gas exchange. In: Zeiger EF, G.D.;Cowan, I.R. ed *Stomatal Function*: Stanford University Press, 445-76.
- Barbour MM, McDowell NG, Tcherkez G, Bickford CP, Hanson DT.** 2007. A new measurement technique reveals rapid post-illumination changes in the carbon isotope composition of leaf-respired CO₂. *Plant Cell and Environment* **30**, 469-82.
- Bernacchi CJ, Portis AR, Nakano H, Von Caemmerer S, Long SP.** 2002. Temperature response of mesophyll conductance. Implications for the determination of Rubisco enzyme kinetics and for limitations to photosynthesis in vivo. *Plant Physiology* **130**, 1992-8.
- Bongi G, Loreto F.** 1989. Gas-Exchange Properties of Salt-Stressed Olive (*Olea europea* L.) Leaves. *Plant Physiology* **90**, 1408-16.
- Boucher J-F, Wetzel S, Munson AD.** 1998. Leaf level response of planted eastern white pine (*Pinus strobus* L.) seven years after intensive silvicultural treatments. *Forest Ecology and Management* **107**, 291-307.
- Bowling DR, Pataki DE, Randerson JT.** 2008. Carbon isotopes in terrestrial ecosystem pools and CO₂ fluxes. *New Phytologist* **178**, 24-40.
- Brodribb TJ, McAdam SAM, Jordan GJ, Feild TS.** 2009. Evolution of stomatal responsiveness to CO₂ and optimization of water-use efficiency among land plants. *New Phytologist* **183**, 839-47.
- Brooks A, Farquhar GD.** 1985. Effect of temperature on the CO₂/O₂ specificity of Ribulose-1,5-bisphosphate carboxylase oxygenase and the rate of respiration in the light - estimates from gas-exchange measurements on spinach. *Planta* **165**, 397-406.
- Brugnoli E, Hubick KT, Von Caemmerer S, Wong SC, Farquhar GD.** 1988. Correlation between the carbon isotope discrimination in leaf starch and sugars of C-3 plants and the ratio of intercellular and atmospheric partial pressures of carbon-dioxide. *Plant Physiology* **88**, 1418-24.
- Bunce J.** 2002. Sensitivity of infrared water vapor analyzers to oxygen concentration and errors in stomatal conductance. *Photosynthesis Research* **71**, 273-6.
- Bunce J.** 2010. Variable responses of mesophyll conductance to substomatal carbon dioxide concentration in common bean and soybean. *Photosynthetica* **48**, 507-12.
- Carelli M, Fahl J, Trivelin P, Queiroz-Voltan R.** 1999. Carbon isotope discrimination and gas exchange in Coffea species grown under different irradiance regimes. *Revista Brasileira de Fisiologia Vegetal* **11**, 5.
- Centritto M, Loreto F, Chartzoulakis K.** 2003. The use of low [CO₂] to estimate diffusional and non-diffusional limitations of photosynthetic capacity of salt-stressed olive saplings. *Plant, Cell & Environment* **26**, 585-94.
- Cernusak LA, Winter K, Aranda J, Turner BL, Marshall JD.** 2007. Transpiration efficiency of a tropical pioneer tree (*Ficus insipida*) in relation to soil fertility. *Journal of Experimental Botany* **58**, 3549-66.
- Cochard H, Venisse J-S, Barigah TS, Brunel N, Herbette S, Guilliot A, Tyree MT, Sakr S.** 2007. Putative role of aquaporins in variable hydraulic conductance of leaves in response to light. *Plant Physiol.* **143**, 122-33.

- Cornic G, Legouallec JL, Briantais JM, Hodges M.** 1989. Effect of dehydration and high light on photosynthesis of 2 C-3 plants (*Phaseolus vulgaris* L. and *Elatostema repens* (Lour) Hall F). *Planta* **177**, 84-90.
- Cowan IR, Farquhar GD.** 1977. Stomatal function in relation to leaf metabolism and environment *Integration of Activity in the Higher Plant*: Society for Experimental Biology, 471-505.
- Craig H.** 1953. The geochemistry of the stable carbon isotopes. *Geochimica Et Cosmochimica Acta* **3**, 53-92.
- Craig H.** 1954. Carbon 13 in plants and the relationships between carbon 13 and carbon 14 variations in nature. *The Journal of Geology* **62**, 35.
- Cregg BM, Olivas-Garcia JM, Hennessey TC.** 2000. Provenance variation in carbon isotope discrimination of mature ponderosa pine trees at two locations in the Great Plains. *Canadian Journal of Forest Research* **30**, 428-39.
- Dawson TE, Ward JK, Ehleringer JR.** 2004. Temporal scaling of physiological responses from gas exchange to tree rings: a gender-specific study of *Acer negundo* (Boxelder) growing under different conditions. *Functional Ecology* **18**, 212-22.
- Dizengremel P.** 2001. Effects of ozone on the carbon metabolism of forest trees. *Plant Physiology and Biochemistry* **39**, 729-42.
- Douthe C, Dreyer E, Epron D, Warren CR.** 2011. Mesophyll conductance to CO₂, assessed from online TDL-AS records of ¹³CO₂ discrimination, displays small but significant short-term responses to CO₂ and irradiance in *Eucalyptus* seedlings. *Journal of Experimental Botany*.
- Duranceau M, Ghashghaie J, Badeck F, Deleens E, Cornic G.** 1999. $\delta^{13}\text{C}$ of CO₂ respired in the dark in relation to $\delta^{13}\text{C}$ of leaf carbohydrates in *Phaseolus vulgaris* L. under progressive drought. *Plant, Cell & Environment* **22**, 515-23.
- Duranceau M, Ghashghaie J, Brugnoli E.** 2001. Carbon isotope discrimination during photosynthesis and dark respiration in intact leaves of *Nicotiana sylvestris*: comparisons between wild type and mitochondrial mutant plants. *Functional Plant Biology* **28**, 65-71.
- During H.** 2003. Stomatal and mesophyll conductances control CO₂ transfer to chloroplasts in leaves of grapevine (*Vitis vinifera* L.). *Vitis* **42**, 65-8.
- Epron D, Godard D, Cornic G, Genty B.** 1995. Limitation of net CO₂ assimilation rate by internal resistances to CO₂ transfer in the leaves of 2 tree species (*Fagus sylvatica* L. and *Castanea sativa* Mill). *Plant Cell and Environment* **18**, 43-51.
- Ethier GJ, Livingston NJ, Harrison DL, Black TA, Moran JA.** 2006. Low stomatal and internal conductance to CO₂ versus Rubisco deactivation as determinants of the photosynthetic decline of ageing evergreen leaves. *Plant, Cell & Environment* **29**, 2168-84.
- Evans J, Loreto F.** 2000. Acquisition and Diffusion of CO₂ in Higher Plant Leaves . In: Leegood R, Sharkey T, Caemmerer S eds. *Photosynthesis: Physiology and Metabolism*: Springer Netherlands, 321-51.
- Evans JR, Kaldenhoff R, Genty B, Terashima I.** 2009. Resistances along the CO₂ diffusion pathway inside leaves. *Journal of Experimental Botany* **60**, 2235-48.
- Evans JR, Sharkey TD, Berry JA, Farquhar GD.** 1986. Carbon isotope discrimination measured concurrently with gas-exchange to investigate CO₂ diffusion in leaves of higher-plants. *Australian Journal of Plant Physiology* **13**, 281-92.
- Evans JR, Von Caemmerer S.** 1996. Carbon dioxide diffusion inside leaves. *Plant Physiology* **110**, 339-46.
- Farquhar GD.** 1983. On the nature of carbon isotope discrimination in C-4 species. *Australian Journal of Plant Physiology* **10**, 205-26.
- Farquhar GD, Ehleringer JR, Hubick KT.** 1989. Carbon isotope discrimination and photosynthesis. *Annual Review of Plant Physiology and Plant Molecular Biology* **40**, 503-37.

- Farquhar GD, Oleary MH, Berry JA.** 1982. On the relationship between carbon isotope discrimination and the inter-cellular carbon-dioxide concentration in leaves. *Australian Journal of Plant Physiology* **9**, 121-37.
- Farquhar GD, Richards RA.** 1984. Isotopic composition of plant carbon correlates with water-use efficiency of wheat genotypes. *Australian Journal of Plant Physiology* **11**, 539-52.
- Farquhar GD, Von Caemmerer S, Berry JA.** 1980. A biochemical-model of photosynthetic CO₂ assimilation in leaves of C-3 species. *Planta* **149**, 78-90.
- Flexas J, Diaz-Espejo A, Berry JA, Cifre J, Galmes J, Kaldenhoff R, Medrano H, Ribas-Carbo M.** 2007a. Analysis of leakage in IRGA's leaf chambers of open gas exchange systems: quantification and its effects in photosynthesis parameterization. *Journal of Experimental Botany* **58**, 1533-43.
- Flexas J, Diaz-Espejo A, Galmes J, Kaldenhoff R, Medrano H, Ribas-Carbo M.** 2007b. Rapid variations of mesophyll conductance in response to changes in CO₂ concentration around leaves. *Plant Cell and Environment* **30**, 1284-98.
- Flexas J, Ortuno MF, Ribas-Carbo M, Diaz-Espejo A, Florez-Sarasa ID, Medrano H.** 2007c. Mesophyll conductance to CO₂ in *Arabidopsis thaliana*. *New Phytologist* **175**, 501-11.
- Flexas J, Ribas-Carbo M, Diaz-Espejo A, Galmes J, Medrano H.** 2008. Mesophyll conductance to CO₂: current knowledge and future prospects. *Plant Cell and Environment* **31**, 602-21.
- Flexas J, Ribas-Carbo M, Hanson DT, Bota J, Otto B, Cifre J, McDowell N, Medrano H, Kaldenhoff R.** 2006. Tobacco aquaporin NtAQP1 is involved in mesophyll conductance to CO₂ *in vivo*. *Plant Journal* **48**, 427-39.
- Gaastra.** 1959. Photosynthesis of crop plants as influenced by light, carbon dioxide, temperature and stomatal diffusion resistance. *Mededelingen van de Landbouwhoogeschool te Wageningen* **59**, 1-68.
- Ghashghaie J, Badeck F, Lanigan GJ, Nogues S, Tcherkez G, Deleens E, Cornic G, Griffiths H.** 2003. Carbon isotope fractionation during dark respiration and photorespiration in C3 plants. *Phytochemistry Reviews* **2**, 145-61.
- Gillon JS.** 1997. Carbon isotope discrimination: interactions between respiration, leaf conductance and photosynthetic capacity. New-castle: University of Newcastle upon Tyne.
- Gillon JS, Griffiths H.** 1997. The influence of (photo)respiration on carbon isotope discrimination in plants. *Plant Cell and Environment* **20**, 1217-30.
- Gorton HL, Herbert SK, Vogelmann TC.** 2003. Photoacoustic analysis indicates that chloroplast movement does not alter liquid-phase CO₂ diffusion in leaves of *Alocasia brisbanensis*. *Plant Physiology* **132**, 1529-39.
- Grossnickle SC, Fan S.** 1998. Genetic variation in summer gas exchange patterns of interior spruce (*Picea glauca* (Moench) Voss times *Picea engelmannii* Parry ex Engelm.). *Canadian Journal of Forest Research* **28**, 831-40.
- Grossnickle SC, Fan S, Russell JH.** 2005. Variation in gas exchange and water use efficiency patterns among populations of western redcedar. *Trees - Structure and Function* **19**, 32-42.
- Guehl J-M, Fort C, Ferhi A.** 1995. Differential response of leaf conductance, carbon isotope discrimination and water-use efficiency to nitrogen deficiency in maritime pine and pedunculate oak plants. *New Phytologist* **131**, 149-57.
- Guy RD, Fogel ML, Berry JA.** 1993. Photosynthetic fractionation of the stable isotopes of oxygen and carbon. *Plant Physiology* **101**, 37-47.
- Hanba YT, Kogami H, Terashima I.** 2003. The effect of internal CO₂ conductance on leaf carbon isotope ratio. *Isotopes in Environmental and Health Studies* **39**, 5 - 13.
- Hanba YT, Shibasaka M, Hayashi Y, Hayakawa T, Kasamo K, Terashima I, Katsuhara M.** 2004. Overexpression of the Barley Aquaporin HvPIP2;1 Increases Internal CO₂

Conductance and CO₂ Assimilation in the Leaves of Transgenic Rice Plants. *Plant and Cell Physiology* **45**, 521-9.

Harley PC, Loreto F, Dimarco G, Sharkey TD. 1992. Theoretical considerations when estimating the mesophyll conductance to CO₂ flux by analysis of the response of photosynthesis to CO₂. *Plant Physiology* **98**, 1429-36.

Harris D.C. 1991. Quantitative Chemical Analysis: WH Freeman and Company, New York.

Hassiotou F, Ludwig M, Renton M, Veneklaas EJ, Evans JR. 2009. Influence of leaf dry mass per area, CO₂, and irradiance on mesophyll conductance in sclerophylls. *Journal of Experimental Botany* **60**, 2303-14.

Heinen RB, Ye Q, Chaumont Fo. 2009. Role of aquaporins in leaf physiology. *Journal of Experimental Botany* **60**, 2971-85.

Holbrook GP, Keys AJ, Leech RM. 1984. Biochemistry of photosynthesis in species of triticum of differing ploidy. *Plant Physiology* **74**, 12-5.

Igamberdiev AU, Bykova NV, Lea PJ, Gardestrom P. 2001. The role of photorespiration in redox and energy balance of photosynthetic plant cells: A study with a barley mutant deficient in glycine decarboxylase. *Physiologia Plantarum* **111**, 427-38.

Ivlev AA, Bykova NV, Igamberdiev AU. 1996. Fractionation of carbon (C-13/C-12) isotopes in glycine decarboxylase reaction. *Febs Letters* **386**, 174-6.

Kim YX, Steudle E. 2009. Gating of aquaporins by light and reactive oxygen species in leaf parenchyma cells of the midrib of Zea mays. *Journal of Experimental Botany* **60**, 547-56.

Kortschak HP, Hartt CE, Burr GO. 1965. Carbon Dioxide Fixation in Sugarcane Leaves. *Plant Physiology* **40**, 209-13.

Lanigan GJ, Betson N, Griffiths H, Seibt U. 2008. Carbon isotope fractionation during photorespiration and carboxylation in senecio. *Plant Physiology* **148**, 2013-20.

Lauteri M, Scartazza A, Guido MC, Brugnoli E. 1997. Genetic variation in photosynthetic capacity, carbon isotope discrimination and mesophyll conductance in provenances of *Castanea sativa* adapted to different environments. *Functional Ecology* **11**, 675-83.

Le Roux X, Bariac T, Sinoquet H, Genty B, Piel C, Mariotti A, Girardin C, Richard P. 2001. Spatial distribution of leaf water-use efficiency and carbon isotope discrimination within an isolated tree crown. *Plant, Cell & Environment* **24**, 1021-32.

Lloyd J, Syvertsen JP, Kriedemann PE, Farquhar GD. 1992. Low conductances for CO₂ diffusion from stomata to the sites of carboxylation in leaves of woody species. *Plant Cell and Environment* **15**, 873-99.

Loreto F, Harley PC, Dimarco G, Sharkey TD. 1992. Estimation of mesophyll conductance to CO₂ flux by 3 different methods. *Plant Physiology* **98**, 1437-43.

Maurel C, Verdoucq L, Luu DT, Santoni V. 2008. Plant aquaporins: Membrane channels with multiple integrated functions. *Annual Review of Plant Biology* **59**, 595-624.

McNevin DB, Badger MR, Kane HJ, Farquhar GD. 2006. Measurement of (carbon) kinetic isotope effect by Rayleigh fractionation using membrane inlet mass spectrometry for CO₂-consuming reactions. *Functional Plant Biology* **33**, 1115-28.

McNevin DB, Badger MR, Whitney SM, von Caemmerer S, Tcherkez GGB, Farquhar GD. 2007. Differences in carbon isotope discrimination of three variants of d-ribulose-1,5-bisphosphate carboxylase/oxygenase reflect differences in their catalytic mechanisms. *Journal of Biological Chemistry* **282**, 36068-76.

Meinzer FC, Goldstein G, Grantz DA. 1990. Carbon Isotope Discrimination in Coffee Genotypes Grown under Limited Water Supply. *Plant Physiology* **92**, 130-5.

Melzer E, O'Leary MH. 1987. Anapleurotic CO₂ fixation by phosphoenolpyruvate carboxylase in C₃ plants. Rockville, MD, ETATS-UNIS: American Society of Plant Biologists.

- Miyazawa S, Kawasaki T, Shinzaki Y, Maeshima M.** 2007. Relationship between mesophyll CO₂ gas diffusion conductance and leaf plasma-membrane-type aquaporin contents in tobacco plants grown under drought conditions. *Photosynthesis Research* **91**, 219-.
- Mook WG, Bommerson JC, Staverman WH.** 1974. Carbon isotope fractionation between dissolved bicarbonate and gaseous carbon dioxide. *Earth and Planetary Science Letters* **22**, 169-76.
- Nier AO.** 1947. A Mass Spectrometer for Isotope and Gas Analysis. *Review of Scientific Instruments* **18**, 14.
- Nier AO, Gulbransen EA.** 1939. Variations in the Relative Abundance of the Carbon Isotopes. *Journal of the American Chemical Society* **61**, 697-8.
- Niinemets U, Diaz-Espejo A, Flexas J, Galmes J, Warren CR.** 2009a. Importance of mesophyll diffusion conductance in estimation of plant photosynthesis in the field. *Journal of Experimental Botany* **60**, 2271-82.
- Niinemets U, Diaz-Espejo A, Flexas J, Galmes J, Warren CR.** 2009b. Role of mesophyll diffusion conductance in constraining potential photosynthetic productivity in the field. *Journal of Experimental Botany* **60**, 2249-70.
- O'leary MH.** 1981. Carbon Isotope Fractionation in Plants. *Phytochemistry* **20**, 553-67.
- O'Leary MH.** 1984. Measurement of the isotope fractionation associated with diffusion of carbon dioxide in aqueous solution. *The Journal of Physical Chemistry* **88**, 823-5.
- O'Leary MH, Rife JE, Slater JD.** 1981. Kinetic and isotope effect studies of maize phosphoenolpyruvate carboxylase. *Biochemistry* **20**, 7308-14.
- Ogée J, Peylin P, Ciais P, Bariac T, Brunet Y, Berbigier P, Roche C, Richard P, Bardoux G, Bonnefond JM.** 2003. Partitioning net ecosystem carbon exchange into net assimilation and respiration using ¹³CO₂ measurements: A cost-effective sampling strategy. *Global Biogeochem. Cycles* **17**, 1070.
- Olivas-Garcia JM, Cregg BM, Hennessey TC.** 2000. Genotypic variation in carbon isotope discrimination and gas exchange of ponderosa pine seedlings under two levels of water stress. *Canadian Journal of Forest Research* **30**, 1581-90.
- Park R, Epstein S.** 1961. Metabolic fractionation of C¹³ & C¹² in plants. *Plant Physiology* **36**, 133-8.
- Peisker M, Apel H** (2001) Inhibition by light of CO₂ evolution from dark respiration: comparison of two gas exchange methods. *Photosynthesis Research* **70**, 291-298.
- Piel C, Frak E, Le Roux X, Genty B.** 2002. Effect of local irradiance on CO₂ transfer conductance of mesophyll in walnut. *Journal of Experimental Botany* **53**, 2423-30.
- Pons TL, Flexas J, von Caemmerer S, Evans JR, Genty B, Ribas-Carbo M, Brugnoli E.** 2009. Estimating mesophyll conductance to CO₂: methodology, potential errors, and recommendations. *Journal of Experimental Botany* **60**, 2217-34.
- Pons TL, Westbeek MHM.** 2004. Analysis of differences in photosynthetic nitrogen-use efficiency between four contrasting species. *Physiologia Plantarum* **122**, 68-78.
- Ponton S, Dupouey J-L, Bréda N, Dreyer E.** 2002. Comparison of water-use efficiency of seedlings from two sympatric oak species: genotype x environment interactions. *Tree Physiology* **22**, 413-22.
- Reibach P, Benedict C.** 1977. Fractionation of stable carbon isotopes by phosphoenolpyruvate carboxylase from C₄ plants. *Plant Physiology* **59**, 4.
- Rodeghiero M, Niinemets Ü, Cescatti A.** 2007. Major diffusion leaks of clamp-on leaf cuvettes still unaccounted: how erroneous are the estimates of Farquhar *et al.* model parameters? *Plant, Cell & Environment* **30**, 1006-22.
- Roeske CA, O'leary MH.** 1984. Carbon isotope effects on the enzyme-catalyzed carboxylation of ribulose biphosphate. *Biochemistry* **23**, 6275-84.

- Rooney MA.** 1988. Short-term carbon isotopic fractionation in plants. Wisconsin: University of Wisconsin-Madison.
- Roupsard O, Gross P, Dreyer E.** 1996. Limitation of photosynthetic activity by CO₂ availability in the chloroplasts of oak leaves from different species and during drought. *Annales Des Sciences Forestieres* **53**, 243-54.
- Roupsard O, Joly H, Dreyer E.** 1998. Variability of initial growth, water-use efficiency and carbon isotope discrimination in seedlings of *Faidherbia albida* (Del.) A. Chev., a multipurpose tree of semi-arid Africa. Provenance and drought effects. *Annales Des Sciences Forestieres* **55**, 329-48.
- Roussel M, Le Thiec D, Montpied P, Ningre N, Guehl J-M, Brendel O.** 2009. Diversity of water use efficiency among *Quercus robur* genotypes: contribution of related leaf traits. *Ann. For. Sci.* **66**, 408.
- Saurer M, Maurer S, Matyssek R, Landolt W, Günthardt-Goerg MS, Siegenthaler U.** 1995. The influence of ozone and nutrition on $\delta^{13}\text{C}$ in *Betula pendula*. *Oecologia* **103**, 397-406.
- Scartazza A, Lauteri M, Guido MC, Brugnoli E.** 1998. Carbon isotope discrimination in leaf and stem sugars, water-use efficiency and mesophyll conductance during different developmental stages in rice subjected to drought. *Australian Journal of Plant Physiology* **25**, 489-98.
- Scott KM, Schwedock J, Schrag DP, Cavanaugh CM.** 2004. Influence of form IA RubisCO and environmental dissolved inorganic carbon on the $\delta^{13}\text{C}$ of the clam-chemoautotroph symbiosis *Solemya velum*. *Environmental Microbiology* **6**, 1210-9.
- Seibt U, Rajabi A, Griffiths H, Berry JA.** 2008. Carbon isotopes and water use efficiency: sense and sensitivity. *Oecologia* **155**, 441-54.
- Sullivan P, Welker J.** 2007. Variation in leaf physiology of *Salix arctica* within and across ecosystems in the High Arctic: test of a dual isotope ($\Delta^{13}\text{C}$ and $\Delta^{18}\text{O}$) conceptual model. *Oecologia* **151**, 372-86.
- Sun ZJ, Livingston NJ, Guy RD, Ethier GJ.** 1996. Stable carbon isotopes as indicators of increased water use efficiency and productivity in white spruce (*Picea glauca* (Moench) Voss) seedlings. *Plant, Cell & Environment* **19**, 887-94.
- Tazoe Y, Von Caemmerer S, Badger MR, Evans JR.** 2009. Light and CO₂ do not affect the mesophyll conductance to CO₂ diffusion in wheat leaves. *Journal of Experimental Botany* **60**, 2291-301.
- Tazoe Y, Von Caemmerer S, Estavillo GM, Evans JR.** 2011. Using tunable diode laser spectroscopy to measure carbon isotope discrimination and mesophyll conductance to CO₂ diffusion dynamically at different CO₂ concentrations. *Plant, Cell & Environment*, no-no.
- Tcherkez G.** 2006. How large is the carbon isotope fractionation of the photorespiratory enzyme glycine decarboxylase? *Functional Plant Biology* **33**, 911-20.
- Tcherkez G, Cornic G, Bligny R, Gout E, Ghashghaie J.** 2005. In vivo respiratory metabolism of illuminated leaves. *Plant Physiology* **138**, 1596-606.
- Tcherkez G, Farquhar G, Badeck F, Ghashghaie J.** 2004. Theoretical considerations about carbon isotope distribution in glucose of C-3 plants. *Functional Plant Biology* **31**, 857-77.
- Tcherkez G, Mahé A, Hodges M** (2011) $^{12}\text{C}/^{13}\text{C}$ fractionations in plant primary metabolism. *Trends in Plant Science* **16**, 499-506.
- Tcherkez G, Mauve C, Lamothe M, Le Bras C, Grapin A.** 2011. The $^{13}\text{C}/^{12}\text{C}$ isotopic signal of day-respired CO₂ in variegated leaves of *Pelargonium × hortorum*. *Plant, Cell & Environment* **34**, 270-83.
- Tcherkez G, Nogues S, Bleton J, Cornic G, Badeck F, Ghashghaie J.** 2003. Metabolic origin of carbon isotope composition of leaf dark-respired CO₂ in French bean. *Plant Physiology* **131**, 237-44.

- Tcherkez G, SchÄufe R, NoguÉS S, Piel C, Boom A, Lanigan G, Barbaroux C, Mata C, Elhani S, Hemming D, Maguas C, Yakir DAN, Badeck FW, Griffiths H, Schnyder H, Ghashghaie J.** 2010. On the $^{13}\text{C}/^{12}\text{C}$ isotopic signal of day and night respiration at the mesocosm level. *Plant, Cell & Environment* **33**, 900-13.
- Terashima I, Hanba YT, Tazoe Y, Vyas P, Yano S.** 2006. Irradiance and phenotype: comparative eco-development of sun and shade leaves in relation to photosynthetic CO_2 diffusion. *Journal of Experimental Botany* **57**, 343-54.
- Terashima I, Ono K.** 2002. Effects of HgCl_2 on CO_2 Dependence of Leaf Photosynthesis: Evidence Indicating Involvement of Aquaporins in CO_2 Diffusion across the Plasma Membrane. *Plant and Cell Physiology* **43**, 70-8.
- Tholen D, Boom C, Noguchi K, Terashima I.** 2007. The effects of chloroplast movement on CO_2 transfer conductance in *Arabidopsis thaliana*. *Plant and Cell Physiology* **48**, S95-S.
- Tholen D, Boom C, Noguchi K, Ueda S, Katase T, Terashima I.** 2008. The chloroplast avoidance response decreases internal conductance to CO_2 diffusion in *Arabidopsis thaliana* leaves. *Plant Cell and Environment* **31**, 1688-700.
- Tholen D, Zhu XG** (2011) The mechanistic basis of internal conductance: A theoretical analysis of mesophyll cell photosynthesis and CO_2 diffusion. *Plant Physiology* **156**, 90-105.
- Valentini R, Epron D, Deangelis P, Matteucci G, Dreyer E.** 1995. In-situ estimation of net CO_2 assimilation, photosynthetic electron flow and photorespiration in turkey oak (*Q. cerris* L.) leaves - diurnal cycles under different levels of water-supply. *Plant Cell and Environment* **18**, 631-40.
- Viil J, Laisk A, Oja V, Parnik T.** 1977. Enhancement of photosynthesis caused by oxygen under saturating irradiance and high CO_2 concentrations. *Photosynthetica* **11**, 251-9.
- Vogel JC.** 1980. Fractionation of the carbon isotopes during photosynthesis. Springer-Verlag: Berlin ;.
- Von Caemmerer S.** 2000. Biochemical models of leaf photosynthesis. Collingwood, Vic. :: CSIRO Publishing.
- Von Caemmerer S, Evans JR.** 1991. Determination of the average partial-pressure of CO_2 in chloroplasts from leaves of several C-3 plants. *Australian Journal of Plant Physiology* **18**, 287-305.
- Von Caemmerer S, Evans JR, Hudson GS, Andrews TJ.** 1994. The kinetics of ribulose-1,5-bisphosphate carboxylase/oxygenase in vivo inferred from measurements of photosynthesis in leaves of transgenic tobacco. *Planta* **195**, 88-97.
- Vrabl D, Vaskova M, Hronkova M, Flexas J, Santrucek J.** 2009. Mesophyll conductance to CO_2 transport estimated by two independent methods: effect of variable CO_2 concentration and abscisic acid. *Journal of Experimental Botany* **60**, 2315-23.
- Vu JCV, Yelenosky G, Bausher MG.** 1985. Photosynthetic Activity in the Flower Buds of 'Valencia' Orange (*Citrus sinensis* [L.] Osbeck). *Plant Physiology* **78**, 420-3.
- Warren CR.** 2006a. Estimating the internal conductance to CO_2 movement. *Functional Plant Biology* **33**, 431-42.
- Warren CR.** 2006b. Why does photosynthesis decrease with needle age in *Pinus pinaster*? *Trees - Structure and Function* **20**, 157-64.
- Warren CR.** 2008a. Does growth temperature affect the temperature responses of photosynthesis and internal conductance to CO_2 ? A test with *Eucalyptus regnans*. *Tree Physiology* **28**, 11-9.
- Warren CR.** 2008b. Soil water deficits decrease the internal conductance to CO_2 transfer but atmospheric water deficits do not. *Journal of Experimental Botany* **59**, 327-34.
- Warren CR, Adams MA.** 2006. Internal conductance does not scale with photosynthetic capacity: implications for carbon isotope discrimination and the economics of water and nitrogen use in photosynthesis. *Plant Cell and Environment* **29**, 192-201.

- Warren CR, Dreyer E.** 2006. Temperature response of photosynthesis and internal conductance to CO₂: results from two independent approaches. *Journal of Experimental Botany* **57**, 3057-67.
- Whelan T, Sackett W, Benedict C.** 1973. Enzymatic Fractionation of Carbon Isotopes by Phosphoenolpyruvate Carboxylase from C₄ Plants. *Plant Physiology* **51**, 4.
- Wickman FE.** 1952. Variations in the Relative Abundance of the Carbon Isotopes in Plants. *Nature* **169**, 1051-.
- Wingate L, Seibt U, Moncrieff JB, Jarvis PG, Lloyd J.** 2007. Variations in C-13 discrimination during CO₂ exchange by *Picea sitchensis* branches in the field. *Plant Cell and Environment* **30**, 600-16.
- Yamori W, Evans JR, Von Caemmerer S.** 2010. Effects of growth and measurement light intensities on temperature dependence of CO₂ assimilation rate in tobacco leaves. *Plant Cell and Environment* **33**, 332-43.
- Yin X, Sun Z, Struik P, Gu J** 2011. Evaluating a new method to estimate the rate of leaf respiration in the light by analysis of combined gas exchange and chlorophyll fluorescence measurements. *Journal of Experimental Botany* **62**, 3489-3499.
- Zhang J, Fins L, Marshall JD.** 1994. Stable carbon isotope discrimination, photosynthetic gas exchange, and growth differences among western larch families. *Tree Physiology* **14**(5), 531-539.
- Zhang JW, Marshall JD** 1995 Variation in Carbon Isotope Discrimination and Photosynthetic Gas Exchange Among Populations of *Pseudotsuga menziesii* and *Pinus ponderosa* in Different Environments. *Functional Ecology* **9**(3), 402-412.